INTERACTION OF STATTIC, A STAT3 INHIBITOR WITH HUMAN SERUM ALBUMIN: SPECTROSCOPIC AND COMPUTATIONAL STUDY

IDA SYAZWANI BINTI MOHD AFFANDI

INSTITUTE OF BIOLOGICAL SCIENCES
FACULTY OF SCIENCE
UNIVERSITY OF MALAYA
KUALA LUMPUR

2017

INTERACTION OF STATTIC, A STAT3 INHIBITOR WITH HUMAN SERUM ALBUMIN: SPECTROSCOPIC AND COMPUTATIONAL STUDY

IDA SYAZWANI BINTI MOHD AFFANDI

DISSERTATION SUBMITTED IN FULFILMENT OF THE REQUIREMENTS FOR THE DEGREE OF MASTER OF SCIENCE

INSTITUTE OF BIOLOGICAL SCIENCES
FACULTY OF SCIENCE
UNIVERSITY OF MALAYA
KUALA LUMPUR

2017

UNIVERSITY OF MALAYA
ORIGINAL LITERARY WORK DECLARATION

Name of Candidate: Ida Syazwani Binti Mohd Affandi [redacted]
Matric No: SGR 150041
Name of Degree: Master of Science
Title of Dissertation: "Interaction of stattic, a STAT3 inhibitor with human serum albumin: Spectroscopic and computational study"

Field of Study: Biochemistry

I do solemnly and sincerely declare that:

(1) I am the sole author/writer of this Work;
(2) This Work is original;
(3) Any use of any work in which copyright exists was done by way of fair dealing and for permitted purposes and any excerpt or extract from, or reference to or reproduction of any copyright work has been disclosed expressly and sufficiently and the title of the Work and its authorship have been acknowledged in this Work;
(4) I do not have any actual knowledge nor do I ought reasonably to know that the making of this work constitutes an infringement of any copyright work;
(5) I hereby assign all and every rights in the copyright to this Work to the University of Malaya ("UM"), who henceforth shall be owner of the copyright in this Work and that any reproduction or use in any form or by any means whatsoever is prohibited without the written consent of UM having been first had and obtained;
(6) I am fully aware that if in the course of making this Work I have infringed any copyright whether intentionally or otherwise, I may be subject to legal action or any other action as may be determined by UM.

Candidate's Signature Date:
(Ida Syazwani Binti Mohd Affandi)

Subscribed and solemnly declared before,

Witness's Signature Date:
Name: Prof. Saad Tayyab
Designation: Supervisor

Witness's Signature Date:
Name: Dr. Saharuddin bin Mohamad
Designation: Supervisor

ABSTRACT

Interaction of stattic (ST), an inhibitor of signal transducer and activation of transcription 3, STAT3 with human serum albumin (HSA), the major transport protein in human blood circulation was investigated using several spectroscopic techniques and molecular docking method. Moderate binding affinity (K_a = 2.60−1.45 × 10^4 M^{-1}) between ST and HSA was revealed from the analysis of the fluorescence quenching titration data at three different temperatures. A decreasing trend of the binding constant with increasing temperature suggested involvement of the static quenching mechanism, thus pointing towards the formation of ST-HSA complex. The complex was supposed to be stabilized by hydrophobic interactions and hydrogen bonds, as indicated by the thermodynamic data (ΔH = −14.9 kJ mol^{-1} and ΔS = +32.8 J mol^{-1} K^{-1}). The far-UV and the near-UV CD spectral results showed slight alteration in the secondary and the tertiary structures of HSA upon ST binding. Whereas ST binding to HSA induced microenvironmental perturbation around protein's aromatic fluorophores, as evident from the three-dimensional fluorescence spectra, it increased protein's thermal stability. Competitive ligand displacement along with molecular docking results suggested Sudlow's site I of HSA as the ST binding site. A comparison of ST binding characteristics of serum albumins for bovine (BSA), porcine (PSA), sheep (SSA) and rabbit (RbSA) showed similarity between HSA and PSA in terms of binding affinity and between HSA and BSA based on warfarin displacement results. Further studies are needed to clarify which of these proteins (PSA or BSA) match closely to HSA in order to be used as a suitable animal model for pharmacological studies.

ABSTRAK

Interaksi stattic (ST), perencat transduser isyarat dan pengaktifan transkripsi 3, STAT3 dengan serum albumin manusia (HSA), protein pengangkutan utama dalam peredaran darah manusia telah dikaji dengan menggunakan beberapa teknik spektroskopi dan kaedah dok molekul. Pertalian pengikat sederhana (Ka = 2.60–1.45 × 10^4 M^{-1}) di antara ST dan HSA didedahkan daripada data analisis pendarfluor pelindapkejutan pentitratan di tiga suhu yang berbeza. Satu trend yang semakin menurun bagi pengikat malar dengan peningkatan suhu mencadangkan penglibatan mekanisme pelindapkejutan statik, sekali gus menunjuk ke arah pembentukan ST-HSA kompleks. Kompleks ini distabil oleh interaksi hidrofobik dan ikatan hidrogen, seperti yang ditunjukkan oleh data termodinamik (ΔH = −14.9 kJ mol^{-1} dan ΔS = +32.8 J mol^{-1} K^{-1}). Keputusan spektrum jauh-UV dan berhampiran-UV CD menunjukkan terdapat sedikit perubahan terhadap struktur sekunder dan tertier HSA apabila diikat dengan ST. Manakala ikatan ST kepada HSA menyebabkan perubahan mikroenvironmental berlaku di sekitar fluorophores aromatik protein, seperti yang terbukti daripada pendarfluor spektrum tiga dimensi, ia meningkatkan kestabilan protein terhadap haba. Kompetitif ligan anjakan protein bersama-sama dengan keputusan dok molekul mencadangkan tapak I Sudlow HSA sebagai tapak pengikat ST. Perbandingan ciri-ciri pengikat ST terhadap serum albumin untuk bovine (BSA), babi (PSA), kambing biri-biri (SSA) dan arnab (RbSA) menunjukkan persamaan antara HSA dan PSA dari segi daya pengikat pertalian dan antara HSA dan BSA berdasarkan keputusan anjakan warfarin. Kajian lanjut diperlukan untuk mengenalpasti di antara protein ini (PSA atau BSA) yang hampir sepadan dengan HSA yang sesuai untuk digunakan sebagai model haiwan untuk kajian farmakologi.

ACKNOWLEDGEMENTS

This dissertation owes its existence to the help, support and inspiration of several people. Firstly, my deepest gratitude goes to both of my supervisors, Professor Saad Tayyab and Dr. Saharuddin Mohamad for their endless support, encouragement and advice throughout my Master journey. Their patience in guiding me from the start until the end of my studies is highly appreciated. It was a golden opportunity to work under them. All the experiences and the knowledge gained throughout this project are something that I am ever grateful for.

My special thanks go to Dr. Zazali Alias, Coordinator of the Biochemistry Programme, Associate Professor Dr. Nurhayati binti Zainal Abidin, Head, Institute of Biological Sciences and Professor Zanariah Abdullah, Dean, Faculty of Science, University of Malaya for providing all the necessary facilities needed in my research.

I would also like to extend my gratitude to Malaysia Genome Institute (MGI) for allowing me to use their CD facility with such reasonable price. Not to forget, Ms. Azyyati Mohd. Padzil for her guidance in handling the machine.

Special thanks are due to Lee Wei Qi, who has been such a good companion during my ups and downs. Her unconditional support, advice and assistance kept me going during the hard time. I am also blessed to have seniors and friends who were very supportive and had been there for me when I needed.

My acknowledgement also goes to the Ministry of Higher Education, Government of Malaysia and the University of Malaya (High Impact Research Grant UM.C/625/1/HIR/Mohe/SC/02) for their financial support in the form of Research Assistantship.

Last but not the least, special thanks are due to my beloved parents and siblings for their support, advice, understanding, patience and prayers.

Ida Syazwani Binti Mohd Affandi

December, 2016

TABLE OF CONTENTS

LIST OF FIGURES

LIST OF TABLES

LIST OF ABBREVIATIONS AND SYMBOLS

Ala	Alanine
ANS	1-Anilinonaphthalene-8-sulfonate
Arg	Arginine
Asp	Aspartic acid
a.u.	Arbitrary unit
BSA	Bovine serum albumin
°C	Degree Celcius
CD	Circular dichroism
cm	Centimeter
Cys	Cysteine
3-D	Three-dimensional
Da	Dalton
DMSO	Dimethyl sulphoxide
DNA	Deoxyribonucleic acid
DZM	Diazepam
e.g.	Latin phrase *exempli gratia* (for example)
Eq.	Equation
ESCC	Esophageal squamous cell carcinoma
FI	Fluorescence intensity
g	Gram
Gln	Glutamine
Glu	Glutamic acid
h	Hour
HSA	Human serum albumin

His	Histidine
i.e.	Latin phrase *id est* (that is)
Ile	Isoleucine
J	Joules
JAK	Janus kinase
K_a	Association / binding constant
K_{sv}	Stern-Volmer constant
k_q	Bimolecular quenching constant
kJ	Kilojoules
L	Liter
Leu	Leucine
Lys	Lysine
M	Molar
mdeg	Milidegree
mg	Milligram
min	Minute
mL	Milliliter
mM	Millimolar
µM	Micromolar
MW	Molecular weight
nm	Nanometer
No.	Number
Phe	Phenylalanine
ppm	Parts per million
Pro	Proline
PSA	Porcine serum albumin

PVDF	Polyvenylidene fluoride
R	Gas constant
r	Correlation coefficient
RbSA	Rabbit serum albumin
Ser	Serine
SH2	Src Homology 2
SSA	Sheep serum albumin
ST	Stattic
STAT	Signal transducer and activator of tanscription
T	Temperature
Trp	Tryptophan
Tyr	Tyrosine
UV	Ultraviolet
V	Voltage
Val	Valine
viz.	Latin phrase *videlicet* (that is to say)
WFN	Warfarin
Å	Angstrom
ΔG	Gibbs free energy change
ΔH	Enthalpy change
ΔS	Entropy change
ε	Extinction coefficient
λ_{em}	Emission wavelength
λ_{ex}	Excitation wavelength
~	Approximate
>	Greater than

Chapter 1

INTRODUCTION

1. INTRODUCTION

Diagnosis of over 14.1 million new cancer patients and 8.2 million deaths each year have made cancer as one of the most life-threatening diseases (Cancer Research UK, 2014). The most commonly used method in treating cancer is chemotherapy, which employs pharmacological agents to treat cancer cells (McKnight, 2003; Corrie, 2008). Despite of their action in killing cancer cells, many of these agents are also toxic to the normal, healthy cells (Skeel & Khleif, 2011). Due to this problem, search for effective drugs to fight cancer is still continued (Krystof & Uldrijan, 2010). Drugs with efficient anticancer potential but minimal effect on normal cells are being discovered from natural sources as well as through chemical synthesis. These drugs usually act as inhibitors against abnormally expressed proteins in cancer cells (Kamal & Burrows, 2009; Krystof & Uldrijan, 2010). Recent *in vivo* studies have reported STAT3 in being constitutively active in a wide range of malignancies including breast, prostate and head and neck tumours as well as multiple myelomas and haematological cancers (Darnell, 1997; Bromberg et al., 1999; Bowman et al., 2000; Levy & Darnell, 2002; Turkson et al., 2004a; Song et al., 2005). This has made it as an attractive molecular target for the development of novel cancer therapies.

Stattic (ST), is a nonpeptidic small molecule that can directly inhibit STAT3 function (Schust et al., 2006) and has shown potential against STAT3-dependent cancer cells such as nasopharynx, ovarian and breast cancers (Yu et al., 2003; Schust et al., 2006; Pan et al., 2013). Several studies on ST have been made to show the mechanism of its anticancer action (Schust et al., 2006; Boengler et al., 2013; Pan et al., 2013) and therefore, it has a high potential in being recognized as a future anticancer drug. Despite its effectiveness in killing cancer cells, information about ST transportation in the blood, its pharmacokinetics and bioavailability has not been reported so far to the best of our knowledge. Therefore, it is important to study the interaction between a particular drug

and plasma proteins at a molecular level to form a sound basis for understanding its pharmacology and toxicity during the chemotherapeutic process (Liu et al., 2007).

Being one of the most abundant proteins in the blood plasma, human serum albumin (HSA) has been commonly used as a reagent in the biological study. It serves as a major transporter in the blood circulation to distribute a large number of endogenous and exogenous ligands including drugs (Peters, 1996; Curry et al., 1998; Petitpas et al., 2001; Kragh-Hansen et al., 2002; Artali et al., 2005). This protein consists of 585 amino acid residues, arranged in a single polypeptide chain in the form of three homologous domains, I, II and III (Peters, 1996). Different ligands may bind to either of the two high affinity ligand binding sites available on HSA, viz. Sudlow's site I and site II, located in subdomains IIA and IIIA, respectively (Sudlow et al., 1976). Presence of a solitary tryptophan residue (Trp-214), located in subdomain IIA is advantageous in using fluorescence spectroscopy to probe the binding of any ligand to the protein (He & Carter, 1992; Peters, 1996). Therefore, this study was undertaken to investigate the interaction between ST and HSA using fluorescence and CD spectroscopy along with molecular docking techniques.

However, before ST can be tested on human subjects, its safety and toxicity has to be evaluated using animal model in order to predict its pharmacological effects on the human system. Since the interaction between a drug and the carrier protein directly affects its pharmacokinetic and pharmacodynamic properties (Peters, 1996; Kragh-Hansen et al., 2002), selection of a suitable animal model possessing close resemblance to the human system in terms of ST-albumin interaction is a prerequisite for preclinical testing. Hence, a comparative study on ST binding characteristics of other serum albumins, *i.e.* sheep (SSA), porcine (PSA), bovine (BSA) and rabbit (RbSA) is essential to select the suitable animal model.

Problem statement

Does ST bind to HSA and form a stable ST-HSA complex? If yes, what are the binding characteristics of ST-HSA interaction and which mammalian albumin shows similar ST binding characteristics?

The following objectives were set to answer the above questions:

1. To study the interaction of ST with HSA in terms of the binding affinity, interactive forces involved and location of the ST binding site.
2. To study ligand-induced changes in the protein conformation and thermal stability.
3. To compare ST binding characteristics of different mammalian serum albumins.

Chapter 2

LITERATURE REVIEW

2. LITERATURE REVIEW

2.1. Signal transducer and activator of transcription proteins (STATs)

A group of latent cytoplasmic proteins, known as signal transducer and activator of transcription proteins (STATs) play a major role in regulating gene expression related to cell cycle, cell survival and immune response (Darnell, 1997; Zhang et al., 2010). There are seven (7) members in the STATs family, *i.e.* STAT1, STAT2, STAT3, STAT4, STAT5A, STAT5B and STAT6. Despite being encoded by individual genes, these proteins possess structurally similar and highly conserved domains, which include the amino-terminal domain (NH2), the coiled-coiled domain (CCD), the DNA-binding domain (DBD), the linker domain and the Src homology 2 (SH2) domain (Zhuang, 2013). STATs can be distinguished from each other on the basis of their carboxy-terminal transcription activation domain (TAD) (Figure 2.1) (Miklossy et al., 2013; Zhuang, 2013).

STATs feature dual roles, serving both as a signal transducer through the cytoplasm and a transcription factor in the nucleus (Darnell et al., 1994; Heinrich et al., 1998). These proteins are activated by either cytokines (Debnath et al., 2012) or growth factors (Yu et al., 2009) through phosphorylation of their tyrosine residues leading to their dimerization (Figure 2.2). Both homodimers and heterodimers with other STAT proteins are formed through reciprocal phosphotyrosine-SH2 domain interactions before their translocation into the nucleus where they bind to specific regions on DNA for further activation of transcription process (Figure 2.2). Non-receptor tyrosine kinases such as Src and Abelson leukemia protein (ABL) can also activate STATs independently without receptor involvement (Yu et al., 1995; Puthier et al., 1999; Yu et al., 2007). Inversely, once the signal has been terminated, STATs are translocated out from the nucleus into the cytoplasm (Figure 2.2) (Ihle, 2001; Leonard, 2001).

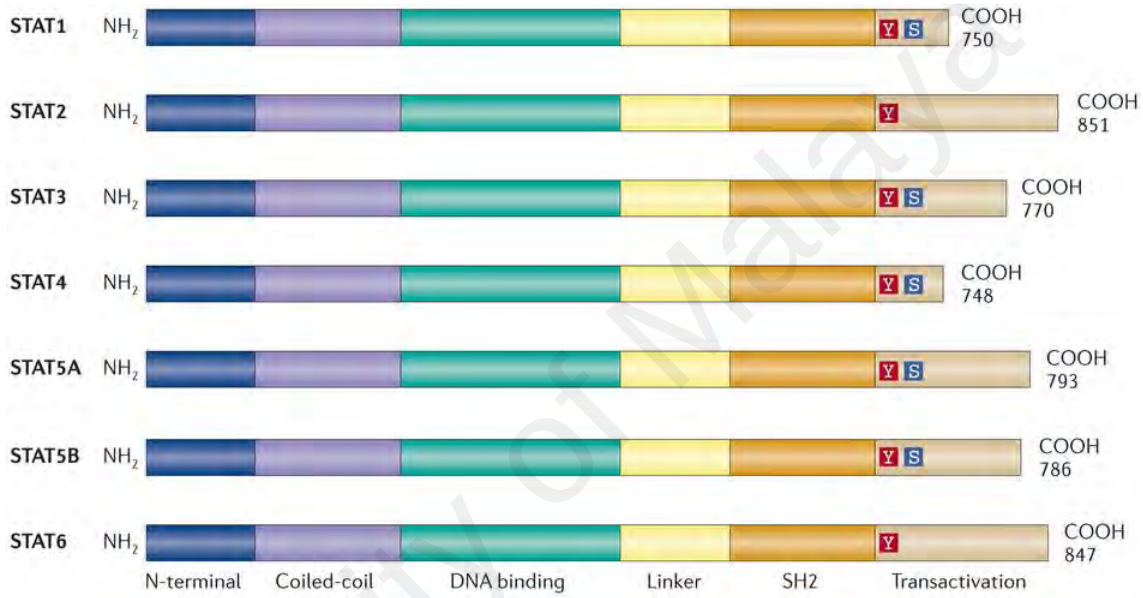

Figure 2.1. Schematic diagram showing the domain structures of STAT protein members. Labels (Y) and (S) refer to tyrosine and serine residues, respectively. (Adapted from Miklossy et al., 2013).

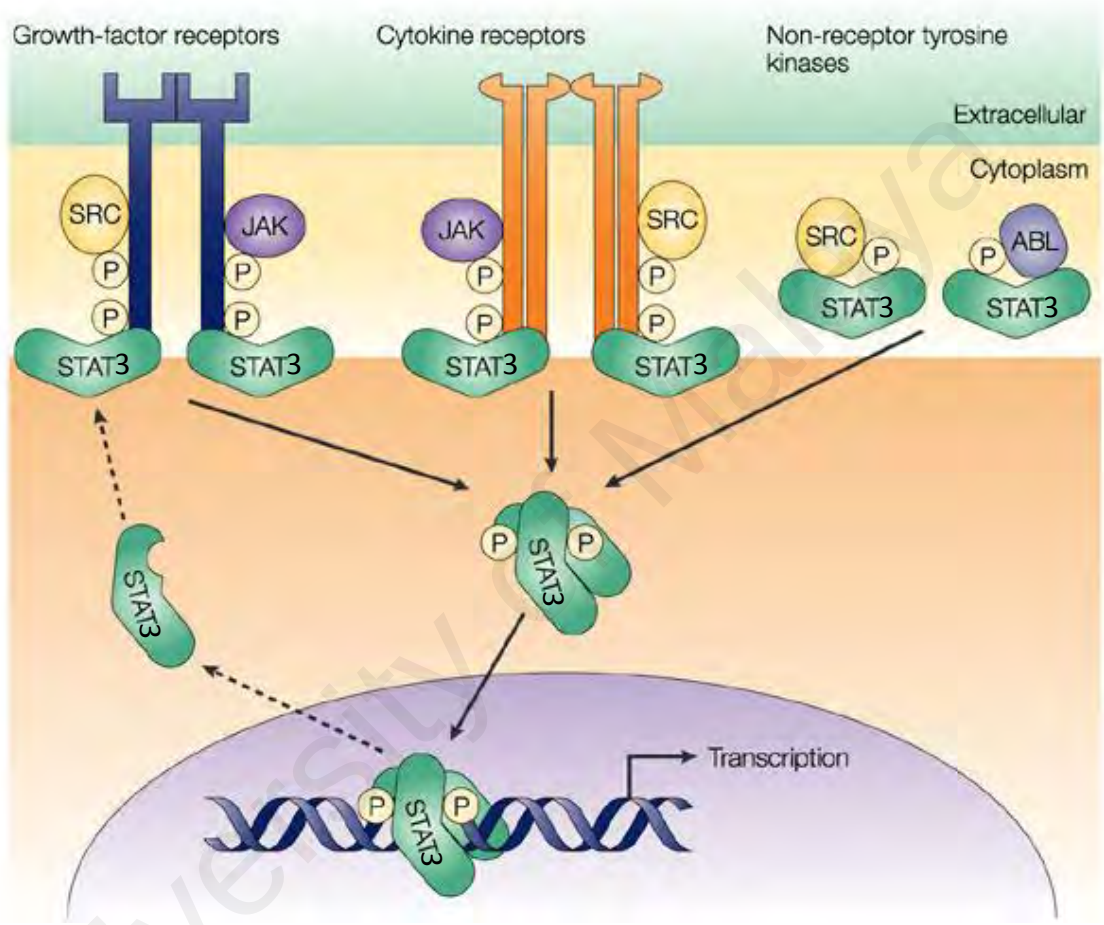

Figure 2.2. Schematic diagram showing the mechanism of STAT3 signaling pathway. (Adapted from Yu & Jove, 2004).

Out of different STAT proteins, STAT3 has been shown to be an important element for early development of an organism, as revealed by the embryonic lethal character of STAT3 null mice (Takeda et al., 1997). Furthermore, STAT3 has also been found participating in the wound healing process in keratinocytes, liver regeneration, mammary involution and cell survival (Akira, 2000; Poli & Alonzi, 2003). Removal of STAT3 by tissue-specific deletion has been shown to increase the apoptotic rate and induce adenoviral infection in both bronchiolar and alveolar epithelial cells, thus suggesting cytoprotective function of this protein (Matsuzaki et al., 2008).

2.2. STAT3 activation and its role in cancer

Activation of STAT3 leads to the regulation of gene expression related to cell cycle, anti-apoptosis, angiogenesis, pro-proliferation, metastasis and invasion/migration (Zhang et al., 2010; Luwor et al., 2013). Therefore, its expression and level of activation varies among the normal tissues and cells depending on their requirement of STAT3 for efficient functioning (Debnath et al., 2012).

In normal cells, activation of STAT3 signalling is a controlled and transient process which can last for half an hour to several hours before being inactivated by various mechanisms. Regulation of STAT3 by various mechanisms is briefly illustrated in Figure 2.3. Binding of cytokines or growth factors to their receptors causes activation of the receptor-associated tyrosine kinase known as Janus kinase (JAK). Upon activation, JAK *trans*-phosphorylates the intracellular domain of the receptor and thus provides the docking site for STAT3. Recruitment of STAT3 to the receptor causes phophorylation of its SH2 domain at a specific tyrosine residue (Tyr-705) by JAK (Lin et al., 2010). This mode of activation is known as JAK/STAT signaling. Phosphorylated STAT3 becomes activated and forms dimers before being translocated into the nucleus for transcriptional activity. Dephosphorylation of tyrosine by protein tyrosine phosphatase (PTP) leads to the inactivation of STAT3 (Muromoto et al., 2008). Upon

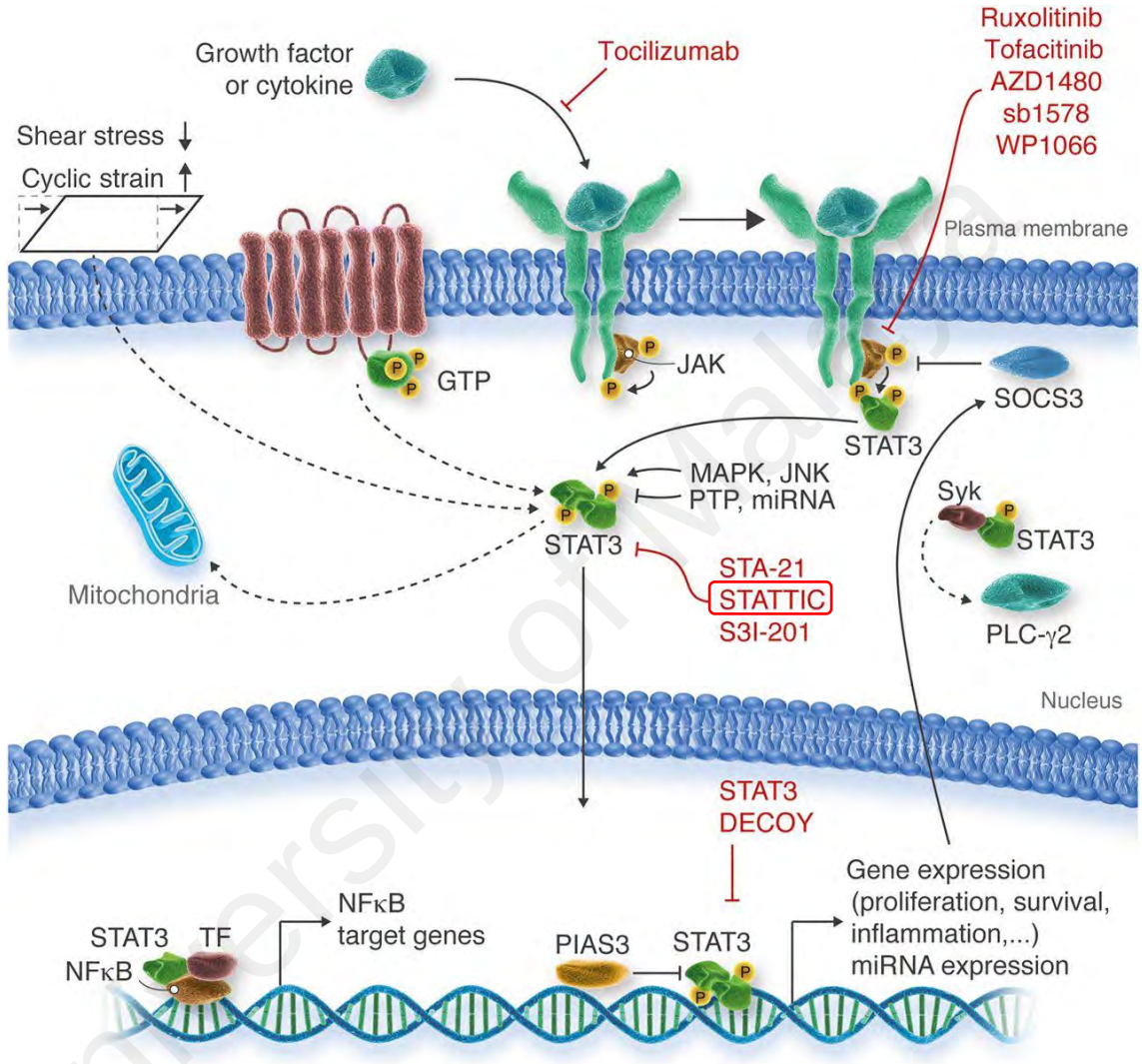

Figure 2.3. Schematic diagram showing the inhibition of STAT3 by regulatory mechanism and targeted therapy inhibitors. (Adapted from Dutzmann et al., 2015).

interaction to the JAK domains or the intracellular portions of the receptors (Naka et al., 1997), suppressors of cytokine signaling 3 (SOCS3) causes disruption or degradation of JAK, thus serves as a negative feedback mechanism of JAK/STAT signaling (Yoshikawa et al., 2001), which results in the reduction of STAT3 activation (Figure 2.3). On the other hand, protein inhibitor of activated STAT3 (PIAS3) that blocks the binding of STAT3 to DNA (Junicho et al., 2000; Shuai, 2000) at the interferon-gamma activated sequence (GAS) within the target gene promoters (Darnell et al., 1994; Junicho et al., 2000) leads to the inhibition of gene transcription activity of STAT3.

Dysregulation or abnormal activation of STAT3 may lead to malignancy as well as induction, development and survival of cancer (Lin et al., 2010). Being constitutively active in many human cancers (Lo et al., 2005; 2007; Alvarez et al., 2007; Abou-Ghazal et al., 2008; Ecker et al., 2008), STAT3 has been found excessively expressed in almost 70 % of the human solid and hematological tumors compared to the normal cells (Zhuang, 2013). STAT3 has been reported to induce cancers of breast (Clevenger, 2004; Ling & Arlinghaus, 2005), prostate (Qin et al., 2008), skin (Chan et al., 2004; Pedranzini et al., 2004) and head and neck (Geiger et al., 2016). Both *in vitro* (cultured cells) and *in vivo* (nude mice) studies have shown expression of mutated dimerizeable STAT3 (STAT3-C) can cause induction of oncogenesis (Bromberg et al., 1999).

Aberrant activity of the upstream signalling pathways is the major contributor of STAT3 abnormal activation in cancerous cells. High level of phosphorylated STAT3 (p-STAT3) is associated with tumor survival by promoting apoptotic resistance as well as facilitating rapid proliferation and tumorigenesis (Page et al., 2011). Due to its critical role in tumor progression and survival, inhibition of STAT3 might give some hope in cancer treatment and thus making it as an attractive molecular target for small molecule therapeutics.

2.3. Stattic: A direct STAT3 inhibitor

Since STAT3 has been known to be involved in the development of several cancers, disruption of its signaling may provide an alternative way in treating these cancers. This can be achieved through several inhibitory mechanisms, one of which involves direct STAT3 inhibition. Small-molecule compounds have been developed to inhibit STAT3 activity and function by targeting its SH2 domain. Since SH2 domain has three proximal binding sub-pockets (Kraskouskaya et al., 2013), inhibition of STAT3 can be accomplished through the binding of the compounds to at least two of these sub-pockets (Park & Li, 2011). One of such compounds is stattic (ST), a STAT3 inhibitory compound. Stattic, whose chemical structure is shown in Figure 2.4, selectively inhibits STAT3 dimerization by blocking the phosphorylation at the SH2 domain (Figure 2.3). An *in vitro* study has shown its ability to prevent the translocation of STAT3 into the nucleus (Kraskouskaya et al., 2013). In a recent communication (Zhang et al., 2015), it has been demonstrated that radioresistant esophageal squamous cell carcinoma (ESCC) both *in vitro* (cultured cell lines) and *in vivo* (xenografted nude mice) systems show an increase in radiosensitivity upon treatment with ST alone or along with radiation, thus suggesting ST treatment as a potential adjuvant therapy in radioresistant ESCC. Similarly, ability of ST to circumvent cisplatin resistance in ovarian cancer (Ji et al., 2013) has made it as an alternative therapy to be used in recurrent cancers displaying constitutively active STAT3.

Other than inhibiting SH2 domain of STAT3, this protein can also be inhibited directly by targeting STAT3 DNA-binding domain. Some of the inhibitors that can directly inhibit STAT3 both at the SH2 and DNA-binding domain are listed in Table 2.1. STAT3 activity can also be inhibited by other therapeutic inhibitors through upstream inhibition, as can be viewed in Figure 2.3.

A

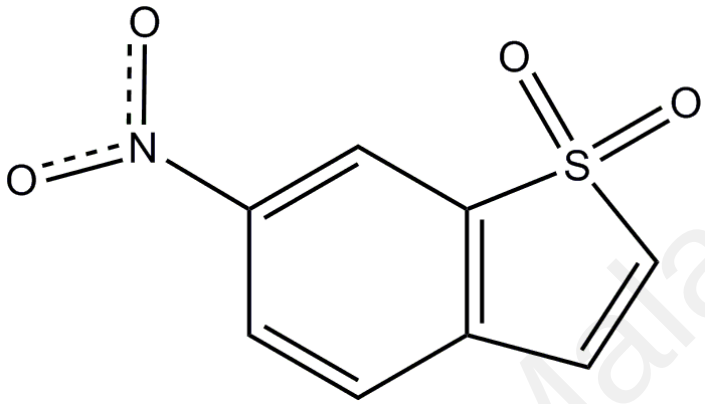

B

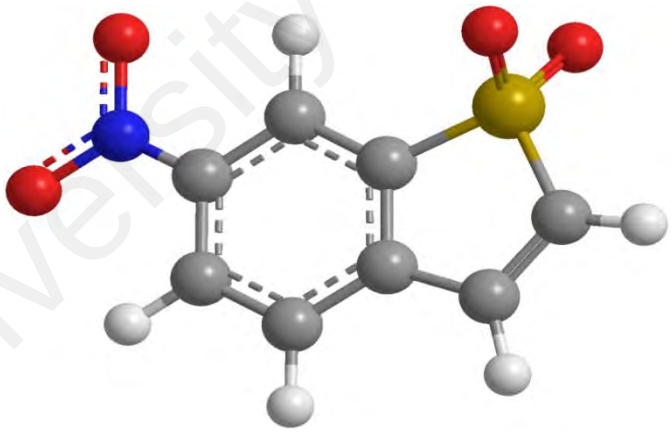

Figure 2.4. Chemical structure (A) and ball-and-stick model (B) of ST.

Table 2.1. Direct inhibition of STAT3 by various therapeutic inhibitors.

	Mechanism	Inhibitors	References
Direct STAT3 inhibitors	STAT3 SH2 domain inhibition	Stattic	(McMurray, 2006) (Ji et al., 2013) (Kraskouskaya et al., 2013)
		STA-21	(Song et al., 2005) (Chen et al., 2007)
		LLL-3 Imatinib	(Mencalha et al., 2010)
		LLL-12	(Lin et al., 2010)
		S31-201	(Siddiquee et al., 2007)
		SF-1-066	(Zhang et al., 2010)
		S31-1757	(Urlam et al., 2013) (Zhang et al., 2013)
	STAT3 DNA-binding domain inhibition	Platinum (IV) – CPA-1 – CPA-7 – Platinum (IV) tetrachloride	(Turkson et al., 2004b; 2005)
		– IS3-295	(Xiong et al., 2014)
		lnS3-54	(Huang et al., 2014)

2.4. Transportation of ST through blood plasma

Upon entering the bloodstream, numerous drugs bind to the plasma proteins in order to be carried to the target site. The interaction between the drug and its carrier protein affects the solubility, pharmacokinetics, pharmacodynamics, therapeutic potential as well as toxicity of the drug in the human system (Peters, 1996; Kragh-Hansen et al., 2002). Besides, protein-bound drugs are protected against metabolism from body's detoxification system (Lindup & Orme, 1981). Human serum albumin (HSA), being the most abundant (representing ~ 60 % of total plasma proteins) and major transporter in blood plasma binds to a large number of endogenous and exogenous compounds (Peters, 1996; Curry et al., 1998; Petitpas et al., 2001; Kragh-Hansen et al., 2002; Artali et al., 2005). Since the information regarding ST transportation, pharmacokinetics and bioavailability remain undefined, it is important to study the interaction between ST and HSA in order to predict its pharmacology and toxicity upon usage in cancer treatment and this will serve as a platform in ST drug design and production (Liu et al., 2007).

2.5 Human serum albumin (HSA)

Encoded by a single gene lying on the long arm of chromosome 4 near the centromere at position q11−22 (Mikkelsen et al., 1977; Harper & Dugaiczyk, 1983; Minghetti et al., 1986), human serum albumin (HSA) is synthesized in the liver. It is a monomeric multi-domain protein and belongs to a family of homologous proteins which has distinct structural features and ligand binding properties. Other members of this family include α-fetoprotein (AFP), afamin (AFM) and vitamin D binding protein (DBP) (Peters, 1996; Fasano et al., 2007).

2.5.1. Physicochemical properties of HSA

Table 2.2 lists a few important physicochemical properties of HSA. Based on the calculation from the amino acid composition, HSA has a molecular mass of 66, 438 Da (Minghetti et al., 1986) that match closely with the value of 66, 479 Da, obtained from the matrix-assisted laser desorption/ionization-time of flight (MALDI-TOF) mass spectrometry (Dockal et al., 1999). In 1992, He and Carter discovered the structure of HSA as a 3-D equilateral triangle with sides and a depth of 80 Å and 30 Å, respectively, based on the x-ray crystallographic results (He & Carter, 1992). From the frequency dispersion of the dielectric constant, an axial ratio of 3:1 was predicted for HSA (Scheider et al., 1976), while its radius of gyration was found to be 26.7 Å (Carter & Ho, 1994). The hydrodynamic parameters of HSA such as sedimentation coefficient and diffusion coefficient were determined to be 4.5 S and 6.1×10^{-7} cm^2 s^{-1}, respectively (Oncley et al., 1947). The values of frictional ratio (1.28:1) and intrinsic viscosity (0.046 dL g^{-1}) of HSA reflected its globular conformation (Oncley et al., 1947; Hunter, 1996). In native form, HSA has the isoelectric point of 4.7 (Peters, 1996) while the value increases to 5.8 for its fatty acid free form (Gianazza et al., 1984). The isoionic point of HSA has been reported as 5.16 (Hughes, 1954). This protein consists of predominant α-helical structure (67 %) with little β-form (10 %) and flexible regions (23 %) between subdomains (Carter & Ho, 1994). A net charge of −19 at the physiological pH (7.4) (Tanford, 1950) contributes to the high solubility of this protein in aqueous environment. At 280 nm, HSA exhibits a specific extinction coefficient of 5.3 (Wallevik, 1973) due to the presence of aromatic amino acid residues (Tyr and Trp).

2.5.2. Structural organization of HSA

As can be viewed from Figure 2.5, the primary structure of HSA is comprised of a single polypeptide chain of 585 amino acid residues. These amino acid residues form

Table 2.2. Physicochemical properties of HSA.

Property	Value	Reference
Molecular mass		
− Amino acid composition	66, 438 Da	(Minghetti et al., 1986)
− MALDI-TOF	66, 479 Da	(Dockal et al., 1999)
Overall dimension	80 × 80 × 30 Å	(He & Carter, 1992)
Axial ratio	3:1	(Scheider et al., 1976)
Radius of gyration	26.7 Å	(Carter & Ho, 1994)
Sedimentation coefficient, $S_{20,W}$	4.5 S	(Oncley et al., 1947)
Diffusion coefficient, $D_{20,W}$	6.1×10^{-7} cm^2 s^{-1}	(Oncley et al., 1947)
Partial specific volume, $\bar{v}_2$	0.733 cm^3 g^{-1}	(Hunter, 1966)
Frictional ratio, f/f$_0$	1.28:1	(Oncley et al., 1947)
Intrinsic viscosity, $[\eta]$	0.046 dL g^{-1}	(Hunter, 1966)
Isoelectic point		
− Native	4.7	(Peters, 1996)
− Defatted	5.8	(Gianazza et al., 1984)
Isoionic point	5.16	(Hughes, 1954)
α-helix	67 %	(Carter & Ho, 1994)
β-form	10 %	(Carter & Ho, 1994)
Net charge per molecule		
− at pH 7.4	−19	(Tanford, 1950)
− amino acid sequence	−15	(Peters, 1996)
$\varepsilon_{1\ cm}^{1\ \%}$ at 280 nm	5.3	(Wallevik, 1973)

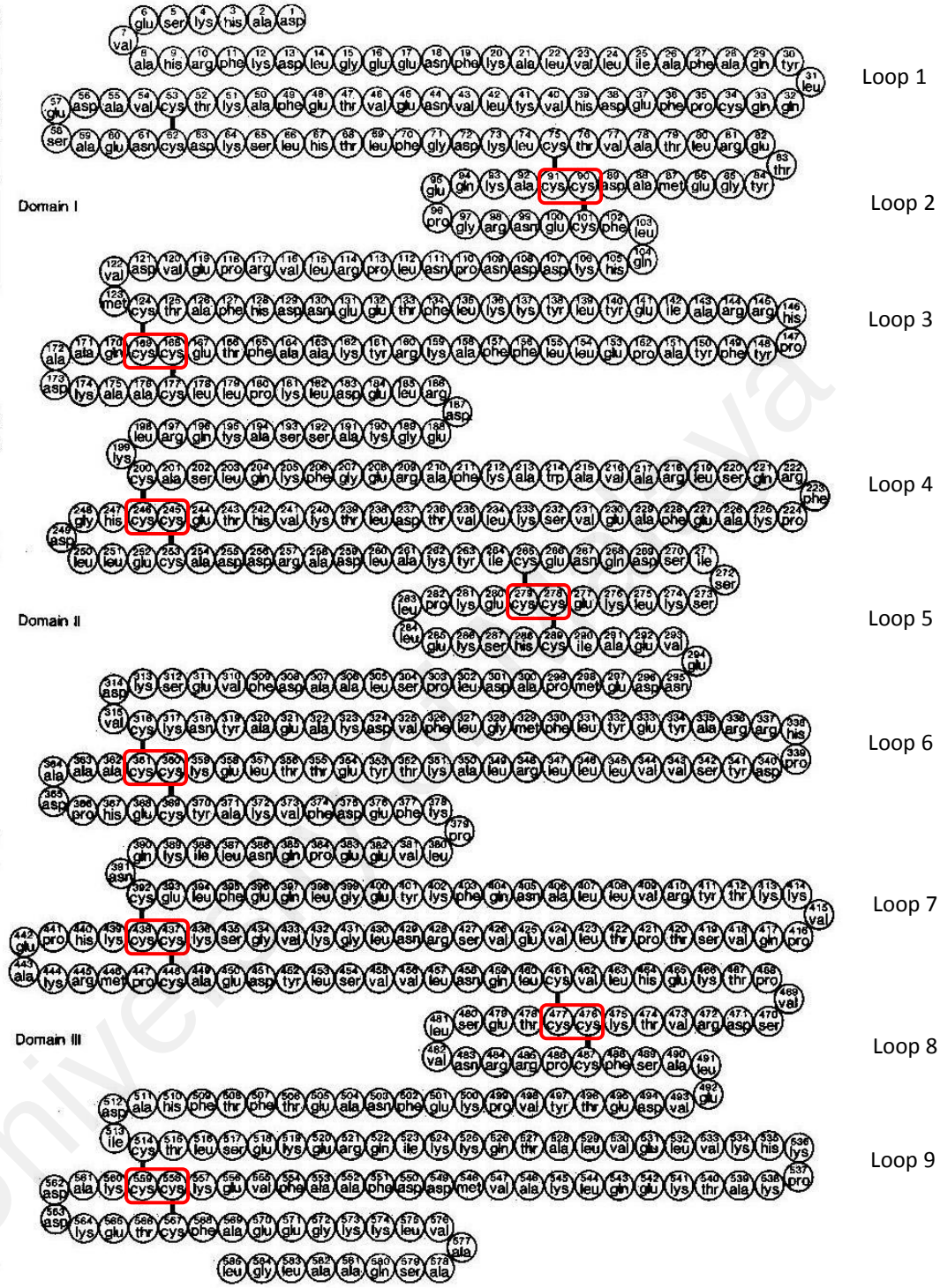

Figure 2.5. Amino acid sequence and disulfide bonding pattern of HSA. The red-colored box refers to the Cys-Cys pairs. (Adapted from Dugaiczyk et al., 1982).

nine loops, arranged in a distinct pattern with eight sequential Cys-Cys pairs (Figure 2.5) and are linked together by 17 disulphide bridges (Figures 2.5 and 2.6). These loops are further grouped into three homologous domains, where each domain is made from triplets of long-short-long loops. These domains are named as domain I, domain II and domain III, which consist of amino acid residues from 1−195, 196−383 and 384−585, respectively. These domains are further divided into subdomains 'A' and 'B', characterized by the presence of the first two loops within each domain, *viz.* 1−2, 4−5 and 7−8 as subdomains IA, IIA and IIIA, respectively; whereas loops 3, 6 and 9 form subdomains IB, IIB and IIIB, respectively (Figure 2.6). These two subdomains, 'A' and 'B' possess six and four α-helices, respectively and the patterns of helices h1−h4 in both subdomains are identical. The extra two short helices in subdomain A, *i.e.* h5 and h6 are antiparallel to each other (Figure 2.6). These helices are connected by the 17 disulfide bridges that are made up from 34 out of 35 cysteine residues present in HSA. The three-dimensional (heart-shaped) structure of HSA, showing different subdomains is illustrated in Figure 2.7.

2.5.3. Functions of HSA

HSA plays an important role in many physiological processes such as regulation of the colloid osmotic pressure (Quinlan et al., 2005), maintainance of blood pH (Figge et al., 1991) and transport of various ligands (Peters, 1996; Curry et al., 1998; Petitpas et al., 2001; Kragh-Hansen et al., 2002; Artali et al., 2005). Besides, it also possesses esterase activity (Dubois-Presle et al., 1995) and acts as an anti-oxidant through its binding to the free copper (Cu^{2+}) ions, thus preventing the production of free radicals (Evans, 2002). HSA acts as a solubilizing agent for the ligands with low aqueous solubility such as fatty acids, amino acids and steroid compounds, which become soluble upon binding to it. It also transports ions including zinc, copper, calcium, iron

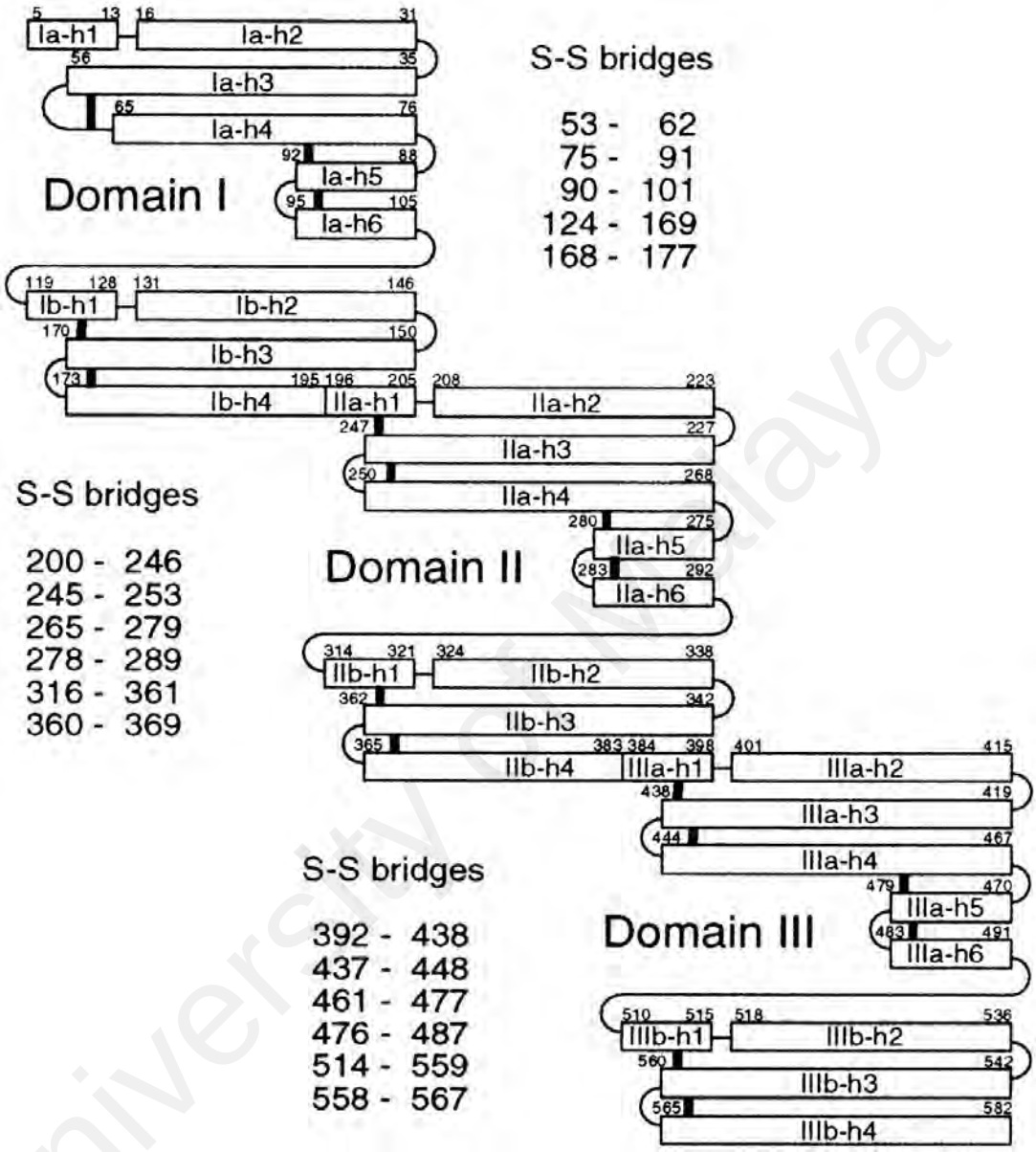

Figure 2.6. Diagram showing helices and disulfide bridges of HSA. Helices are represented by rectangles, and loops and turns by thin lines. Disulfide bridges are drawn with thick lines. (Adapted from Sugio et al., 1999).

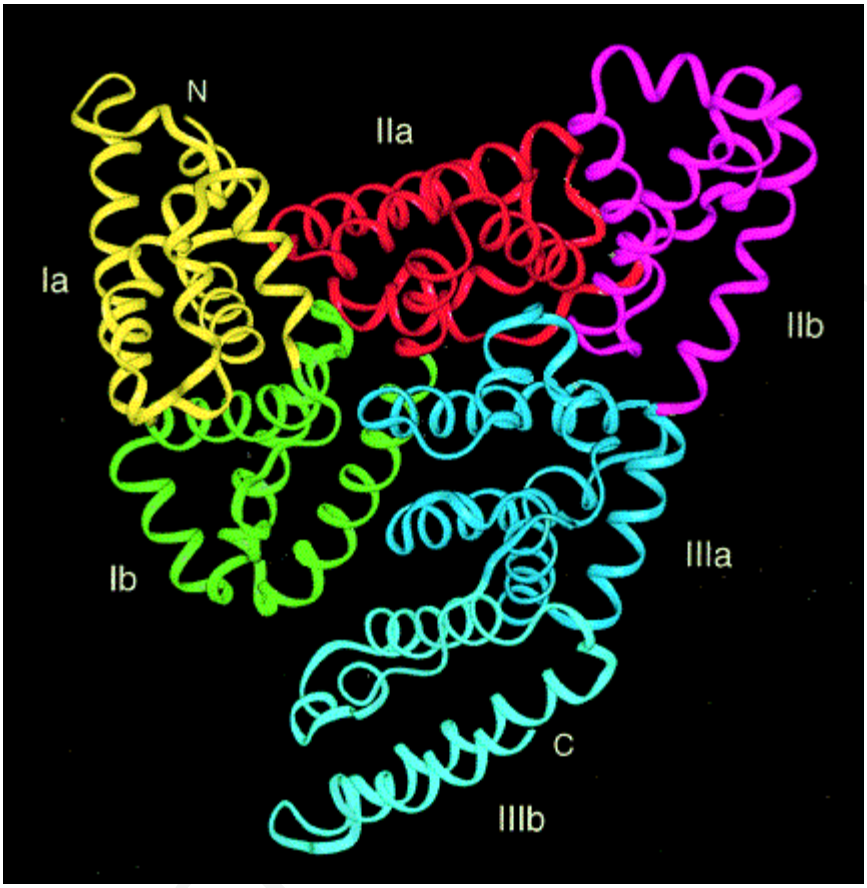

Figure 2.7. Three-dimensional structure of HSA. Each subdomain is marked with a different color as follows: IA, yellow; IB, green; IIA, red; IIB, purple; IIIA, blue and IIIB, cyan. The N- and C-termini are marked as N and C, respectively. (Adapted from Sugio et al., 1999).

and chloride through the circulatory system (Peters, 1996) and acts as an important depot protein for nitric oxide, a key signaling molecule (Stamler et al., 1992). Transportation of bilirubin to the liver for detoxification by HSA has made this protein as a toxic waste carrier (Knudsen et al., 1986). Other than binding to endogenous ligands, HSA also binds to exogenous molecules such as drugs (Peters, 1996; Kragh-Hansen et al., 2002) and potential toxic compounds (Tunç et al., 2014; Zhang et al., 2013).

2.5.4. Ligand binding and binding sites of HSA

In 1975, a fluorescent probe displacement study had identified two specific ligand binding sites, namely, site I and site II, on HSA (Sudlow et al., 1975). Through peptic and tryptic digestion results, locations of these binding sites were identified in domains II and III, respectively (Sudlow et al., 1975; Bos et al., 1988). Crystallographic studies further characterized the location of site I in subdomain IIA and site II in subdomain IIIA (Carter & Ho, 1994; Curry et al., 1998; Sugio et al., 1999). Majority of the ligands have been reported to bind reversibly to either of these binding sites (Peters, 1996; Curry et al., 1998) with an association constant ranging between 10^4 to 10^6 M^{-1} (Carter & Ho, 1994; Kragh-Hansen et al., 2002). A few of the ligands that bind to site I and site II of HSA are shown in Figure 2.8. A brief description of these sites is given below.

2.5.4.1. Site I

Site I consists of two nonpolar clusters together with a pair of centrally-located polar residues, formed by Tyr-150, His-242 and Arg-257 (at the bottom) along with Lys-195, Lys-199, Arg-218 and Arg-222 at the entrance of the pocket (Ghuman et al., 2005). Due to its large and flexible binding region, site I can bind to various ligands including large size molecules (*e.g.* bilirubin) and able to accommodate more than one

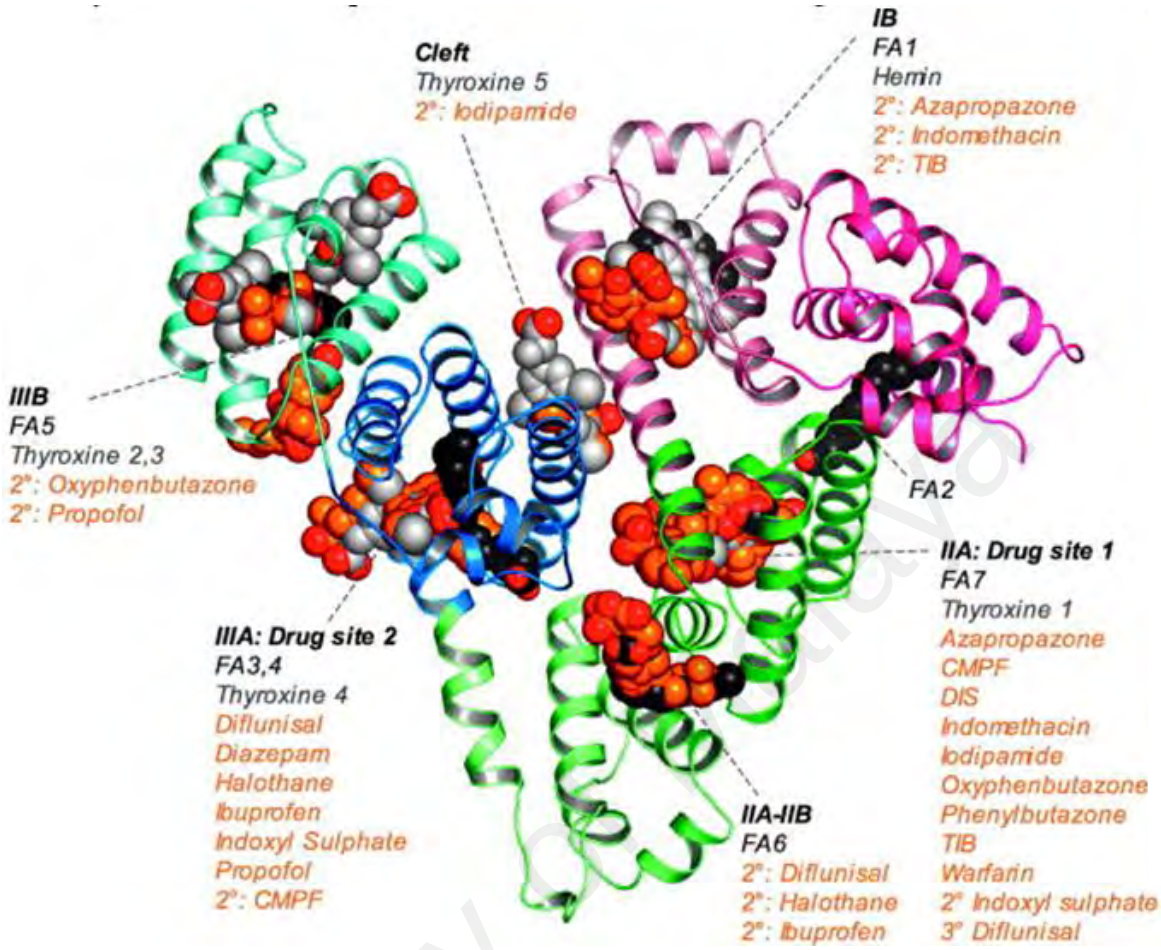

Figure 2.8. Diagram showing ligand binding sites of HSA. Individual subdomains are colored differently and ligands are depicted as space-filling models. Oxygen atoms are colored red. All other atoms in fatty acids, other endogenous ligands (hemin and thyroxine) and drugs are colored black, grey and orange, respectively. (Adapted from Ghuman et al., 2005).

ligands at the same time (Kragh-Hansen et al., 1988). Generally, ligands that bind to this site with high affinity are classified as dicarboxylic acids or negatively charged bulky heterocyclic molecules (Kragh-Hansen et al., 2002). In terms of its structural make-up, site I has been reported to possess two overlapping binding sites based on its mutual interaction between warfarin and azapropazone, with the presence of lone Trp residue (Trp-214), situated in the non-overlapping region of the warfarin site (Fehske et al., 1982). However, different studies have proposed the existence of two independent binding regions within site I (Kragh-Hansen et al., 1985; 1988), while Yamasaki and his colleges (Yamasaki et al., 1996) suggested the presence of three binding regions within this site, *i.e.* Ia, Ib and Ic for the binding of warfarin, azapropazone and butamben, respectively.

2.5.4.2. Site II

Nonpolar nature of site II is characterized by the lining of the pocket by hydrophobic side chains while presence of a single dominant polar patch that centered around Tyr-411 and Arg-410 near the entrance creates the polar environment of this site. Due to both polar and apolar features of site II, most of the ligands that bind to this site are typically aromatic carboxylic acids with a negatively charged group at one end of the molecule facing away from the hydrophobic center (Kragh-Hansen et al., 2002). Unlike site I, site II does not possess any overlapping binding sites and large molecules rarely bind to this locus due to the smaller and narrower size of this site (Kragh-Hansen et al., 2002). Site II is also less flexible and the binding of a ligand is usually influenced by stereoselectivity, as evident by the stronger binding affinity of L-Trp (~100 times higher) compared to its D-isomer (Kragh-Hansen et al., 2002). In addition, slight modification of the ligands (substitution with a small group) may affect their binding, as revealed by the inability of the fluorinated diazepam to bind to site II, which is well known as the preferred binding site of diazepam (Chuang & Otagiri, 2001).

2.6. Mammalian serum albumins

Animal models have been widely used in modern biomedical research since early of the 20th century (Ericsson et al., 2013) in order to predict the pharmacological and toxicological effects of drugs before being tested on human subjects. However, the conclusion drawn are only valid for the interspecies that closely match with the human system in terms of ligand metabolism, physiology, absorption and distribution (Martinez, 2011). Animals that have close phylogenetic relationship or anatomically similar to human and possess similar biochemical and physiological response throughout the investigation are usually selected as a suitable animal models (Simon & Maibach, 2000).

The pharmacological effect of ST in human system can also be predicted based on animal model. Through a comparative study using serum albumins of five different mammalian species, *i.e.* HSA, BSA, SSA, PSA, and RbSA, those showing similarity to HSA in terms of ST binding characteristics can be selected as suitable animal model(s) for preclinical testing. These mammalian serum albumins were used due to their similar characteristics in relation to HSA. BSA, SSA and PSA are composed of 583 amino acid residues while HSA and RbSA possess 585 and 584 amino acid residues, respectively. As shown in Table 2.3, these albumins have high content of cysteine and charged amino acids but low amount of tryptophan, glycine and methionine (Brown & Shockley, 1982; Peters, 1985). Due to the high percentage of total charged residues and the presence of 17 disulfide bridges, these albumins show similar solubility and stability characteristics. Whereas these albumins possess a single Trp residue located in loop 4, BSA, PSA and SSA are characterized by the presence of an additional Trp residue in a homologous site in loop 3 (Peters, 1996). A comparison of the complete amino acid sequences of these proteins (Figure 2.9, Table 2.4) shows a high degree of similarity among them in terms of both amino acid sequence (72−92 %) and molecular weight (66, 015 − 66, 798 Da)

Table 2.3. Amino acid compositions of different mammalian albumins.

Amino acid	No. of residues				
	Human[a]	Bovine[a]	Sheep[b]	Porcine[c]	Rabbit[d]
Alanine	62	46	50	50	54
Arginine	24	23	22	26	22
Asparagine	17	14	14	13	12
Aspartic acid	36	40	44	37	43
Cysteine	35	35	35	35	35
Glutamic acid	62	59	56	61	56
Glutamine	20	20	19	20	14
Glycine	12	16	17	16	20
Histidine	16	17	18	18	23
Isoleucine	8	14	13	23	16
Leucine	61	61	61	62	62
Lysine	59	59	60	57	57
Methionine	6	4	4	-	1
Phenylalanine	31	27	28	29	24
Proline	24	28	28	30	29
Serine	24	28	25	23	26
Threonine	28	34	31	26	27
Tryptophan	1	2	2	2	1
Tyrosine	18	20	20	22	24
Valine	41	36	36	33	38
Total	**585**	**583**	**583**	**583**	**584**

Taken from:

[a] (Peters, 1996)

[b] (Brown et al., 1989)

[c] NCBI PDB Accession No. NP_001075813

[d] (Weinstock & Baldwin, 1988)

	1 10	20	30	40	50
Human[a]	DAHKSEVAHR	FKDLGEENFK	ALVLIAFAQY	LQQCPFEDHV	KLVNEVTEFA
Bovine[b]	DTHKSEIAHR	FKDLGEEHFK	GLVLIAFSQY	LQQCPFDEHV	KLVNELTEFA
Sheep[c]	DTHKSEIAHR	FNDLGEENFQ	GLVLIAFSQY	LQQCPFDEHV	KLVKELTEFA
Porcine[d]	DTYKSEIAHR	FKDLGEQYFK	GLVLIAFSQH	LQQCPYEEHV	KLVREVTEFA
Rabbit[e]	EAHKSEIAHR	FNDVGEEHFI	GLVLITFSQY	LQKCPYEEHA	KLVKEVTDLA

	60	70	80	90	100
Human	KTCVADESAE	NCDKSLHTLF	GDKLCTVATL	RETYGEMADC	CAKQEPERNE
Bovine	KTCVADESHA	GCEKSLHTLF	GDELCKVASL	RETYGDMADC	CEKQEPERNE
Sheep	KTCVADESHA	GCDKSLHTLF	GDELCKVATL	RETYGDMADC	CEKQEPERNE
Porcine	KTCVADESAE	NCDKSIHTLF	GDKLCAIPSL	REHYGDLADC	CEKEEPERNE
Rabbit	KACVADESAA	NCDKSLHDIF	GDKICALPSL	RDTYGDVADC	CEKKEPERNE

	110	120	130	140	150
Human	CFLQHKDDNP	NLPRLVRPEV	DVMCTAFHDN	EETFLKKYLY	EIARRHPYFY
Bovine	CFLSHKDDSP	DLPKL-KPDP	NTLCDEFKAD	EKKFWGKYLY	EIARRHPYFY
Sheep	CFLNHKDDSP	DLPKL-KPEP	DTLCAEFKAD	EKKFWGKYLY	EVARRHPYFY
Porcine	CFLQHKNDNP	DIPKL-KPDP	VALCADFQED	EQKFWGKYLY	EIARRHPYFY
Rabbit	CFLHHKDDKP	DLPPFARPEA	DVLCKAFHDD	EKAFFGHYLY	EVARRHPYFY

	160	170	180	190	200
Human	APELLFFAKR	YKAAFTECCQ	AADKAACLLP	KLDELRDEGK	ASSAKQRLKC
Bovine	APELLYYANK	YNGVFQECCQ	AEDKGACLLP	KIETMREKVL	ASSARQRLRC
Sheep	APELLYYANK	YNGVFQECCQ	AEDKGACLLP	KIDAMREKVL	ASSARQRLRC
Porcine	APELLYYAII	YKDVFSECCQ	AADKAACLLP	KIEHLREKVL	TSAAKQRLKC
Rabbit	APELLYYAQK	YKAILTECCE	AADKGACLTP	KLDALEGKSL	ISAAQERLRC

	210	220	230	240	250
Human	ASLQKFGERA	FKAWAVARLS	QRFPKAEFAE	VSKLVTDLTK	VHTECCHGDL
Bovine	ASIQKFGERA	LKAWSVARLS	QKFPKAEFVE	VTKLVTDLTK	VHKECCHGDL
Sheep	ASIQKFGERA	LKAWSVARLS	QKFPKADFTD	VTKIVTDLTK	VHKECCHGDL
Porcine	ASIQKFGERA	FKAWSLARLS	QRFPKADFTE	ISKIVTDLAK	VHKECCHGDL
Rabbit	ASIQKFGDRA	YKAWALVRLS	QRFPKADFTD	ISKIVTDLTK	VHKECCHGDL

	260	270	280	290	300
Human	LECADDRADL	AKYICENQDS	ISSKLKECCE	KPLLEKSHCI	AEVENDEMPA
Bovine	LECADDRADL	AKYICDNQDT	ISSKLKECCD	KPLLEKSHCI	AEVEKDAIPE
Sheep	LECADDRADL	AKYICDHQDA	LSSKLKECCD	KPVLEKSHCI	AEVDKDAVPE
Porcine	LECADDRADL	AKYICENQDT	ISTKLKECCD	KPLLEKSHCI	AEAKRDELPA
Rabbit	LECADDRADL	AKYMCEHQET	ISSHLKECCD	KPILEKAHCI	YGLHNDETPA

	310	320	330	340	350
Human	DLPSLAADFV	ESKDVCKNYA	EAKDVFLGMF	LYEYARRHPD	YSVVLLLRLA
Bovine	NLPPLTADFA	EDKDVCKNYQ	EAKDAFLGSF	LYEYSRRHPE	YAVSVLLRLA
Sheep	NLPPLTADFA	EDKEVCKNYQ	EAKDVFLGSF	LYEYSRRHPE	YAVSVLLRLA
Porcine	DLNPLEHDFV	EDKEVCKNYK	EAKDVFLGTF	LYEYSRRHPD	YSVSLLLRIA
Rabbit	GLPAVAEEFV	EDKDVCKNYE	EAKDLFLGKF	LYEYSRRHPD	YSVVLLLRLG

Cont...

	360	370	380	390	400
Human	KTYETTLEKC	CAAADPHECY	AKVFDEFKPL	VEEPQNLIKQ	NCELFKQLGE
Bovine	KEYEATLEEC	CAKDDPHACY	STVFDKLKHL	VDEPQNLIKQ	NCDQFEKLGE
Sheep	KEYEATLEDC	CAKEDPHACY	ATVFDKLKHL	VDEPQNLIKK	NCELFEKHGE
Porcine	KIYEATLEDC	CAKEDPPACY	ATVFDKFQPL	VDEPKNLIKQ	NCELFEKLGE
Rabbit	KAYEATLKKC	CATDDPHACY	AKVLDEFQPL	VDEPKNLVKQ	NCELYEQLGD

	410	420	430	440	450
Human	YKFQNALLVR	YTKKVPQVST	PTLVEVSRNL	GKVGSKCCKH	PEAKRMPCAE
Bovine	YGFQNALIVR	YTRKVPQVST	PTLVEVSRSL	GKVGTRCCTK	PESERMPCTE
Sheep	YGFQNALIVR	YTRKAPQVST	PTLVEISRSL	GKVGTKCCAK	PESERMPCTE
Porcine	YGFQNALIVR	YTKKVPQVST	PTLVEVARKL	GLVGSRCCKR	PEEERLSCAE
Rabbit	YNFQNALLVR	YTKKVPQVST	PTLVEISRSL	GKVGSKCCKH	PEAERLPCVE

	460	470	480	490	500
Human	DYLSVVLNQL	CVLHEKTPVS	DRVTKCCTES	LVNRRPCFSA	LEVDETYVPK
Bovine	DYLSLILNRL	CVLHEKTPVS	EKVTKCCTES	LVNRRPCFSA	LTPDETYVPK
Sheep	DYLSLILNRL	CVLHEKTPVS	EKVTKCCTES	LVNRRPCFSD	LTLDETYVPK
Porcine	DYLSLVLNRL	CVLHEKTPVS	EKVTKCCTES	LVNRRPCFSA	LTPDETYKPK
Rabbit	DYLSVVLNRL	CVLHEKTPVS	EKVTKCCSES	LVDRRPCFSA	LGPDETYVPK

	510	520	530	540	550
Human	EFNAETFTFH	ADICTLSEKE	RQIKKQTALV	ELVKHKPKAT	KEQLKAVMDD
Bovine	AFDEKLFTFH	ADICTLPDTE	KQIKKQTALV	ELLKHKPKAT	EEQLKTVMEN
Sheep	PFDEKFFTFH	ADICTLPDTE	KQIKKQTALV	ELLKHKPKAT	DEQLKTVMEN
Porcine	EFVEGTFTFH	ADLCTLPEDE	KQIKKQTALV	ELLKHKPHAT	EEQLRTVLGN
Rabbit	EFNAETFTFH	ADICTLPETE	RKIKKQTALV	ELVKHKPHAT	NDQLKTVVGE

	560	570	580	585
Human	FAAFVEKCCK	ADDKETCFAE	EGKKLVAASQ	AALGL
Bovine	FVAFVDKCCA	ADDKEACFAV	EGPKLVVSTQ	TALA
Sheep	FVAFVDKCCA	ADDKEGCFVL	EGPKLVASTQ	AALA
Porcine	FAAFVQKCCA	APDHEACFAV	EGPKFVIEIR	GILA
Rabbit	FTALLDKCCS	AEDKEACFAV	EGPKLVESSK	ATLG

Figure 2.9. Amino acid sequences of different mammalian albumins. Positions of identical residues in the amino acid sequences are shown in red color.

Taken from:

[a] (Minghetti et al., 1986)

[b] EMBL Accession No. M73993

[c] (Brown et al., 1989)

[d] (Weinstock & Baldwin, 1988)

[e] NCBI PDB Accession No. NP_001075813

Table 2.4. Molecular weight and sequence similarity score of different mammalian serum albumins.

Organism	MW (Da)	Protein sequence similarity score*				
		Human	Bovine	Porcine	Rabbit	Sheep
Human	66 472	1	0.77	0.77	0.75	0.76
Bovine	66 433		1	0.80	0.72	0.92
Porcine	66 798			1	0.75	0.78
Rabbit	66 015				1	0.73
Sheep	66 328					1

*(Huang & Miller, 1991)

(Adapted from Michaud et al., 2009). Copyright Wiley-VCI. (Reproduced with permission).

(Michaud et al., 2009). Although these albumins show similarities in several characteristics, many other species-specific factors may influence their performance *in vivo*.

Chapter 3

MATERIALS AND METHODS

3. MATERIALS AND METHODS

3.1. Materials

3.1.1. Proteins

Human serum albumin (HSA), essentially fatty acid-free (Lot 068K7538V) as well as other mammalian serum albumins, *viz*. bovine serum albumin (BSA) (Lot 011M7406V); rabbit serum albumin (RbSA) (Lot 104K7560); sheep serum albumin (SSA) (Lot 117K7540) and porcine serum albumin (PSA) (Lot 084K7636) were purchased from Sigma-Aldrich Co., USA. The purity of these proteins was 96–99 %. These proteins were used as such without further purification.

3.1.2. Drug

Stattic (ST) (Empirical formula: $C_8H_5NO_4S$, Molecular weight: 211.19) was supplied by Sigma-Aldrich Co., USA

3.1.3. Reagents used in drug displacement studies

Warfarin (WFN) (Lot 104K1261) and 1-anilinonaphthalene-8-sulfonate (ANS) (Lot 104K2510) were procured from Sigma-Aldrich Co., USA. Diazepam (DZM) (Lot 107.1B0.2) was the product of Lipomed AG, Switzerland.

3.1.4. Miscellaneous

Analytical grade samples of sodium dihydrogen phosphate, *di*-sodium hydrogen phosphate were obtained from SYSTERM®, Malaysia. Standard buffers of pH 7.0 and pH 10.0 were supplied by Sigma-Aldrich Co., USA. Analytical grade dimethyl sulphoxide (DMSO) and polyvinylidene fluoride (PVDF) membrane filters (0.45 μm pore size) were purchased from Merck Millipore, Germany. Cellulose nitrate membrane filters (0.45 μm pore size) were supplied by Whatman®, England.

All-glass distilled water or ultrapure (Type 1) water produced by Milli-Q Water Purification System (Merck Millipore, Germany) was used throughout this study. All experiments were performed at 25 °C unless otherwise stated.

3.2. Methods

3.2.1 pH measurements

Measurements of pH of different solutions were made on a delta 320 pH meter (Mettler-Toledo GmbH, Switzerland), attached with a HA405-K2/120 combination electrode. Standard buffers of pH 7.0 and pH 10.0 were used to calibrate the pH meter for pH measurements in the neutral and alkaline pH ranges, respectively. The least count of the pH meter was 0.01 pH unit.

3.2.2. Preparation of protein solutions

Sodium phosphate buffer (60 mM, pH 7.4) was used to prepare all working solutions throughout this study. The protein stock solutions were prepared in the above buffer, filtered through PVDF membrane filters and their concentrations were determined spectrophotometrically, using molar absorption coefficients of 36,500 M^{-1} cm^{-1} for HSA (Painter et al., 1998), 43,827 M^{-1} cm^{-1} for BSA, 43,385 M^{-1} cm^{-1} for both RbSA and PSA and 42,925 M^{-1} cm^{-1} for SSA, at 280 nm (Khan et al., 2013). These protein stock solutions were stored at 4 °C and were used within a week.

3.2.3. Preparation of ligand solutions

To prepare the stock solutions of DZM and ST, 10 mg of their crystals were dissolved in 10 mL DMSO and were diluted with the buffer to obtain the desired concentrations for the working solutions.

For the preparation of WFN stock solution, a few crystals of it were dissolved in 10 mL DMSO, diluted to the desired concentration with the buffer and its concentration was determined spectrophotometrically, using a molar absorption coefficient of 13,610 M^{-1} cm^{-1} at 310 nm (Twine et al., 2003).

The stock solution of ANS was prepared by dissolving a few of its crystals in desired volume of the buffer and a molar absorption coefficient of 5,000 M^{-1} cm^{-1} at 350 nm was used to determine its concentration (Mulqueen & Kronman, 1982).

3.2.4. Fluorescence measurements

Fluorescence intensity of protein solutions was measured on a Jasco FP-6500 spectrofluorometer (Jasco International Co., Japan), using a 1 cm path length quartz cuvette, positioned in a thermostatically-controlled cell holder. The fluorescence spectra were collected in the wavelength range, 310–400 nm, using an excitation wavelength (λ_{ex}) of 295 nm. Both excitation and emission bandwidths were set at 10 nm, while the response time, scanning rate and the detector voltage were fixed at 1 s, 500 nm min^{-1} and 240 V, respectively.

Three-dimensional (3-D) fluorescence spectra of HSA (3 μM) solutions in free form as well as in the presence of ST (ST: HSA molar ratio of 5:1 and 10:1) were executed under the following conditions: excitation wavelength range, 220–360 nm with data interval of 5 nm; emission wavelength range, 220–500 nm with data interval of 1 nm. Rest of the parameters were maintained as described above.

3.2.5. Absorption measurements

PerkinElmer Lambda 25 UV/VIS double-beam spectrometer (PerkinElmer Inc., USA) was used for absorption measurements, using quartz cells of 1 cm path length. Absorbance values of the protein and the drug solutions at respective wavelengths were

measured against suitable blanks, prepared in the same way but without the protein or the drug.

3.2.6. Circular dichroism measurements

Circular dichroism (CD) spectra were recorded on a Jasco J-815 spectropolarimeter (Jasco International Co., Japan), equipped with a cell holder attached to a water bath. The far-UV (200−250 nm) CD spectra were recorded using the protein solution (1 μM HSA) in a 1 mm path length cuvette while near-UV (250−300 nm) CD spectral measurements were made by using a protein concentration and cuvette path length of 10 μM and 10 mm, respectively. The CD spectra were measured as an average of 4 scans, using a scan speed of 100 nm min^{-1} and a response time of 1 s.

3.2.7. ST-HSA interaction

The interaction between ST and HSA was studied using fluorescence quenching titration method as described earlier (Feroz et al., 2015).

3.2.7.1. Fluorescence quenching titration

A fixed concentration (3 μM) of HSA was titrated with increasing concentrations (3−45 μM with 3 μM intervals) of ST by adding increasing volumes (0.09−1.35 mL) of the stock ST solution (100 μM) to a fixed volume of (0.3 mL) of the stock protein solution (30 μM) taken in different tubes. The total volume in each tube was made to 3.0 mL by adding respective volumes of the buffer and the tubes were shaken well. After incubation for 1 h at 25 °C for equilibrium attainment, the fluorescence spectra were recorded in the wavelength range, 310−400 nm, using λ_{ex} = 295 nm.

The titration was also performed at two other temperatures (15 and 45 °C) in the same way except that 1 h incubation was made at respective temperature and the

fluorescence spectra were recorded after 6 min of equilibration at these temperatures in the cuvette (Feroz et al., 2015).

3.2.7.2. Data analysis

Inner filter effect correction

The fluorescence spectra were subjected to the inner filter effect correction due to absorption of the fluorescence light and reabsorption of the emitted light by the ligand, according the following equation (Lakowicz, 2006):

$$F_{cor} = F_{obs}\, 10^{(A_{ex}+A_{em}/2)} \quad (1)$$

where F_{cor} and F_{obs} are the corrected and the observed fluorescence intensity values, respectively. A_{ex} and A_{em} refer to the difference in the absorbance values of the protein samples at the excitation and emission wavelengths, respectively, upon addition of ST. The corrected values of the fluorescence intensity were transformed into relative fluorescence intensity (Relative FI) by taking the fluorescence intensity of the protein in the absence of ST as 100.

Quenching and binding parameters

In order to analyze the quenching mechanism involved in the ST-HSA system, fluorescence data at three different temperatures were treated according to the Stern-Volmer equation (Lakowicz, 2006):

$$F_0/F = K_{sv}[Q] + 1 = k_q\tau_0[Q] + 1 \quad (2)$$

where F_0 and F are the fluorescence intensity values in the absence and the presence of the quencher, respectively; K_{sv} is the Stern-Volmer constant; $[Q]$ is the concentration of the quencher; k_q is the bimolecular quenching constant and τ_0 is the fluorophore lifetime of HSA in the absence of quencher. Values of K_{sv} were obtained from the slope of the

plots between F_0/F and [Q], while k_q values were calculated by substituting the value of τ_0 as 6.38×10^{-9} s for HSA (Abou-Zied & Al-Shihi, 2008) in the following equation:

$$k_q = K_{sv}/\tau_0 \quad (3)$$

The following equation was employed to obtain the values of the association constant, K_a for ST-HSA interaction at three different temperatures (Bi et al., 2004):

$$\log (F_0 - F)/F = n \log K_a - n \log [1/([L_T]-(F_0-F)[P_T]/F_0)] \quad (4)$$

where n is the Hill coefficient, while $[L_T]$ and $[P_T]$ represent the total ligand and total protein concentrations, respectively.

Thermodynamic parameters

The thermodynamic parameters, *viz.* enthalpy change (ΔH) and entropy change (ΔS) of ST-HSA interaction were determined by treating the fluorescence quenching data according to the van't Hoff equation (Wallevik, 1973):

$$\ln K_a = -\Delta H/RT + \Delta S/R \quad (5)$$

where T is the absolute temperature (273 + ___°C) and R is the gas constant (8.3145 J mol^{-1} K^{-1}). Values of ΔH and ΔS were obtained from the slope and the intercept, respectively of the van't Hoff plot between ln K_a and $1/T$.

The Gibbs energy change of the reaction, ΔG was calculated by substituting the values of ΔH and ΔS into the following equation:

$$\Delta G = \Delta H - T\Delta S \quad (6)$$

3.2.8. Thermal stability studies

Thermal stability of HSA was studied both in the absence and the presence of ST, using fluorescence spectroscopy. Prior to the fluorescence measurements, ST-HSA

mixtures in different molar ratios (5:1, 10:1 and 15:1) were incubated at 25 °C for 1 h. Values of the fluorescence intensity of HSA (3 μM) and ST-HSA mixtures were recorded at 343 nm at different temperatures between 25 and 80 °C with 5 °C increment, after an equilibration time of 6 min at each temperature. The data were presented as relative fluorescence intensity at 343 nm ($RFI_{343\ nm}$) against temperature by taking the value of $RFI_{343\ nm}$ as 100 at 25 °C.

3.2.9. Ligand displacement studies

Competitive ligand displacement experiments were performed to allocate ST binding site on HSA, using site-specific markers, WFN and DZM for site I and site II, respectively. Mixtures of 1:1 WFN / DZM and HSA (3 μM each), pre-incubated at 25 °C for 1 h were titrated with increasing ST concentrations (0−45 μM with 3 μM intervals). Whereas, WFN-HSA fluorescence spectra (360−480 nm) were recorded using an excitation wavelength of 335 nm, fluorescence spectra for DZM-HSA mixtures were studied in the wavelength range, 310−400 nm, upon excitation at 295 nm.

ANS displacement experiments were also performed in two different sets to confirm ST binding site on HSA. In the first set of experiments, HSA (3 μM) was titrated with increasing concentrations (0−45 μM with 3 μM intervals) of ST / ANS and the fluorescence spectra (310−400 nm) were recorded after 1 h incubation at 25 °C, using an excitation wavelength of 295 nm. Alternatively, ANS-HSA (1:1) mixture (pre-incubated for 1 h at 25 °C) was titrated with increasing ST concentrations (0−45 μM with 3 μM intervals) and the ANS fluorescence spectra (400−600 nm) were recorded after additional 1 h incubation at 25 °C, using 370 nm as an excitation wavelength.

3.2.10. Computational studies

The structure of ST was constructed and geometry was optimized with MMFF94 force field (Halgren, 1996) using Avogadro Software (Hanwell et al., 2012) and exported as a mol2 file. Docking, visualization and rendering simulation were performed using AutoDock 4.2 (Goodsell et al., 1996) and AutoDockTools 1.5.6 (Sanner, 1999) at the Academic Grid Malaysia Infrastructure. The crystal structure of HSA (PDB code 1BM0, 2.5 Å resolution) was downloaded from the Protein Data Bank (Berman et al., 2000). Water molecules were removed and the atomic coordinates of chain A of 1BM0 were stored in a separate file and used as input for AutoDockTools, where polar hydrogens, Kollman charges and solvation parameters were added. In the case of the ligand (ST), nonpolar hydrogens were merged and rotatable bonds were defined. The two binding sites (subdomains IIA and IIIA) were defined using two grids of 70 × 70 × 70 points each with a grid space of 0.375 Å, centered at coordinates x = 35.26, y = 32.41 and z = 36.46 for subsite IIA and x = 14.42, y = 23.55 and z = 23.31 for subsite IIIA, respectively. Lamarckian genetic algorithm with local search was used as the search engine, with a total of 100 runs for each binding site. In each run, a population of 150 individuals with 27,000 generations and 2,500,000 energy evaluations were employed. Operator weights for crossover, mutation and elitism were set at 0.8, 0.02 and 1.0, respectively. For the local search, default parameters were used. Cluster analysis was performed on docked results using a root-mean-square deviation (rmsd) tolerance of 2.0 Å. The protein-ligand complex was visualized and analyzed using AutoDockTools.

3.2.11. ST-serum albumin interactions

Fluorescence quenching titration method was used to study the interaction between ST and different mammalian serum albumins. A fixed albumin concentration

(3 μM), taken in different tubes, was titrated with increasing ST concentrations (3–45 μM, with 3 μM intervals) in a total volume of 3.0 mL. The mixtures were incubated at 25 °C for 1 h and the fluorescence spectra were recorded in the same way as mentioned above in section 3.2.7.1.

The binding parameters, K_{sv} and K_a for ST-albumin interaction were determined by analyzing the fluorescence quenching data in the same way as described in section 3.2.7.2. The values of ΔG for the binding reaction were obtained by substituting the K_a values into the following equation:

$$\Delta G = -\mathrm{RT} \ln K_a \quad (7)$$

3.2.12. Warfarin displacement from various albumin complexes

Sudlow's site I marker, WFN and different serum albumins were mixed in 1:1 molar ratio (3 μM each) and incubated for 1 h at 25 °C. The mixtures were then titrated with increasing ST concentrations (3−45 μM, with 3 μM intervals) and the fluorescence spectra were recorded after 1 h incubation at 25 °C in the wavelength range, 360−480 nm using an excitation wavelength of 335 nm.

3.2.13. Statistical analysis

All experiments were carried out in triplicates independently and the results are presented as ± SD. Statistical data processing and graphs plotting were done with the help of OriginPro 8.5 software (OriginLab Corp., USA).

Chapter 4

RESULTS AND DISCUSSION

4. RESULTS AND DISCUSSION

4.1. ST-HSA interaction

Fluorescence spectroscopy has been widely used to study the interaction between the ligand and the protein (Mi et al., 2014; Divsalar & Khodabakhshian, 2015; Shahlaei et al., 2015). Due to the presence of a solitary tryptophan (Trp-214) residue, located in subdomain IIA of HSA (Peters, 1996), it is advantageous to use fluorescence spectroscopy to probe the binding of ST to HSA.

4.1.1. ST-induced quenching of protein fluorescence

The interaction of ST with HSA was studied by measuring Trp fluorescence of the protein in the absence and the presence of increasing ST concentrations. As depicted in Figure 4.1, free HSA showed strong fluorescence intensity at 343 nm (spectrum 1), whereas ST alone was almost non-fluorescent under similar conditions. However, addition of ST resulted in a gradual decrease of HSA fluorescence intensity (spectra 2−16), showing ~47% quenching at 45 μM ST concentration (inset of Figure 4.1) along with 2 nm blue shift in the emission maxima. These changes in the fluorescence characteristics indicated binding of ST to HSA, as similar results have been reported earlier in several ligand-binding studies (Sulkowska et al., 2003; 2008; Wang et al., 2009; Shah & Bano, 2011; Khan et al., 2012; Tunc et al., 2014; Kabir et al., 2016; Yasmeen et al., 2017). Occurrence of the blue shift in the emission maxima reflected changes in the microenvironment around Trp residue, suggesting increase in the hydrophobicity or decrease in the polarity upon ST interaction (Rinco et al., 2009; Zhang et al., 2009).

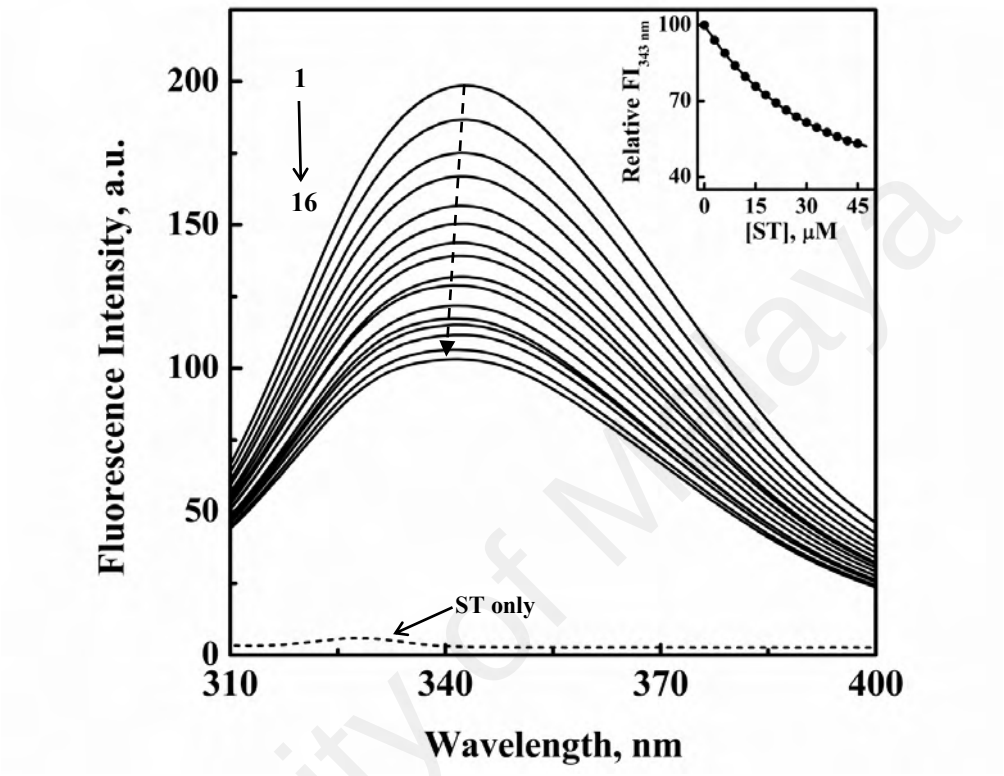

Figure 4.1. ST-induced fluorescence quenching of HSA in 60 mM sodium phosphate buffer, pH 7.4 at 25 °C. The fluorescence spectrum of 3 μM HSA is shown at the top while spectra 2−16 were obtained in the presence of 3−45 μM ST with 3 μM intervals (λ_{ex}= 295 nm). The fluorescence spectrum of free ST is also included. The inset shows decrease in the relative fluorescence intensity of HSA at 343 nm ($FI_{343\ nm}$) with increasing ST concentrations.

4.1.2. Quenching mechanism and binding affinity

Quenching of the fluorescence intensity may be driven by either dynamic or static quenching, which can be differentiated by their temperature dependence. Higher temperatures will induce faster diffusion of molecules, which leads to a larger collisional quenching. In contrast, destabilization of the reversibly-bound complexes occurs at higher temperatures, resulting in a decrease in the static quenching (Lakowicz, 2006). In order to verify the quenching mechanism involved in the ST-HSA system, fluorescence data, obtained at three different temperatures were treated according to Eq. 2 and the resulting linear Stern-Volmer plots are shown in Figure 4.2. Values of the Stern-Volmer constant, K_{sv} were obtained from the slope of these plots and are listed in Table 4.1. A decrease in the K_{sv} value with increasing temperature clearly suggested that ST-induced fluorescence quenching was due to the static quenching process. The bimolecular quenching constant, k_q values, calculated at different temperatures were found to be 3.93×10^{12}, 3.12×10^{12} and 2.23×10^{12} M^{-1} s^{-1} at 15, 25 and 45 °C, respectively. These values were higher than the maximum dynamic quenching constant (2×10^{10} M^{-1} s^{-1}), reported for a diffusion-controlled process (Ware, 1962), thus supporting the involvement of static quenching mechanism in the ST-HSA system.

For a drug to perform its pharmacological activity, it must first be in its free form to diffuse from the blood circulation into the target tissue or organ (Wang et al., 1997). A low binding affinity between a drug and the transport protein causes short lifetime or poor distribution of the drug in the blood, whereas strong binding affinity leads to lower free drug concentration and thus lowers its pharmacodynamic effect (Sjöholm & Ljungstedt, 1973; Gao et al., 2004). To evaluate the binding affinity between ST and HSA, values of the association constant, K_a for ST-HSA interaction at different temperatures were obtained from the double logarithmic plots, shown in Figure 4.3 and the values are included in Table 4.1. An inverse correlation between K_a and temperature

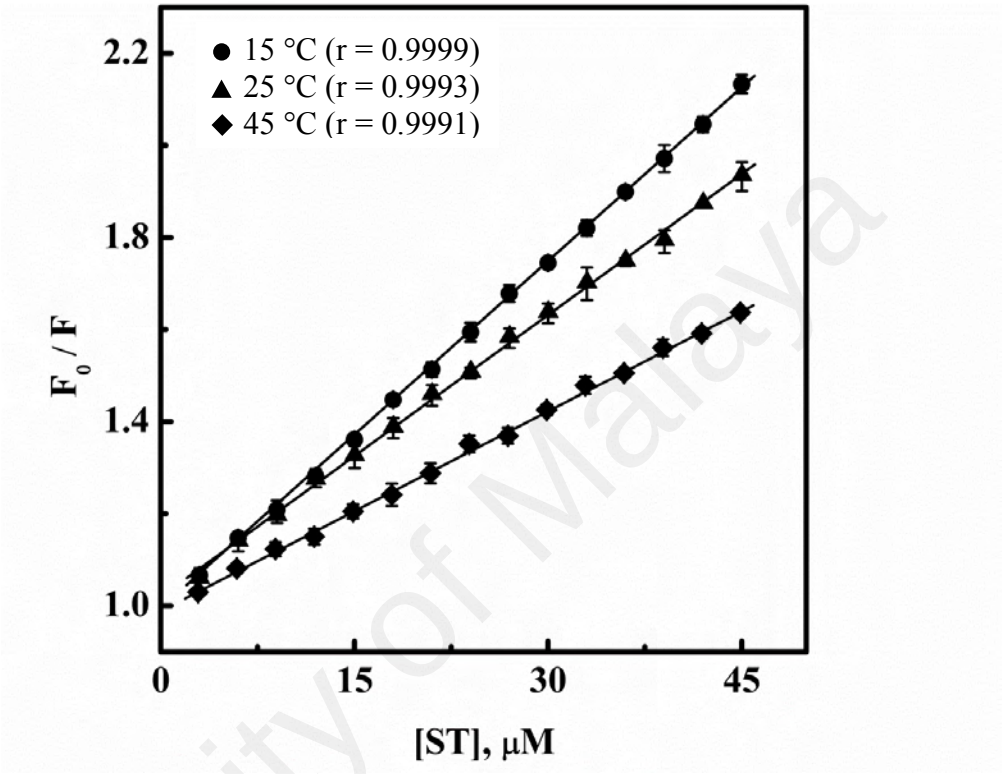

Figure 4.2. Stern-Volmer plots for the fluorescence quenching data of ST-HSA system at three different temperatures, *i.e.*, 15 °C, 25 °C and 45 °C.

Table 4.1. Binding constants and relative thermodynamic parameters of ST–HSA interaction.

T (°C)	$K_{sv} \times 10^4$ (M^{-1})	$K_a \times 10^4$ (M^{-1})	ΔS (J mol^{-1} K^{-1})	ΔH (kJ mol^{-1})	ΔG (kJ mol^{-1})
15	2.51 ± 0.01	2.60 ± 0.03	+32.8	–14.9	– 24.4
25	1.99 ± 0.03	2.13 ± 0.03			– 24.7
45	1.42 ± 0.02	1.45 ± 0.05			– 25.3

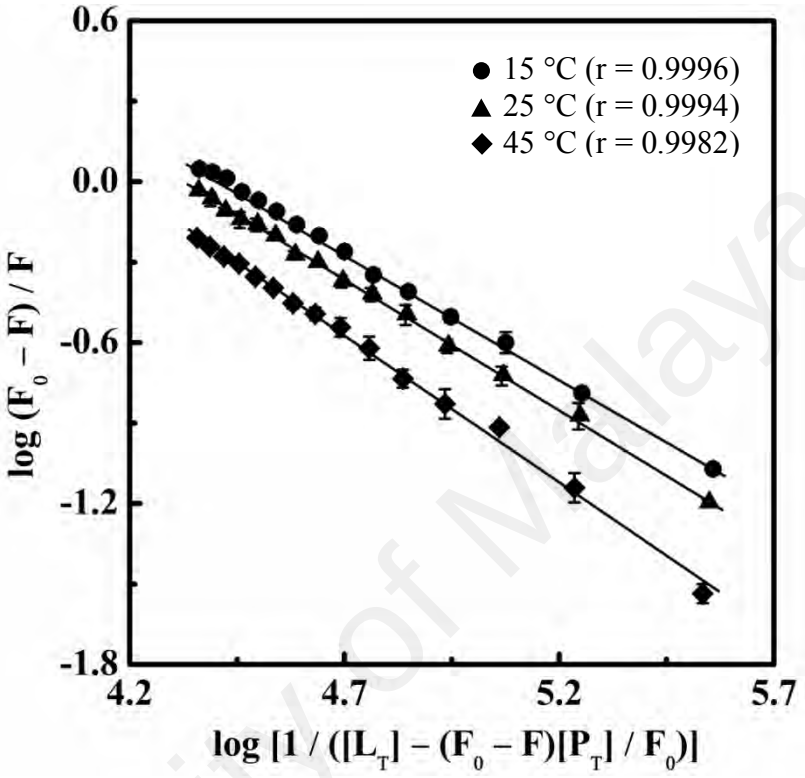

Figure 4.3. Linear plots of log $(F_0 - F) / F$ versus log $[1 / ([L_T] - (F_0 - F)[P_T] / F_0)]$ for the fluorescence quenching data of ST-HSA system at three different temperatures, *i.e.*, 15 °C, 25 °C and 45 °C.

simply reflected temperature-induced weakening of the forces involved in the ligand-protein complex formation. Binding of ST to HSA was found to be reversible with moderate binding affinity, as the K_a values had fallen within the range, $1-15 \times 10^4\ M^{-1}$ (Dufour & Dangles, 2005). Many ligands have been reported to bind HSA with moderate binding affinity (Yue et al., 2008; Varlan & Hillebrand, 2010; Feroz et al., 2012; Afrin et al., 2014; Feroz et al., 2015). The moderate affinity between ST and HSA seems beneficial for ST transportation in the body, as it can be easily dissociated and diffused upon reaching the target site (Peters, 1996).

4.1.3. Interactive forces

There are several non-covalent forces *i.e.* hydrogen bonds, electrostatic interactions, hydrophobic interactions and van der Waals forces known to be involved in the complexation of a ligand with a protein (Olsson et al., 2008). Prediction of the binding forces involved in ST-HSA interaction can be made with the help of the thermodynamic parameters, ΔH and ΔS. Values of these parameters were obtained from the van't Hoff plot, shown in Figure 4.4, while the values of ΔG were calculated by substituting the values of ΔH and ΔS into Eq. 6. These values of ΔH, ΔS and ΔG are listed in Table 4.1. The interaction of ST with HSA is believed to be a spontaneous process at all temperatures due to the negative sign of ΔG values. A positive sign of ΔS suggests involvement of both hydrophobic and electrostatic interactions in the complex formation (Ross & Subramanian, 1981). In view of the presence of a benzene ring and a heterocyclic ring in the ST structure (Figure 2.1), it seems plausible to assume the involvement of hydrophobic interactions in ST-HSA complex formation through non-polar residues of HSA. Since ST lacks any charged group, it seems unlikely to involve electrostatic interactions in the formation of ST-HSA complex. A negative value of ΔH supports the formation of hydrogen bonds in low dielectric medium (Ross & Subramanian, 1981). Due to the presence of polar groups in the ST structure, formation

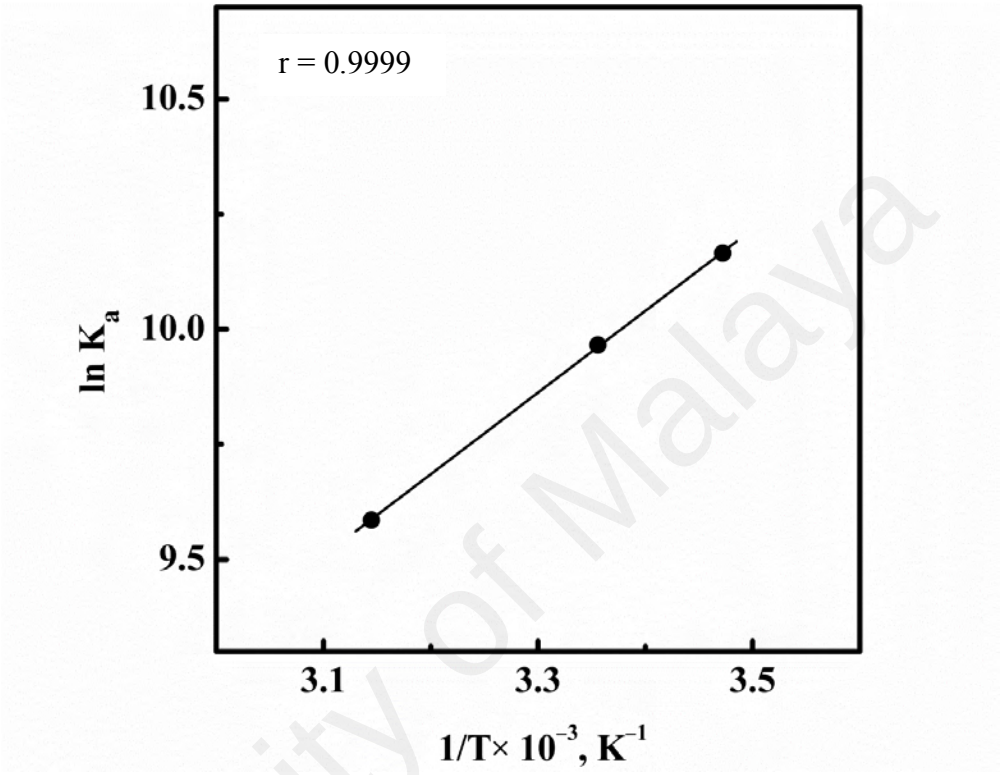

Figure 4.4. van't Hoff plot for ST-HSA interaction. Values of K_a were obtained from the double logarithmic plots, shown in Figure 4.3.

of hydrogen bonds between ST and HSA seems possible. Therefore, both hydrophobic interactions and hydrogen bonds appear to stabilize the ST-HSA complex. Furthermore, our molecular docking results also predicted the location of ST binding site as a deep hydrophobic cleft and participation of several hydrogen bonds in ST-HSA complex formation.

4.1.4. ST-induced structural/microenvironmental changes in HSA

Ligand-protein interaction might be accompanied by conformational changes in the protein. Changes in the secondary and the tertiary structures of HSA upon ST binding were evaluated by the far-UV and the near-UV CD spectra, respectively. Figure 4.5 depicts the far-UV CD spectrum of HSA (1 μM), which exhibited two minima at 209 and 222 nm, thus characterized the presence of α-helical structure in the protein (Reed et al., 1975). A slight decrease in the CD spectral signals at these wavelengths was observed in the presence of ST (4 μM), which indicated alteration in the secondary structures of the protein, thus implying the formation of ST-HSA complex. Similar results have been reported earlier, showing CD spectral changes of HSA in the presence of different ligands (Trynda-Lemiesz et al., 1999; Ding et al., 2010; Khan et al., 2012; Shahabadi et al., 2015; Bhat et al., 2016).

The near-UV CD spectra of HSA (10 μM) in the absence and the presence of ST (40 μM) were characterized by the presence of two minima around 261 and 269 nm (Figure 4.6) due to the presence of the disulfide bonds and aromatic chromophores in the protein (Lee & Hirose, 1992; Uversky et al., 1997). A slight change in the CD spectral signals, observed in the presence of ST suggested alteration around the aromatic residues and disulphide bonds in the protein due to tertiary structural changes. Therefore, ST binding to HSA produced slight changes in both secondary and tertiary structures of the protein.

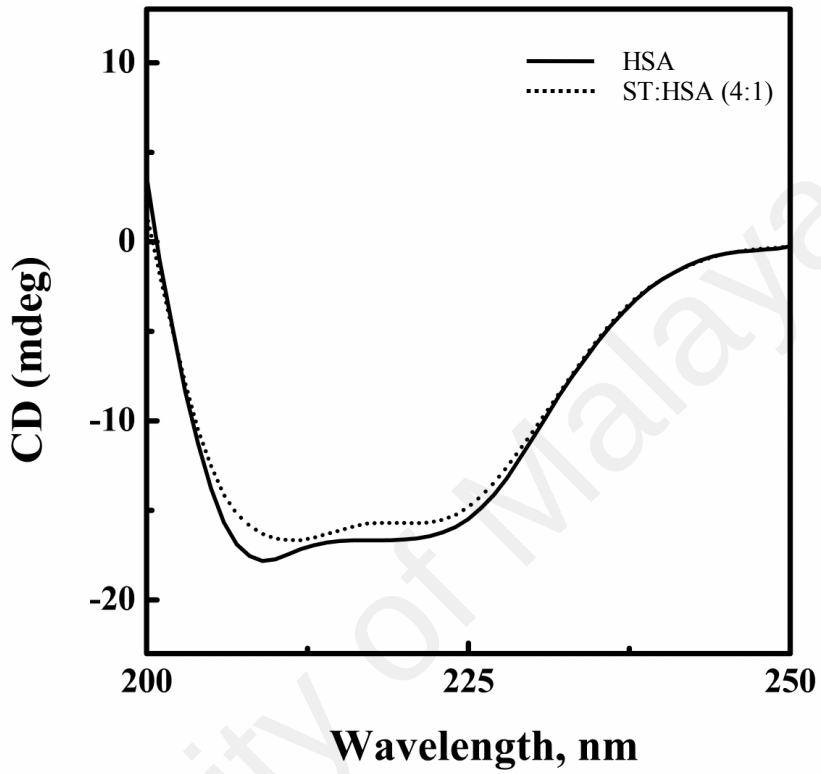

Figure 4.5. Far-UV CD spectra of HSA in free form and its complex with ST at ST:HSA molar ratio of 4:1 in 60 mM sodium phosphate buffer, pH 7.4 at 25 °C. The protein concentration and cuvette path length were 1 μM and 1 mm, respectively.

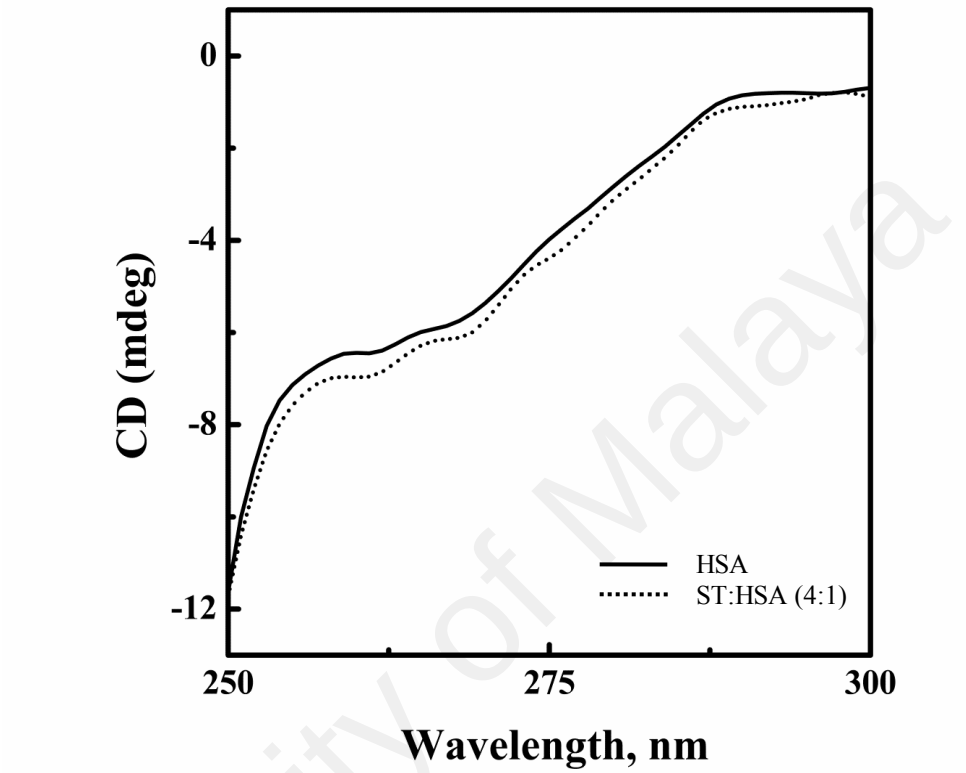

Figure 4.6. Near-UV CD spectra of HSA in free form and its complex with ST at ST:HSA molar ratio of 4:1 in 60 mM sodium phosphate buffer, pH 7.4 at 25 °C. The protein concentration and cuvette path length were 10 μM and 10 mm, respectively.

Information about the microenvironmental changes around aromatic fluorophores (Trp and Tyr) of HSA in the presence of ST was obtained from the 3-D fluorescence spectra. 3-D fluorescence spectra and corresponding contour maps of HSA in the absence as well as the presence of 5 and 10 molar excess of ST are shown in Figures 4.7, 4.8 and 4.9, respectively. The characteristics of these spectra, peak position and the intensity are listed in Table 4.2. Peak '*a*' (λ_{ex}= λ_{em}) refers to the Rayleigh scattering peak while peak '*b*' ($2\lambda_{ex}$= λ_{em}) represents the second-order scattering peak (Lakowicz, 2006). The two other peaks (Figure 4.7), labelled as '*1*' (λ_{ex}= 280 nm) and '*2*' (λ_{ex}= 235 nm) characterize the spectral behaviour of Trp and Tyr residues of HSA (Lakowicz, 2006). Addition of ST to HSA produced significant reduction in the fluorescence intensity and red shift in the emission maxima of both peaks '*1*' and '*2*' (Figure 4.8). Whereas 35% reduction in the fluorescence intensity along with 2 nm red shift was observed in peak '*1*', peak '*2*' experienced 45% reduction in the intensity along with 4 nm red shift in the presence of 5 molar excess of ST (Table 4.2). These changes became more pronounced at higher ST:HSA molar ratio (Figure 4.9), showing 53% reduction in the fluorescence intensity along with 4 nm red shift for peak '*1*' and 64% reduction in the intensity along with 6 nm red shift for peak '*2*' (Table 4.2). These results suggested significant changes in the microenvironment around aromatic fluorophores due to the binding of ST to HSA.

4.1.5 Thermal stability of HSA

Binding of small molecules to proteins often shows changes in their thermal unfolding behaviour (González et al., 1999; Layton & Hellinga, 2010). To investigate the effect of ST binding on the thermal stability of HSA, temperature-dependent titration experiments were performed. The fluorescence intensity of HSA in the absence and the presence of ST (ST: HSA molar ratios of 5:1, 10:1 and 15:1) was monitored at 343 nm in the temperature range, 25−80 °C. As shown in Figure 4.10, a continuous

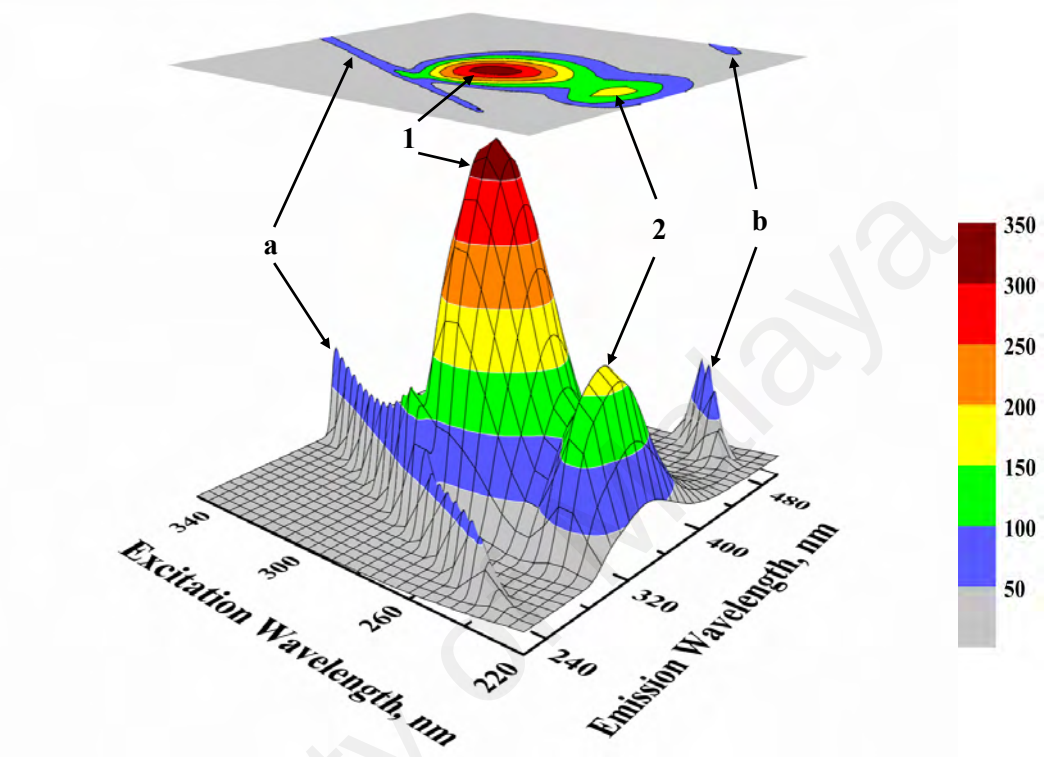

Figure 4.7. Three-dimensional fluorescence spectrum and corresponding contour map of HSA (3 μM) in 60 mM sodium phosphate buffer, pH 7.4 at 25 °C.

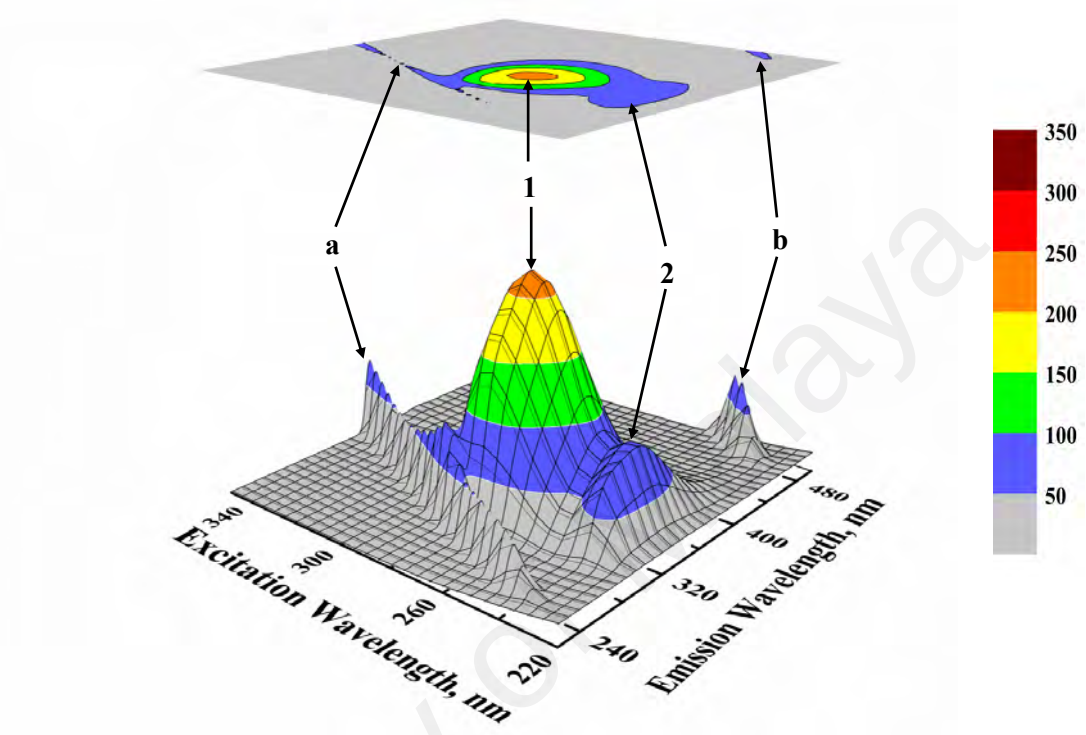

Figure 4.8. Three-dimensional fluorescence spectrum and corresponding contour map of HSA (3 μM) in the presence of 15 μM ST in 60 mM sodium phosphate buffer, pH 7.4 at 25 °C.

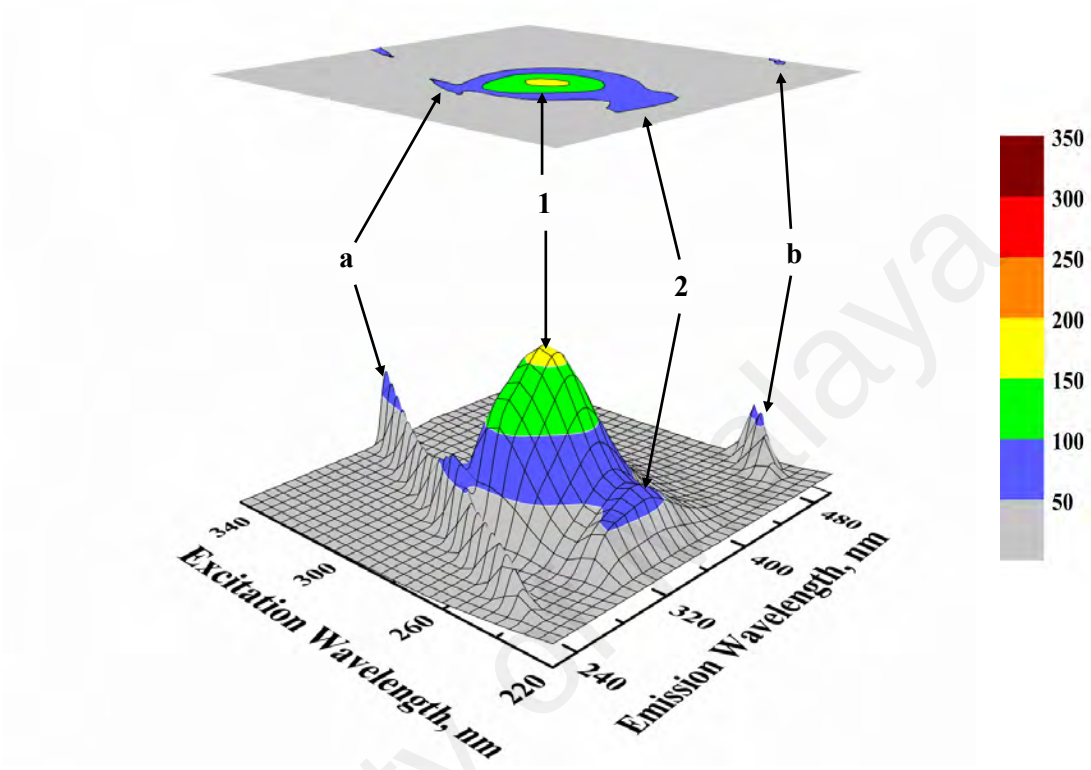

Figure 4.9. Three-dimensional fluorescence spectrum and corresponding contour map of HSA (3 μM) in the presence of 30 μM ST in 60 mM sodium phosphate buffer, pH 7.4 at 25 °C.

Table 4.2. Characteristics of the three-dimensional fluorescence spectra of HSA and ST–HSA complexes at pH 7.4, 25 °C.

System	Peak number	Peak position [$\lambda_{ex}/\lambda_{em}$, nm/nm]	Intensity
HSA	a	220/220 → 350/350	19.0 → 87.8
	b	250/500	90.7
	1	280/335	319.3
	2	235/332	166.2
[ST]:[HSA]= 5 : 1	a	220/220 → 350/350	19.5 → 73.8
	b	250/500	72.9
	1	280/337	207.2
	2	235/336	92.2
[ST]:[HSA]= 10 : 1	a	220/220 → 350/350	19.9 → 73.4
	b	250/500	61.4
	1	280/339	150.8
	2	235/338	60.1

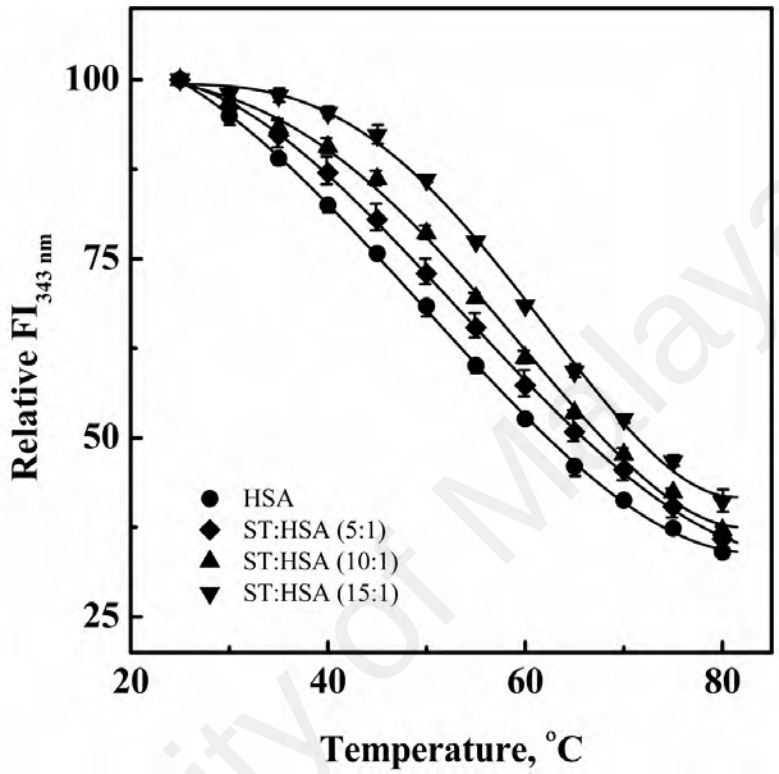

Figure 4.10. Thermal denaturation profiles of HSA (3 μM) in the absence and the presence of 15, 30 and 45 μM ST in 60 mM sodium phosphate buffer, pH 7.4 in the temperature range, 25–80 °C, as studied by fluorescence measurements at 343 nm upon excitation at 295 nm.

decrease in the fluorescence intensity of HSA was observed up to 70 °C, which sloped off thereafter. Similar decrease has been reported earlier in the thermal stability profile of HSA (Picó, 1997; Flora et al., 1998). Interestingly, addition of ST in increasing concentrations produced gradual thermal stabilization of HSA throughout the temperature range. These results clearly suggested increase in the thermal stability of HSA due to ST-HSA complex formation, as presence of non-covalent forces that stabilized this complex would require higher energy to be broken down (Yeggoni et al., 2014).

4.1.6. ST binding site

HSA has two well-known ligand binding sites namely, Sudlow's site I and site II, located in subdomains IIA and IIIA, respectively, which enable most physiological ligands to bind HSA with high affinity (Sudlow et al., 1976; Peters, 1996). These sites can be characterized based on the binding of high affinity drugs, which serve as specific site markers such as warfarin, indomethacin and phenylbutazone that bind to site I; ibuprofen, ketoprofen and diazepam that bind to site II of HSA (Curry, 2002). These specific site markers are commonly used to allocate the binding site of any unknown ligand on HSA. Therefore, competitive ligand displacement experiments were performed with WFN and DZM as the site I and site II markers, respectively.

ST-induced displacement of WFN from WFN-HSA (1:1) complex was evident from the gradual decrease in the fluorescence intensity of WFN-HSA complex at 383 nm with increasing ST concentrations (Figure 4.11). As shown in the inset of Figure 4.11, ~ 40% quenching was noticed at the highest ST concentration. It is important to note that the free forms of WFN, HSA and ST as well as ST-HSA complex did not show any significant fluorescence intensity at 383 nm (spectra '*a*'–'*d*' in Figure 4.11). Such decrease in the fluorescence intensity of WFN-HSA complex in the presence of ST clearly suggested ST-induced displacement of WFN from site I of HSA.

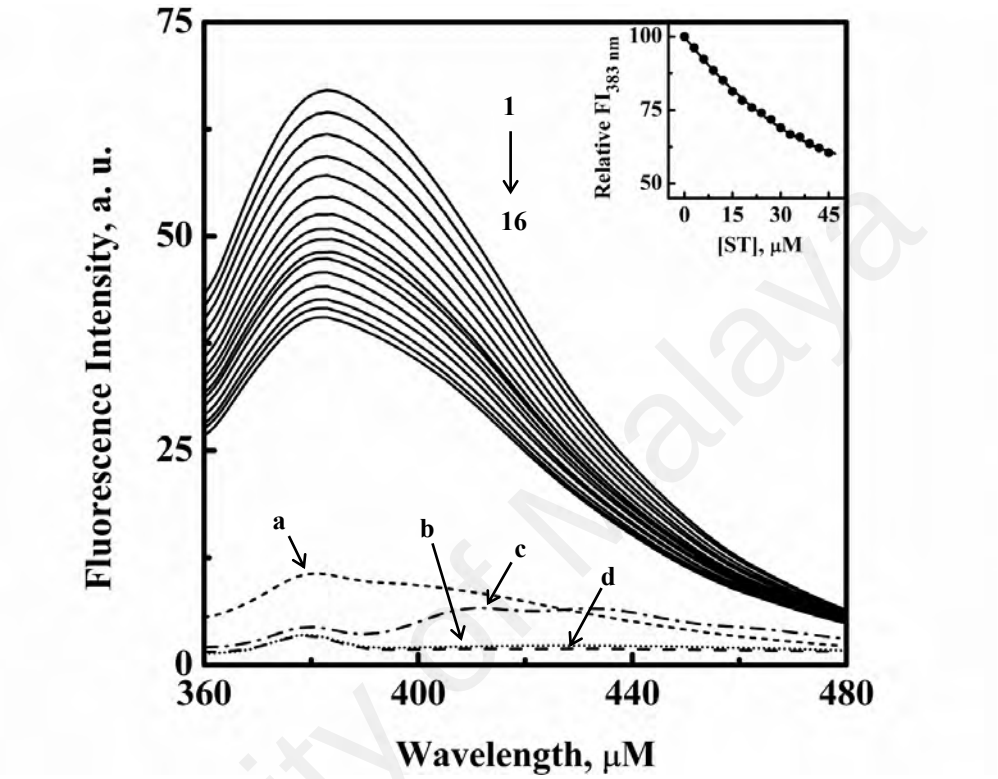

Figure 4.11. Fluorescence spectrum of WFN-HSA (1:1) complex in the absence (spectrum 1) and the presence (spectra 2−16) of increasing ST concentrations (3−45 μM with 3 μM intervals) in 60 mM sodium phosphate buffer, pH 7.4 at 25 °C, upon excitation at 335 nm. The labelled spectra refer to (a) 3 μM WFN, (b) 3 μM HSA, (c) 15:1 ST-HSA complex and (d) 45 μM ST. The inset shows decrease in the relative fluorescence intensity of WFN-HSA complex at 383 nm with increasing ST concentrations.

To investigate the possibility of ST binding to site II of HSA, changes in the fluorescence intensity at 343 nm of HSA and DZM-HSA (1:1) complex were monitored in the presence of increasing ST concentrations. As can be seen from Figure 4.12, no significant difference was noticed in the ST-induced decrease in the fluorescence intensity of HSA and DZM-HSA complex. These results clearly demonstrated that binding of ST to HSA remained unaffected by the presence of DZM on HSA, thus suggesting separate binding sites of ST and DZM on HSA.

In order to verify the above finding, ANS was also used to support the exclusion of site II as the ST binding site on HSA. Previous studies have reported one high-affinity ANS binding site, located in subdomain IIIA (Sudlow's site II) and at least three low-affinity ANS binding sites on HSA (Bagatolli et al., 1996; Cattoni et al., 2009). In the first set of experiments, HSA (3 μM) was titrated with increasing concentrations (3−45 μM with 3 μM intervals) of ST or ANS. Both ST and ANS produced quenching in the fluorescence intensity of HSA at 343 nm. However, quenching produced by ANS was more pronounced compared to ST, as ~87% quenching of HSA fluorescence was observed at 45 μM ANS concentration compared to ~48% quenching, observed with similar concentration of ST (Figure 4.13). From these results, it seems that binding of these two ligands occurred at separate sites on HSA. Similar quenching results of HSA fluorescence with ANS have been shown in an earlier study (Ding et al., 2010). In the second set of experiments, ANS-HSA complex was titrated with increasing ST concentrations and its fluorescence intensity was recorded at 466 nm, using an excitation wavelength of 370 nm. Interestingly, reduction in the fluorescence intensity of ANS-HSA complex was only up to ~35% at the highest ST concentration, as shown in Figure 4.13. In view of the small extent of fluorescence quenching of ANS-HSA complex by added ST, it appears that such ANS displacement might have occurred from the secondary low affinity sites of ANS rather than the primary ANS binding site

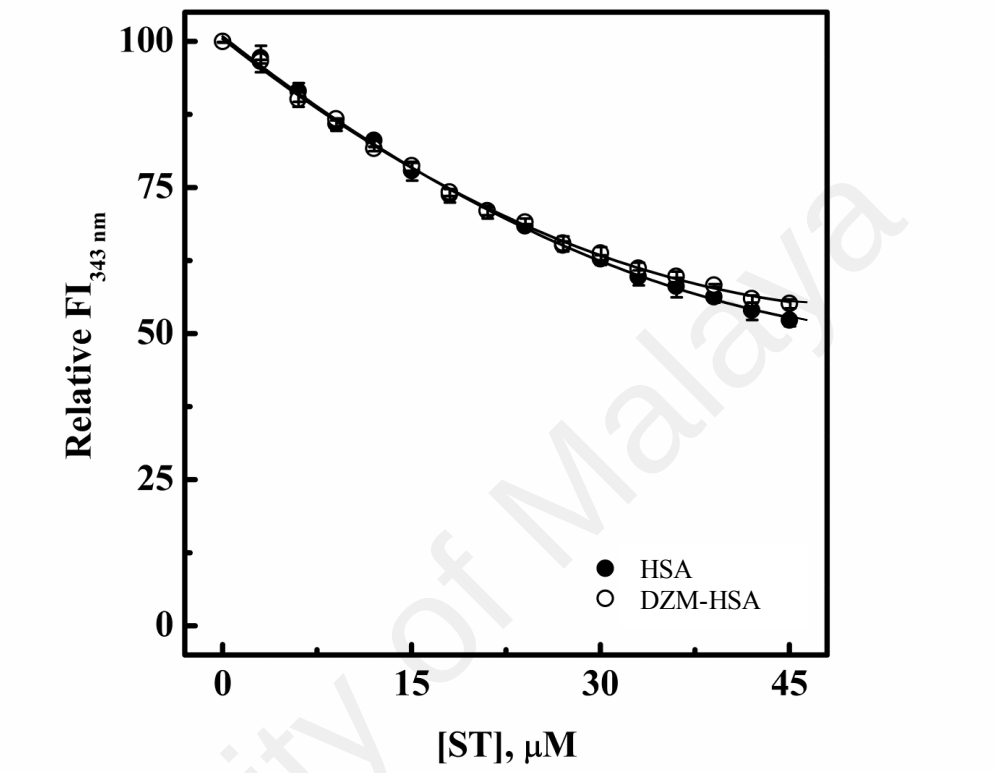

Figure 4.12. Plots showing decrease in the relative fluorescence intensity at 343 nm ($FI_{343\ nm}$) of HSA (3 μM) and DZM-HSA (1:1) complex with increasing (3−45 μM) ST concentrations.

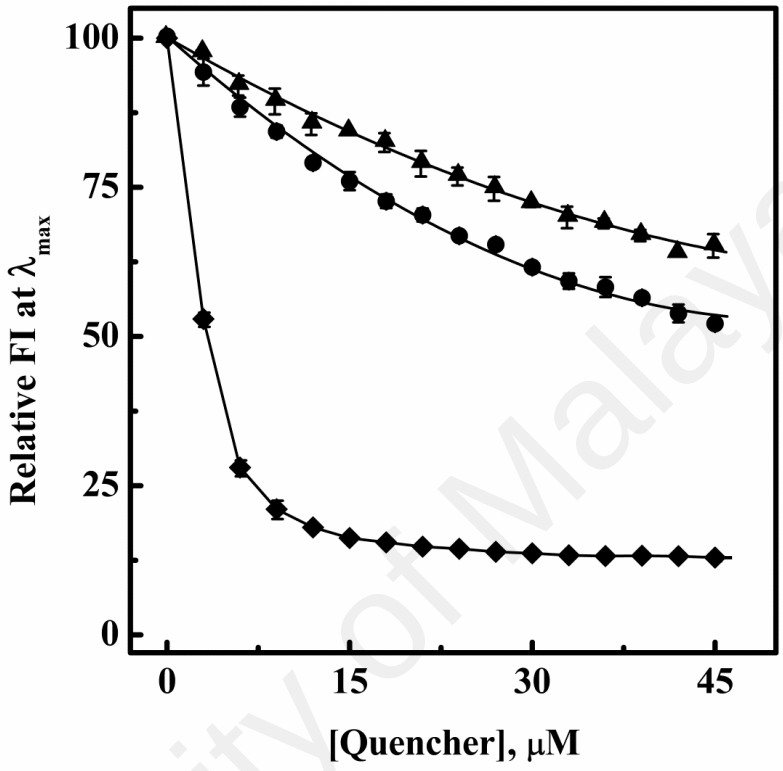

Figure 4.13. Plots showing decrease in the relative fluorescence intensity at 343 nm of HSA with increasing concentrations (3−45 μM) of ANS (◆) and ST (●) upon excitation at 295 nm. Titration results of ANS-HSA complex with increasing ST concentrations are shown by (▲), as obtained at 466 nm upon excitation at 370 nm. All experiments were performed in 60 mM sodium phosphate buffer, pH 7.4 at 25 °C.

(Sudlow's site II), located in subdomain IIIA. Therefore, these results were in agreement with those obtained from the DZM displacement studies and supported the exclusion of site II as the ST binding site on HSA. Furthermore, our docking results also supported the competitive drug displacement results.

4.1.7. Molecular docking results

A molecular modeling study was conducted to predict the binding site of ST in HSA and to confirm the results of the displacement experiments described above. As shown in Figure 4.14, cluster analysis for the binding site I showed a total of 11 multimember conformational clusters from 100 docking runs with the lowest mean binding energy of −32.00 kJ mol^{-1}. The highest populated cluster possessed 35 conformations. However, the conformation with the lowest binding energy (−32.26 kJ mol^{-1}) did not belong to the highest populated cluster. On the other hand, at the binding site II, 9 multimember conformational clusters, with lowest mean binding energy of −29.27 kJ mol^{-1} were identified. The highest populated cluster was comprised of 40 conformations. Since the docking energy of the most favorable conformation in site I was lower than the one in site II, site I (subdomain IIA) can be predicted as the preferential binding site of ST on HSA. These results were in accordance with the drug displacement results discussed above.

Binding orientation analysis was then performed using the predicted binding model with the lowest docking energy (−32.26 kJ mol^{-1}). As shown in Figure 4.15, the binding site (characterized by the amino acid residues available within 5 Å distance to the ligand) was found to be a hydrophobic cleft lined by the amino acid residues: Tyr-150, Glu-153, Phe-157, Arg-160, Glu-188, Ala-191, Ser-192, Ser-193, Lys-195, Gln-196, Lys-199, Trp-214, Arg-218, Leu-219, Arg-222, Leu-238, His-242, Arg-257, Ser-287, His-288, Ala-291, Glu-292, Pro-447, Cys-448, Asp-451 and Tyr-452. Presence of hydrophobic amino acid residues at the ST binding site in HSA was in accord with the

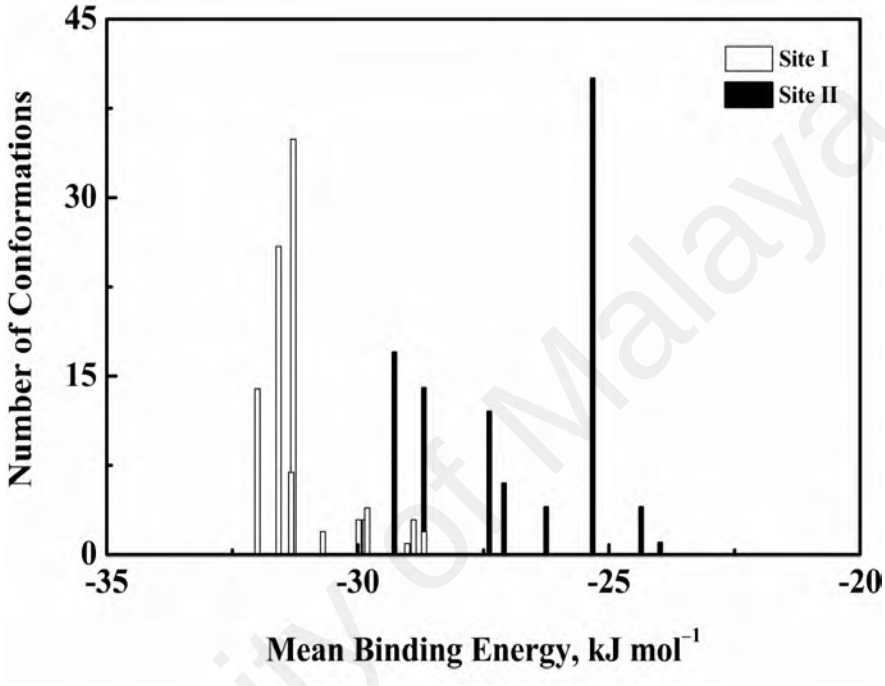

Figure 4.14. Cluster analysis of ST docking to HSA crystal structure (1BM0) at Sudlow's site I and site II, as obtained from a total of 100 docking runs for each site.

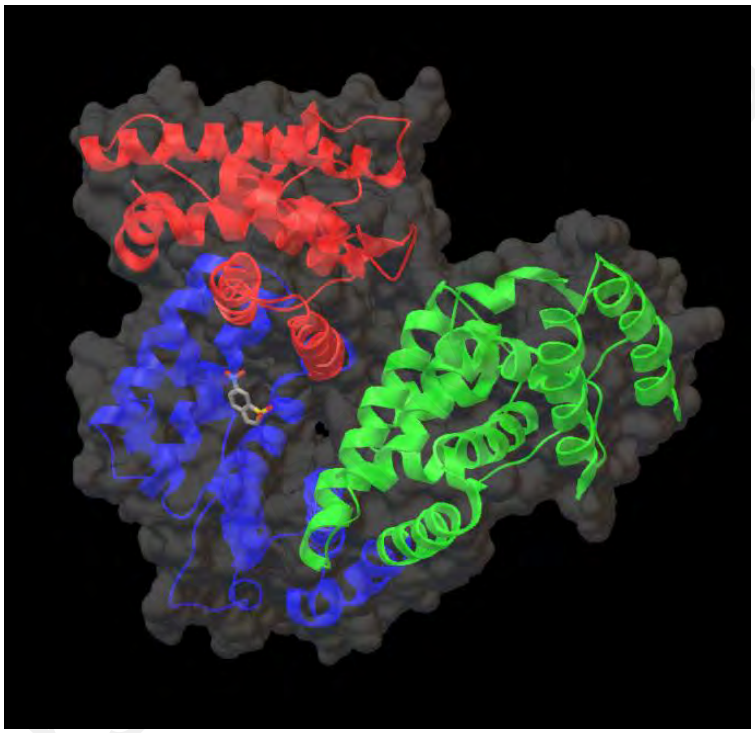

Figure 4.15. Predicted binding orientation of the lowest docking energy conformation of ST (ball and stick rendered) in the Sudlow's site I (subdomain IIA) of HSA (1BM0). Three major domains of HSA, namely, I, II and III are represented in red, blue and green, respectively.

involvement of hydrophobic force in ST-HSA interaction. Furthermore, in the ST-HSA complex docking conformation at the site I, five hydrogen bonds were predicted (Figure 4.16, Table 4.3), which also supported our thermodynamic data (Table 4.1), suggesting involvement of hydrogen bonds along with hydrophobic forces in ST-HSA complex formation.

4.2. ST-serum albumin interactions

4.2.1. ST-induced quenching of albumins' fluorescence

Fluorescence spectra of different mammalian serum albumins, *i.e.* HSA, SSA, PSA, BSA and RbSA in their free form as well as in the presence of increasing ST concentrations are illustrated in Figure 4.17A−E. Variation in the fluorescence intensity observed among these proteins (spectrum 1) is due to the difference in the number of Trp residues present in these albumins, which is the main contributor of the fluorescence intensity upon excitation at 295 nm (Lakowicz, 2006). Proteins with two Trp residues, namely, BSA, SSA and PSA produced relatively higher fluorescence intensity compared to those possessing single Trp residue, *i.e.* HSA and RbSA (Table 4.4) (Pajot, 1976). Meanwhile, location of the Trp residue(s) in the three-dimensional structure of the proteins could explain the difference in the emission maxima of these albumins (Lakowicz, 2006), which falls within the range, 343−345 nm (Table 4.4).

A significant decrease in the fluorescence intensity of these proteins was observed upon addition of increasing ST concentrations (spectra 2−16; Figure 4.17). As discussed in section 4.1.1., such quenching was suggestive of ST binding to these albumins. Although all these albumins produced quenching in protein fluorescence, quantitative differences were noticed among them. In order to compare the quenching pattern observed with these albumins, fluorescence data were normalized by taking the fluorescence intensity of the free protein at its emission maxima as 100. Figure 4.18 shows decrease in the relative fluorescence intensity of different serum albumins at their

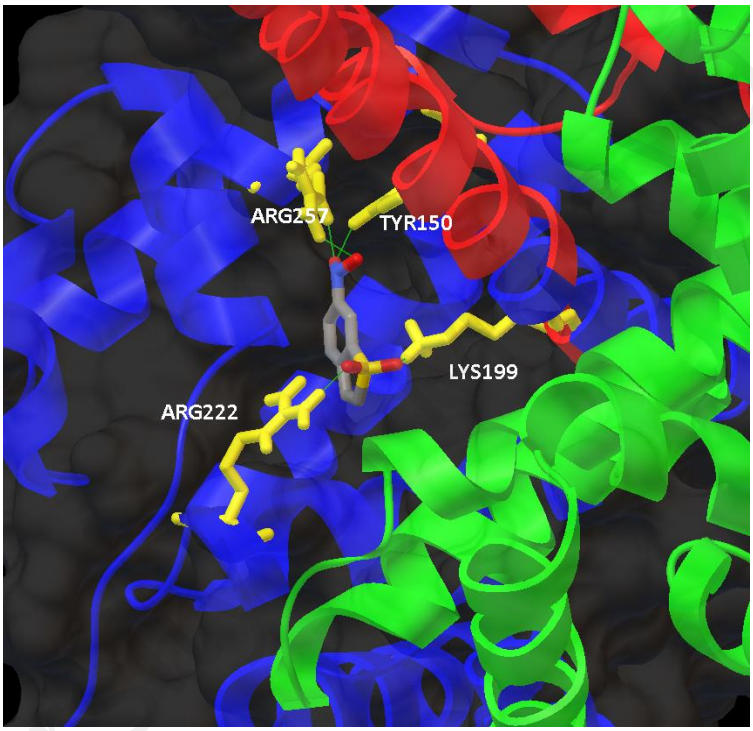

Figure 4.16. The zoomed-in view of the binding site showing hydrogen bonds (green) formed between ST and amino acid side chains of HSA.

Table 4.3. Predicted hydrogen bonds between interacting atoms of the amino acid residues of HSA (1BM0) and ST at site I.

Binding site	Protein (HSA) atom	Ligand (ST) atom	Distance (Å)
Site I	TYR−150: HH	O (sulfonyl)	2.16
	LYS−199: HZ1	O (sulfonyl)	1.83
	ARG−222: HH21	O (nitro)	1.90
	ARG−257: HE	O (nitro)	2.06
	ARG−257: HH22	O (nitro)	2.06

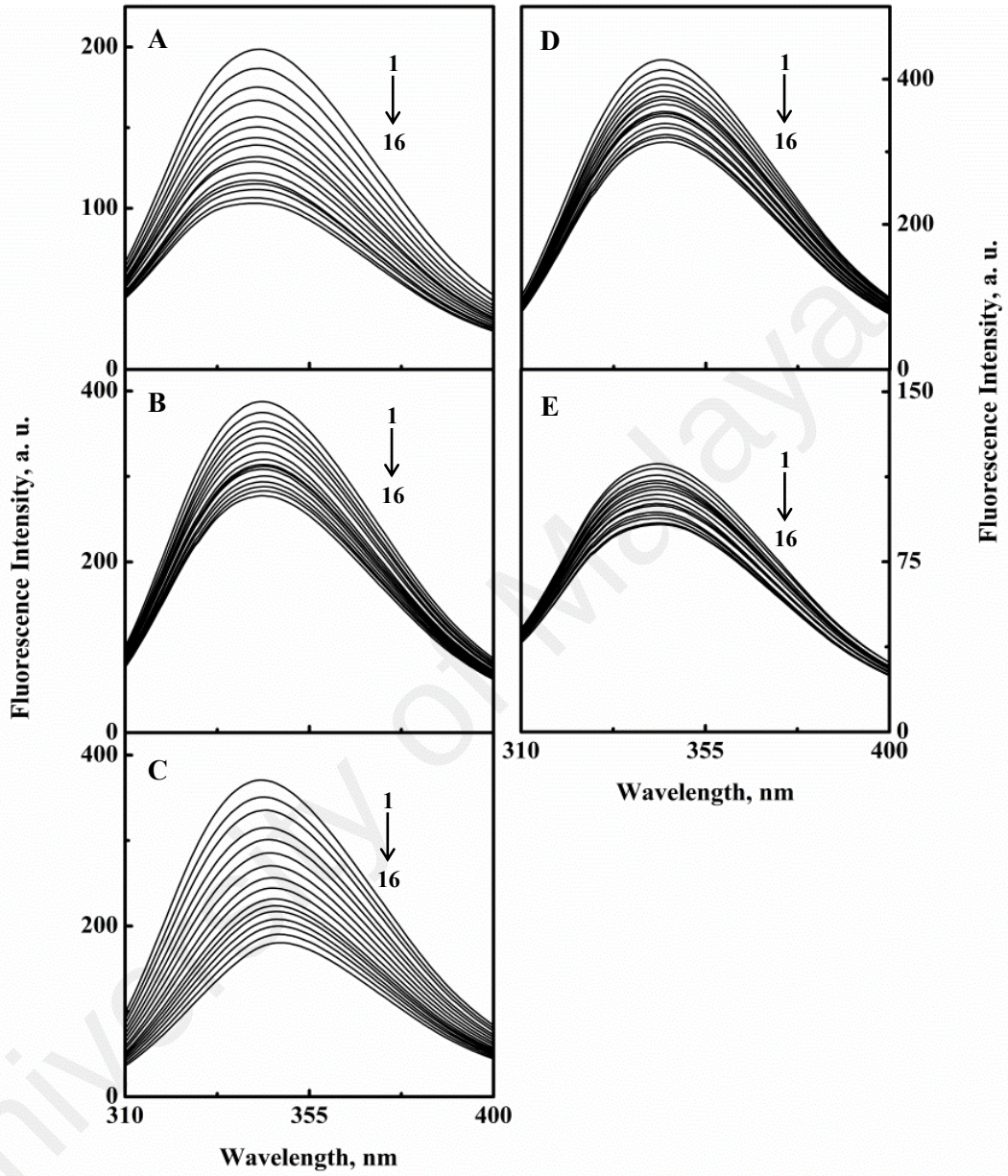

Figure 4.17. Fluorescence spectra of different mammalian serum albumins (3 μM) in the absence (spectrum 1) and the presence (spectra 2−16) of increasing ST concentrations (3−45 μM with 3 μM intervals) in 60 mM sodium phosphate buffer, pH 7.4 at 25 °C, upon excitation at 295 nm. The different serum albumins were: HSA (A); SSA (B); PSA (C); BSA (D) and RbSA (E).

Table 4.4. Fluorescence characteristics of different mammalian albumins in free form and their complexes with ST.

Albumin	Intensity (a.u.)	Emission maximum (nm)	Trp residues	% Quenching [ST]:[Albumin] = 15:1
HSA	199	343	Trp-214	46.8 ± 0.14
SSA	388	343	Trp-134, Trp-213	28.5 ± 0.50
PSA	371	343	Trp-134, Trp-213	52.7 ± 0.37
BSA	427	345	Trp-134, Trp-213	26.6 ± 0.30
RbSA	118	343	Trp-214	26.1 ± 0.05

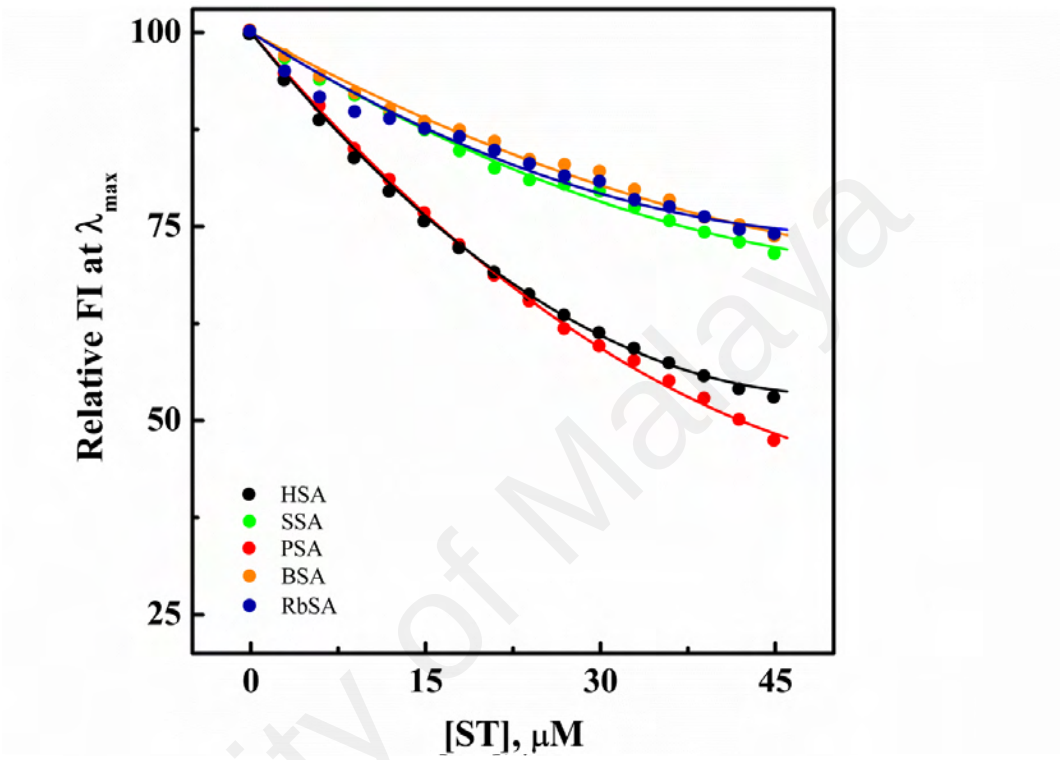

Figure 4.18. Plots showing decrease in the relative fluorescence intensity of different serum albumins at their emission maxima with increasing ST concentrations, as obtained from the results shown in Figure 4.17.

emission maxima with increasing ST concentrations. As evident from Figure 4.18, BSA, SSA and RbSA produced lesser extent of quenching compared to HSA and PSA, which showed higher degree of quenching at all ST concentrations. Quantitatively, ~ 26 %, ~ 27 % and ~ 28 % quenching were observed for RbSA, BSA and SSA, respectively, compared to HSA and PSA that produced ~ 47 % and ~ 53 % quenching, respectively, at the highest (15:1) ST/albumin molar ratio (Table 4.4). Such differences in the ST-induced quenching of albumin fluorescence were not uncommon, as similar patterns have been observed in several ligand binding studies (Sheng et al., 2010; Samari et al., 2012; Feroz et al., 2015).

4.2.2. Binding parameters

To characterize the quenching mode involved in the ST-induced quenching of albumins' fluorescence, fluorescence quenching data were analyzed following the treatments based on Eq. 2. Figure 4.19 shows the Stern-Volmer plots for different ST-albumin systems while the K_{sv} values are listed in Table 4.5. It should be noted that the Stern-Volmer plot for ST-PSA system showed an upward deviation at higher ST concentrations. Therefore, experimental points falling in the linear zone were selected for regression analysis. Similar to the quenching pattern (Figure 4.18), higher values of K_{sv} were obtained for PSA and HSA compared to SSA, RbSA and BSA. Using a value of τ_0 (fluorophore lifetime in the absence of quencher) for different mammalian albumins as 10^{-8} s (Lakowicz, 2006), calculations of k_q values for different ST-albumin systems were made according to Eq. 3. These values were found to be in the order of 10^{12} M^{-1} s^{-1} (HSA and PSA) and 10^{11} M^{-1} s^{-1} (SSA, RbSA and BSA), which were larger than the highest value reported for the diffusion-controlled process, ~10^{10} M^{-1} s^{-1} (Lakowicz, 2006). Such k_q values supported the formation of ST-albumin complexes.

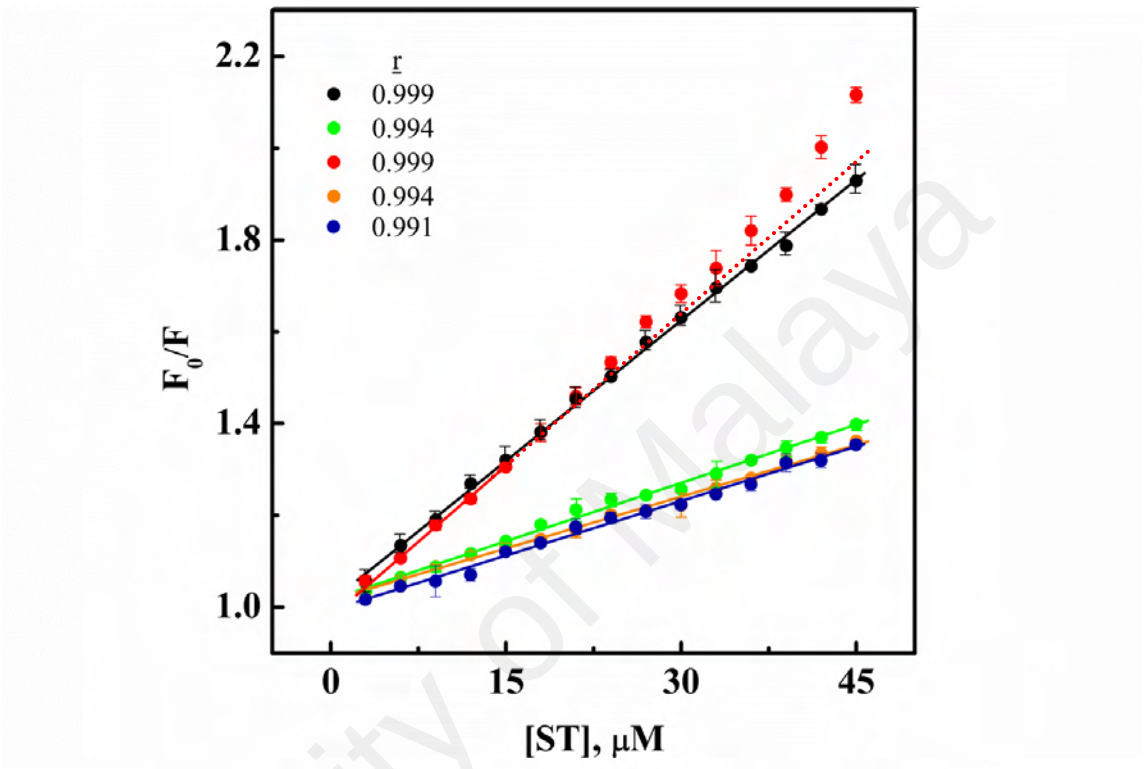

Figure 4.19. Stern-Volmer plots for the fluorescence quenching data of different ST-albumin systems at 25 °C. The data were obtained from the Figure 4.17. The symbols used to represent each albumin are similar as shown in Figure 4.18.

Table 4.5. Binding parameters for ST-albumin interactions.

Albumin	K_{sv} (M^{-1})	K_a (M^{-1})	ΔG (kJ mol^{-1})
HSA	$(1.99 \pm 0.03) \times 10^4$	$(2.13 \pm 0.04) \times 10^4$	−24.7
SSA	$(8.50 \pm 0.15) \times 10^3$	$(7.95 \pm 0.14) \times 10^3$	−22.3
PSA	$(2.09 \pm 0.07) \times 10^4$	$(2.44 \pm 0.06) \times 10^4$	−25.0
BSA	$(8.00 \pm 0.02) \times 10^3$	$(6.67 \pm 0.06) \times 10^3$	−21.8
RbSA	$(7.90 \pm 0.32) \times 10^3$	$(6.61 \pm 0.31) \times 10^3$	−21.8

Therefore, ST-induced quenching of these albumins' fluorescence can be described as the static quenching phenomenon.

The fluorescence quenching data were also treated according to Eq. 4 to determine the binding affinity between ST and serum albumins. Values of the association constant, K_a for different ST-albumin systems were obtained from the linear double logarithmic plots (Figure 4.20) and are listed in Table 4.5. Binding affinity of ST to these albumins was found to follow the order: PSA>HSA>SSA>BSA/RbSA. Furthermore, these albumins can be classified into two groups based on their ST-binding affinity. Whereas PSA and HSA showed relatively higher affinity, SSA, RbSA and BSA can be grouped together with relatively lower ST binding affinity (Table 4.5). Although these albumins share a strong similarity in terms of the sequence and protein characteristics, binding affinity of a ligand to proteins depends on the degree of phylogenetic relationship (Day & Myszka, 2003). This explains the variation in the binding affinity among these albumins.

The values of Gibbs free energy change, ΔG, as calculated using Eq. 7 suggested feasible binding reactions between ST and albumins (Ross & Subramanian, 1981).

4.2.3. ST-induced warfarin displacement

As discussed in sections 4.1.6. and 4.1.7., Sudlow's site I has been suggested as the preferred binding site of ST on HSA. In view of this, similar study of WFN displacement from different albumin complexes upon addition of ST was made. As evident from Figure 4.21A–E, significant quenching in the fluorescence intensity of WFN-albumin complexes at 382 nm (spectrum 1) was observed upon addition of increasing ST concentrations (spectra 2–16). Such reduction in the fluorescence intensity at 382 nm clearly suggested displacement of WFN from these albumins by added ST. It should be noted that values of the fluorescence intensity of WFN, serum

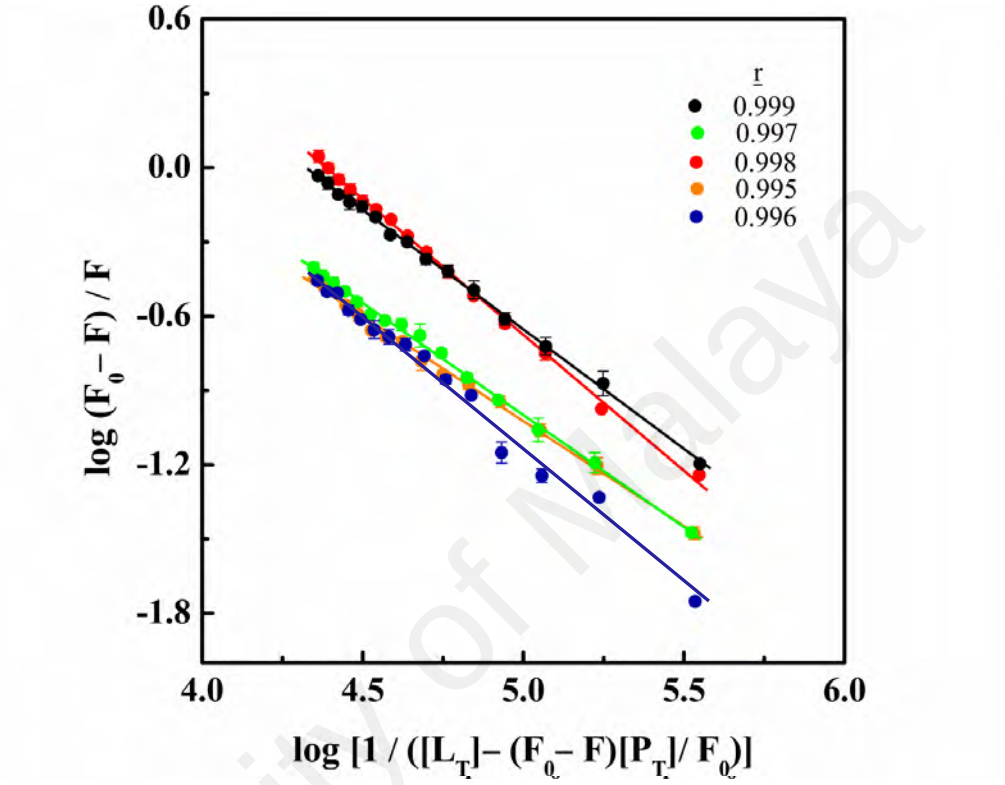

Figure 4.20. Double logarithmic plots of log (F_0 − F) / F versus log [1 / ([L_T] − (F_0 − F)[P_T] / F_0)] for the fluorescence quenching data of the ST-albumin systems. The symbols used to represent each albumin are similar as shown in Figure 4.18.

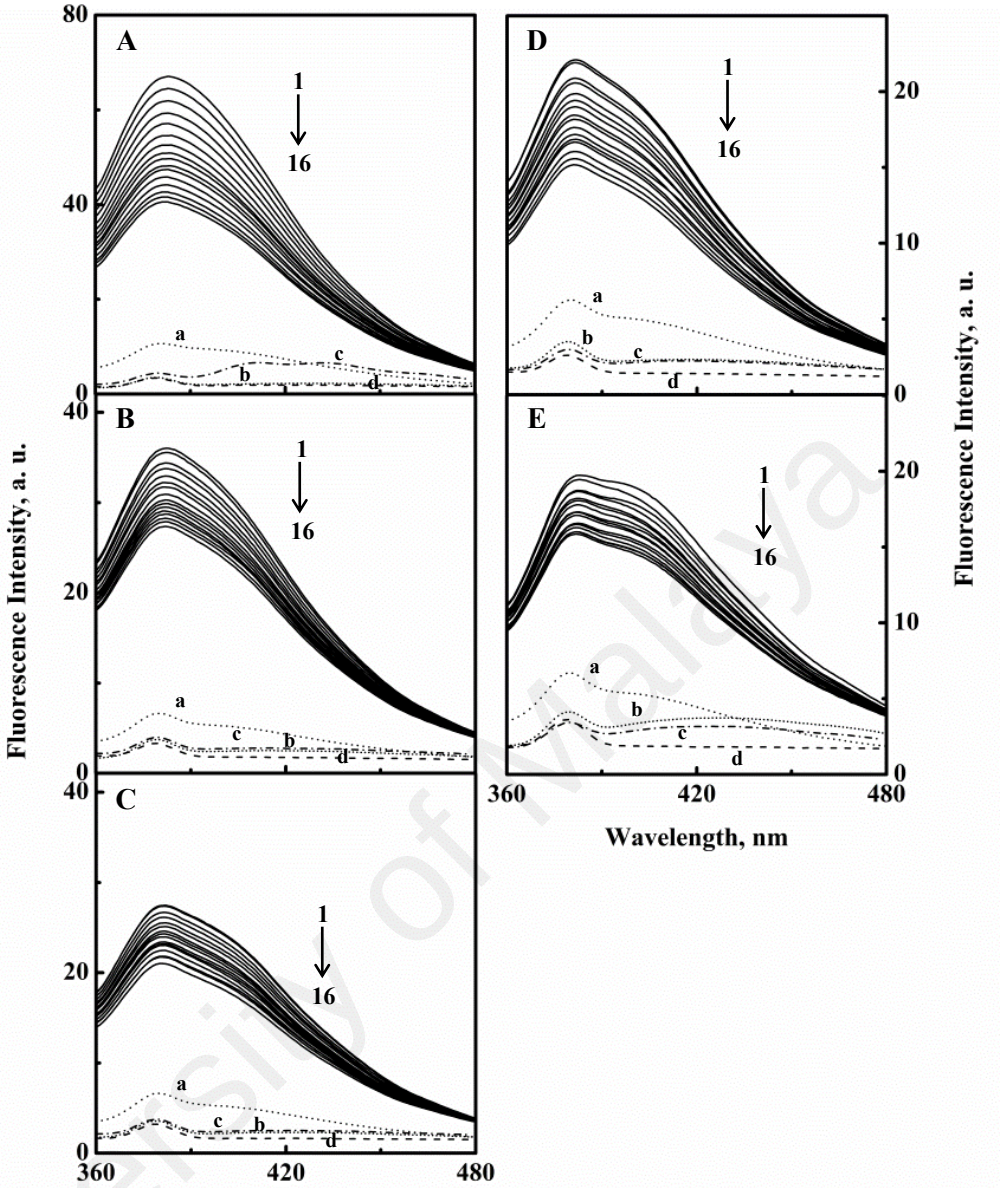

Figure 4.21. Fluorescence spectra of WFN-albumin (1:1) complexes (3 μM each) in the absence (spectrum 1) and the presence (spectra 2−16) of increasing ST concentrations (3−45 μM with 3 μM intervals) in 60 mM sodium phosphate buffer, pH 7.4 at 25 °C, upon excitation at 335 nm. The different serum albumin commplexes were: HSA (A); SSA (B); PSA (C); BSA (D) and RbSA (E). The labelled spectra refer to (a) 3 μM WFN, (b) 3 μM serum albumin, (c) 15:1 ST-albumin complex and (d) 45 μM ST.

albumin, ST-albumin complex and ST (spectra '*a*'−'*d*') were either weak or insignificant at this wavelength.

Although ST-induced displacement of WFN from different WFN-albumin complexes were significant, quantitative difference were noticed. This can be clearly seen from Figure 4.22, showing decrease in the relative fluorescence intensity at 382 nm (Relative $FI_{382\ nm}$) for different WFN-albumin complexes with increasing ST concentrations. A comparison of the percentage quenching observed with these complexes at ST:albumin molar ratio of 15:1 shows similarity between BSA and HSA, while SSA, PSA and RbSA form a separate group (Table 4.6).

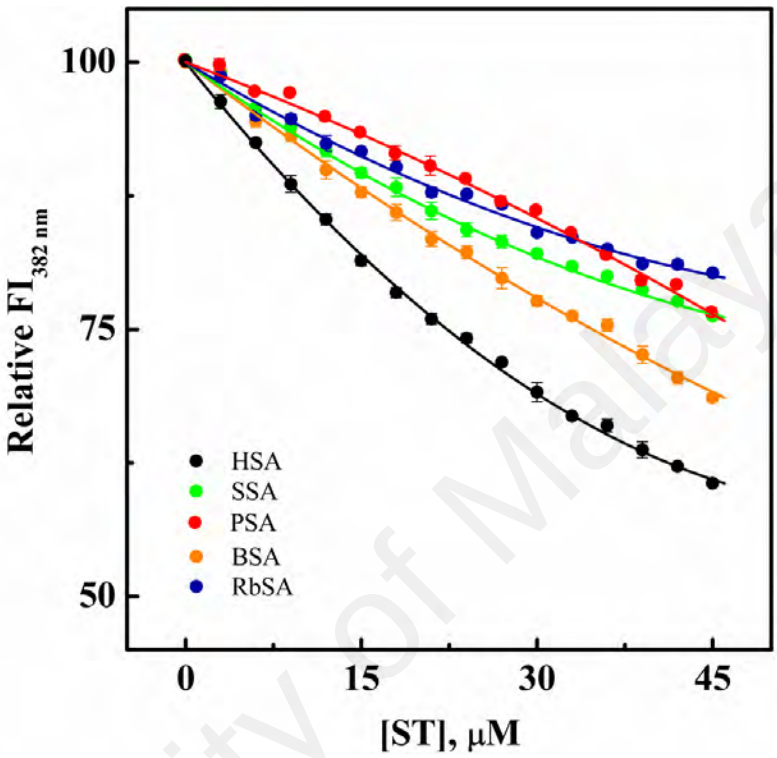

Figure 4.22. Plots showing decrease in the relative fluorescence intensity of different WFN-albumin complexes at 382 nm with increasing ST concentrations.

Table 4.6. ST-induced WFN displacement from WFN-albumin complexes.

Albumin	% Quenching [ST]:[Albumin] = 15:1
HSA	39.5 ± 0.07
SSA	24.0 ± 0.01
PSA	23.6 ± 0.37
BSA	31.4 ± 0.43
RbSA	19.8 ± 0.12

Chapter 5

CONCLUSION

5. CONCLUSION

In summary, this study describes moderate binding affinity between ST and HSA. The complex (ST-HSA) was stabilized by hydrophobic interactions and hydrogen bonds. Secondary and tertiary structural changes in the protein, microenvironmental perturbation around aromatic fluorophores and increased thermal stability of the protein were noticed upon ST binding. Sudlow's site I of HSA, located in subdomain IIA was suggested to be the preferred binding site of ST. Based on the binding parameters, PSA showed close similarity to HSA in the ST binding characteristics. However, results from the WFN displacement experiments showed similarity between BSA and HSA. Further studies are needed to confirm which of these proteins (PSA or BSA) has close resemblance to HSA in order to be used as a suitable animal model in pharmacological studies.

REFERENCES

REFERENCES

Abou-Ghazal, M., Yang, D. S., Qiao, W., Reina-Ortiz, C., Wei, J., Kong, L. Y., Fuller, G. N., Hiraoka, N., Priebe, W., Sawaya, R., & Heimberger, A. B. (2008). The incidence, correlation with tumor-infiltrating inflammation, and prognosis of phosphorylated STAT3 expression in human gliomas. *Clinical Cancer Research*, *14*: 8228−8235.

Abou-Zied, O. K., & Al-Shihi, O. I. (2008). Characterization of subdomain IIA binding site of human serum albumin in its native, unfolded, and refolded states using small molecular probes. *Journal of the American Chemical Society, 130*: 10793−10801.

Afrin, S., Rabbani, G., & Khan, R. H. (2014). Spectroscopic and calorimetric studies of interaction of methimazole with human serum albumin. *Journal of Luminescence, 151*: 219−223.

Akira, S. (2000). Roles of STAT3 defined by tissue-specific gene targeting. *Oncogene*, *19*: 2607−2611.

Alvarez, J. V., Mukherjee, N., Chakravarti, A., Robe, P., Zhai, G., Chakladar, A., Loeffler, J., Black, P., & Frank, D. A. (2007). A STAT3 gene expression signature in gliomas is associated with a poor prognosis. *Translational Oncogenomics*, *2*: 99−105.

Artali, R., Bombieri, G., Calabi, L., & Del Pra, A. (2005). A molecular dynamics study of human serum albumin binding sites. *Il Farmaco, 60*: 485−495.

Bagatolli, L. A., Kivatinitz, S. C., Aguilar, F., Soto, M. A., Sotomayor, P., & Fidelio, G. D. (1996). Two distinguishable fluorescent modes of 1-anilino-8-naphthalenesulfonate bound to human albumin. *Journal of Fluorescence, 6*: 33−40.

Berman, H. M., Westbrook, J., Feng, Z., Gilliland, G., Bhat, T. N., Weissig, H., Shindyalov, I. N., & Bourne, P. E. (2000). The protein data bank. *Nucleic Acids Research, 28*: 235−242.

Bhat, S. A., Bhat, W. F., & Bano, B. (2016). Spectroscopic evaluation of the interaction between pesticides and chickpea cystatin: Comparative binding and toxicity analyses. *Environmental Science: Processes & Impacts, 18*: 872−881.

Bi, S., Ding, L., Tian, Y., Song, D., Zhou, X., Liu, X., & Zhang, H. (2004). Investigation of the interaction between flavonoids and human serum albumin. *Journal of Molecular Structure, 703*: 37−45.

Boengler, K., Ungefug, E., Heusch, G., & Schulz, R. (2013). The STAT3 inhibitor stattic impairs cardiomyocyte mitochondrial function through increased reactive oxygen species formation. *Current Pharmaceutical Design, 19*: 6890−6895.

Bos, O. J., Remijn, J. P., Fischer, M. J., Wilting, J., & Janssen, L. H. (1988). Location and characterization of the warfarin binding site of human serum albumin: A comparative study of two large fragments. *Biochemical Pharmacology*, *37*: 3905−3909.

Bowman, T., Garcia, R., Turkson, J., & Jove, R. (2000). STATs in oncogenesis. *Oncogene, 19*: 2474−2489.

Bromberg, J. F., Wrzeszczynska, M. H., Devgan, G., Zhao, X. Y., Pestell, R. G., Albanese, C., & Darnell, J. E. (1999). *Stat3* as an oncogene. *Cell, 98*: 295−303.

Brown, J. R., & Shockley, P. (1982). Serum albumin: Structure and characterization of its ligand binding sites. In P. C. Jost & O. H. Griffith (Eds.), *Lipid-Protein Interactions* (pp. 25−68). New York: Wiley.

Brown, W. M., Dziegielewska, K. M., Foreman, R. C., & Saunders, N. R. (1989). Nucleotide and deduced amino acid sequence of sheep serum albumin. *Nucleic Acids Research*, *17*: 10495.

Cattoni, D. I., Kaufman, S. B., & Flecha, F. L. G. (2009). Kinetics and thermodynamics of the interaction of 1-anilino-naphthalene-8-sulfonate with proteins. *Biochimica et Biophysica Acta - Proteins and Proteomics, 1794*: 1700−1708.

Cancer Research UK (2014). Worldwide cancer incidence statistics. Retrieved on March 18, 2016, from http://www.cancerresearchuk.org/healthprofessional/cancerstatistics/worldwidecancer/incidence.

Carter, D. C., & Ho, J. X. (1994). Structure of serum albumin. *Advances in Protein Chemistry*, *45*: 153−203.

Chan, K. S., Sano, S., Kiguchi, K., Anders, J., Komazawa, N., Takeda, J., & DiGiovanni, J. (2004). Disruption of Stat3 reveals a critical role in both the

initiation and the promotion stages of epithelial carcinogenesis. *The Journal of Clinical Investigation*, *114*: 720−728.

Chen, C. L., Loy, A., Cen, L., Chan, C., Hsieh, F. C., Cheng, G., Wu, B., Qualman, S. J., Kunisada, K., Yamauchi-Takihara, K., & Lin, J. (2007). Signal transducer and activator of transcription 3 is involved in cell growth and survival of human rhabdomyosarcoma and osteosarcoma cells. *BMC Cancer, 7*: 111.

Chuang, V. T. G., & Otagiri, M. (2001). Flunitrazepam, a 7-nitro-1, 4-benzodiazepine that is unable to bind to the indole-benzodiazepine site of human serum albumin. *Biochimica et Biophysica Acta - Protein Structure and Molecular Enzymology*, *1546*: 337−345.

Clevenger, C. V. (2004). Roles and regulation of stat family transcription factors in human breast cancer. *The American Journal of Pathology*, *165*: 1449−1460.

Corrie, P. G. (2008). Cytotoxic chemotherapy: Clinical aspects. *Medicine, 36*: 24−28.

Curry, S. (2002). Beyond expansion: Structural studies on the transport roles of human serum albumin. *Vox Sanguinis, 83*: 315−319.

Curry, S., Mandelkow, H., Brick, P., & Franks, N. (1998). Crystal structure of human serum albumin complexed with fatty acid reveals an asymmetric distribution of binding sites. *Nature Structural & Molecular Biology, 5*: 827−835.

Darnell Jr., J. E. (1997). STATs and gene regulation. *Science, 27*: 1630−1635.

Darnell Jr., J. E., Kerr, I. M., & Stark, G. R. (1994). Jak-STAT pathways and transcriptional activation in response to IFNs and other extracellular signaling proteins. *Science*, *264*: 1415−1420.

Day, Y. S., & Myszka, D. G. (2003). Characterizing a drug's primary binding site on albumin. *Journal of Pharmaceutical Sciences*, *92*: 333−343.

Debnath, B., Xu, S., & Neamati, N. (2012). Small molecule inhibitors of signal transducer and activator of transcription 3 (Stat3) protein. *Journal of Medicinal Chemistry*, *55*: 6645−6668.

Ding, F., Liu, W., Zhang, L., Yin, B., & Sun, Y. (2010). Sulfometuron-methyl binding to human serum albumin: Evidence that sulfometuron-methyl binds at the Sudlow's site I. *Journal of Molecular Structure, 968*: 59−66.

Divsalar, A., & Khodabakhshian, S. (2015). Probing the binding site of a new synthesized anti-cancer compound to HSA via competitive ligand binding method. *Journal of Molecular Liquids*, *206*: 82−88.

Dockal, M., Carter, D. C., & Rüker, F. (1999). The three recombinant domains of human serum albumin. Structural characterization and ligand binding properties. *The Journal of Biological Chemistry*, *274*: 29303−29310.

Dubois-Presle, N., Lapicque, F., Maurice, M. H., Fournel-Gigleux, S., Magdalou, J., Abiteboul, M., Siest, G., & Netter, P. (1995). Stereoselective esterase activity of human serum albumin toward ketoprofen glucuronide. *Molecular Pharmacology*, *47*: 647−653.

Dufour, C., & Dangles, O. (2005). Flavonoid–serum albumin complexation: Determination of binding constants and binding sites by fluorescence spectroscopy. *Biochimica et Biophysica Acta - General Subjects, 1721*: 164−173.

Dugaiczyk, A., Law, S. W., & Dennison, O. E. (1982). Nucleotide sequence and the encoded amino acids of human serum albumin mRNA. *Proceedings of the National Academy of Sciences of the United States of America*, *79*: 71−75.

Dutzmann, J., Daniel, J. M., Bauersachs, J., Hilfiker-Kleiner, D., & Sedding, D. G. (2015). Emerging translational approaches to target STAT3 signaling and its impact on vascular disease. *Cardiovascular Research*, *106*: 365−374.

Ericsson, A. C., Crim, M. J., & Franklin, C. L. (2013). A brief history of animal modeling. *Missouri Medicine*, *110*: 201–205.

Ecker, A., Simma, O., Hoelbl, A., Kenner, L., Beug, H., Moriggl, R., & Sexl, V. (2008). The dark and the bright side of Stat3: Proto-oncogene and tumor-suppressor. *Frontiers in Bioscience (Landmark Edition)*, *14*: 2944−2958.

Evans, T. W. (2002). Review article: Albumin as a drug—Biological effects of albumin unrelated to oncotic pressure. *Alimentary Pharmacology & Therapeutics*, *16*: 6−11.

Fasano, M., Fanali, G., Leboffe, L., & Ascenzi, P. (2007). Heme binding to albuminoid proteins is the result of recent evolution. *International Union of Biochemistry and Molecular Biology Life, 59*: 436–440.

Fehske, K. J., Schläfer, U., Wollert, U., & Müller, W. E. (1982). Characterization of an important drug binding area on human serum albumin including the high-affinity binding sites of warfarin and azapropazone. *Molecular Pharmacology*, *21*: 387−393.

Feroz, S. R., Mohamad, S. B., Bujang, N., Malek, S. N. A., & Tayyab, S. (2012). Multispectroscopic and molecular modeling approach to investigate the interaction of flavokawain B with human serum albumin. *Journal of Agricultural and Food Chemistry, 60*: 5899−5908.

Feroz, S. R., Mohamad, S. B., Lee, G. S., Malek, S. N. A., & Tayyab, S. (2015). Supramolecular interaction of 6-shogaol, a therapeutic agent of *Zingiber officinale* with human serum albumin as elucidated by spectroscopic, calorimetric and molecular docking methods. *Phytomedicine, 22*: 621−630.

Figge, J., Rossing, T. H., & Fencl, V. (1991). The role of serum proteins in acid-base equilibria. *The Journal of Laboratory and Clinical Medicine*, *117*: 453−467.

Flora, K., Brennan, J. D., Baker, G. A., Doody, M. A., & Bright, F. V. (1998). Unfolding of acrylodan-labeled human serum albumin probed by steady-state and time-resolved fluorescence methods. *Biophysical Journal, 75*: 1084−1096.

Gao, H., Lei, L., Liu, J., Kong, Q., Chen, X., & Hu, Z. (2004). The study on the interaction between human serum albumin and a new reagent with antitumour activity by spectrophotometric methods. *Journal of Photochemistry and Photobiology A: Chemistry, 167*: 213–221.

Geiger, J. L., Grandis, J. R., & Bauman, J. E. (2016). The STAT3 pathway as a therapeutic target in head and neck cancer: Barriers and innovations. *Oral Oncology*, *56*: 84−92.

Ghuman, J., Zunszain, P. A., Petitpas, I., Bhattacharya, A. A., Otagiri, M., & Curry, S. (2005). Structural basis of the drug-binding specificity of human serum albumin. *Journal of Molecular Biology*, *353*: 38−52.

Gianazza, E., Frigerio, A., Astrua-Testori, S., & Righetti, P. G. (1984). The behavior of serum albumin upon isoelectric focusing on immobilized pH gradients. *Electrophoresis*, *5*: 310−312.

González, M., Argaraña, C. E., & Fidelio, G. D. (1999). Extremely high thermal stability of streptavidin and avidin upon biotin binding. *Biomolecular Engineering, 16*: 67−72.

Goodsell, D. S., Morris, G. M., & Olson, A. J. (1996). Automated docking of flexible ligands: Applications of AutoDock. *Journal of Molecular Recognition, 9*: 1−5.

Halgren, T. A. (1996). Merck molecular force field. I. Basis, form, scope, parameterization, and performance of MMFF94. *Journal of Computational Chemistry, 17*: 490−519.

Hanwell, M. D., Curtis, D. E., Lonie, D. C., Vandermeersch, T., Zurek, E., & Hutchison, G. R. (2012). Avogadro: An advanced semantic chemical editor, visualization, and analysis platform. *Journal of Cheminformatics, 4*: 1−17.

Harper, M. E., & Dugaiczyk, A. (1983). Linkage of the evolutionarily-related serum albumin and alpha-fetoprotein genes within q11-22 of human chromosome 4. *American Journal of Human Genetics*, *35*: 565−572.

He, X. M., & Carter, D. C. (1992). Atomic structure and chemistry of human serum albumin. *Nature, 358*: 209−215.

Heinrich, P. C., Behrmann, I., Müller-Newen, G., Schaper, F., & Graeve, L. (1998). Interleukin-6-type cytokine signalling through the gp130/Jak/STAT pathway. *Biochemical Journal*, *334*: 297−314.

Huang, W., Dong, Z., Wang, F., Peng, H., Liu, J. Y., & Zhang, J. T. (2014). A small molecule compound targeting STAT3 DNA-binding domain inhibits cancer cell proliferation, migration, and invasion. *ACS Chemical Biology*, *9*: 1188−1196.

Huang, X., & Miller, W. (1991). A time-efficient, linear-space local similarity algorithm. *Advances in Applied Mathematics*, *12*: 337−357.

Hughes, W. L. (1954). The proteins of blood plasma. In H. Neurath & K. Bailey (Eds.), *The Proteins* (pp. 663−754). New York: Academic Press.

Hunter, M. J. (1966). A method for the determination of protein partial specific volumes. *The Journal of Physical Chemistry*, *70*: 3285−3292.

Ihle, J. N. (2001). The Stat family in cytokine signaling. *Current Opinion in Cell Biology*, *13*: 211−217.

Ji, T., Gong, D., Han, Z., Wei, X., Yan, Y., Ye, F., Ding, W., Wang, J., Xia, X., Li, F., Hu, W., Lu, Y., Wang, S., Zhou, J., Ma, D., & Gao, Q. (2013). Abrogation of

constitutive Stat3 activity circumvents cisplatin resistant ovarian cancer. *Cancer Letters*, *341*: 231−239.

Junicho, A., Matsuda, T., Yamamoto, T., Kishi, H., Korkmaz, K., Saatcioglu, F., Fuse, H., & Muraguchi, A. (2000). Protein inhibitor of activated STAT3 regulates androgen receptor signaling in prostate carcinoma cells. *Biochemical and Biophysical Research Communications*, *278*: 9−13.

Kabir, M. Z., Feroz, S. R., Mukarram, A. K., Alias, Z., Mohamad, S. B., & Tayyab, S. (2016). Interaction of tyrosine kinase inhibitor, vandetanib with human serum albumin as studied by fluorescence quenching and molecular docking. *Journal of Biomolecular Structure and Dynamics, 34*: 1693−1704.

Kamal, A., & Burrows, F. J. (2009). Hsp90 inhibitors as selective anticancer drug*s. Discovery Medicine, 4*: 277−280.

Khan, A. B., Khan, J. M., Ali, M. S., & Khan, R. H. (2012). Interaction of amphiphilic drugs with human and bovine serum albumins. *Spectrochimica Acta Part A: Molecular and Biomolecular Spectroscopy, 97*: 119−124.

Khan, J. M., Chaturvedi, S. K., & Khan, R. H. (2013). Elucidating the mode of action of urea on mammalian serum albumins and protective effect of sodium dodecyl sulfate. *Biochemical and Biophysical Research Communications*, *441*: 681-688.

Knudsen, A., Pedersen, A. O., & Brodersen, R. (1986). Spectroscopic properties of bilirubin-human serum albumin complexes: A stoichiometric analysis. *Archives of Biochemistry and Biophysics*, *244*: 273−284.

Kragh-Hansen, U. (1985). Relations between high-affinity binding sites of markers for binding regions on human serum albumin. *Biochemical Journal*, *225*: 629−638.

Kragh-Hansen, U. (1988). Evidence for a large and flexible region of human serum albumin possessing high affinity binding sites for salicylate, warfarin, and other ligands. *Molecular Pharmacology*, *34*: 160−171.

Kragh-Hansen, U., Chuang, V. T. G., & Otagiri, M. (2002). Practical aspects of the ligand- binding and enzymatic properties of human serum albumin. *Biological and Pharmaceutical Bulletin, 25*: 695−704.

Kraskouskaya, D., Duodu, E., Arpin, C. C., & Gunning, P. T. (2013). Progress towards the development of SH2 domain inhibitors. *Chemical Society Reviews*, *42*: 3337−3370.

Krystof, V., & Uldrijan, S. (2010). Cyclin-dependent kinase inhibitors as anticancer drugs. *Current Drug Targets, 11*: 291−302.

Lakowicz, J. R. (2006). *Principles of Fluorescence Spectroscopy*. (3rd ed.) (pp. 954). New York: Plenum Press.

Lakowicz, J. R., & Weber, G. (1973). Quenching of fluorescence by oxygen. Probe for structural fluctuations in macromolecules. *Biochemistry*, *12*: 4161−4170.

Layton, C. J., & Hellinga, H. W. (2010). Thermodynamic analysis of ligand-induced changes in protein thermal unfolding applied to high-throughput determination of ligand affinities with extrinsic fluorescent dyes. *Biochemistry, 49*: 10831−10841.

Lee, J. Y., & Hirose, M. (1992). Partially folded state of the disulfide-reduced form of human serum albumin as an intermediate for reversible denaturation. *The Journal of Biological Chemistry, 267*: 14753−14758.

Leonard, W. J. (2001). Role of Jak kinases and STATs in cytokine signal transduction. *International Journal of Hematology*, *73*: 271−277.

Levy, D. E., & Darnell, J. E. (2002). STATs: Transcriptional control and biological impact. *Nature Reviews Molecular Cell Biology, 3*: 651−662.

Lin, L., Hutzen, B., Li, P. K., Ball, S., Zuo, M., DeAngelis, S., Foust, E., Sobo, M., Friedman, L., Bhasin, D., Cen, L., Li, C., & Lin, J. (2010). A novel small molecule, LLL12, inhibits STAT3 phosphorylation and activities and exhibits potent growth-suppressive activity in human cancer cells. *Neoplasia*, *12*: 39−50.

Lindup, W. E., & Orme, M. C. (1981). Plasma protein binding of drugs. *British Medical Journal, 282*: 212−214.

Ling, X., & Arlinghaus, R. B. (2005). Knockdown of STAT3 expression by RNA interference inhibits the induction of breast tumors in immunocompetent mice. *Cancer Research*, *65*: 2532−2536.

Liu, M., Zhu, L. Y., Qu, X. K., Sun, D. Z., Li, L. W., & Lin, R. S. (2007). Studies on the binding of paeonol and two of its isomers to human serum albumin by using microcalorimetry and circular dichroism. *The Journal of Chemical Thermodynamics, 39*: 1565−1570.

Lo, H. W., Hsu, S. C., Ali-Seyed, M., Gunduz, M., Xia, W., Wei, Y., Bartholomeusz, G., Shih, J. Y., & Hung, M. C. (2005). Nuclear interaction of EGFR and STAT3 in the activation of the iNOS/NO pathway. *Cancer Cell*, *7*: 575−589.

Lo, H. W., Hsu, S. C., Xia, W., Cao, X., Shih, J. Y., Wei, Y., Abbruzzese, J. L., Hortobagyi, G. N., & Hung, M. C. (2007). Epidermal growth factor receptor cooperates with signal transducer and activator of transcription 3 to induce epithelial-mesenchymal transition in cancer cells via up-regulation of TWIST gene expression. *Cancer Research*, *67*: 9066−9076.

Luwor, R. B., Stylli, S. S., & Kaye, A. H. (2013). The role of Stat3 in glioblastoma multiforme. *Journal of Clinical Neuroscience*, *20*: 907−911.

Martinez, M. N. (2011). Factors influencing the use and interpretation of animal models in the development of parenteral drug delivery systems. *The American Association of Pharmaceutical Scientists Journal*, *13*: 632−649.

Matsuzaki, Y., Besnard, V., Clark, J. C., Xu, Y., Wert, S. E., Ikegami, M., & Whitsett, J. A. (2008). STAT3 regulates ABCA3 expression and influences lamellar body formation in alveolar type II cells. *American Journal of Respiratory Cell and Molecular Biology*, *38*: 551−558.

McKnight, J. A. (2003). Principles of chemotherapy. *Clinical Techniques in Small Animal Practice, 18*: 67−72.

McMurray, J. S. (2006). A new small-molecule Stat3 inhibitor. *Chemistry & Biology*, *13*: 1123−1124.

Mencalha, A. L., Du Rocher, B., Salles, D., Binato, R., & Abdelhay, E. (2010). LLL-3, a STAT3 inhibitor, represses BCR-ABL-positive cell proliferation, activates apoptosis and improves the effects of Imatinib mesylate. *Cancer Chemotherapy and Pharmacology*, *65*: 1039−1046.

Mi, R., Hu, Y. J., Fan, X. Y., Ouyang, Y., & Bai, A. M. (2014). Exploring the site-selective binding of jatrorrhizine to human serum albumin: Spectroscopic and molecular modeling approaches. *Spectrochimica Acta Part A: Molecular and Biomolecular Spectroscopy*, *117*: 163−169.

Michaud, F. T., Garnier, A., Lemieux, L., & Duchesne, C. (2009). Multivariate analysis of single quadrupole LC-MS spectra for routine characterization and quantification of intact proteins. *Proteomics*, *9*: 512−520.

Mikkelsen, M., Jacobsen, P., & Henningsen, K. (1977). Possible localization of Gc-system on chromosome 4. Loss of long arm 4 material associated with father-child incompatibility within the Gc-system. *Human Heredity*, *27*: 105−107.

Miklossy, G., Hilliard, T. S., & Turkson, J. (2013). Therapeutic modulators of STAT signalling for human diseases. *Nature Reviews Drug Discovery*, *12*: 611−629.

Minghetti, P. P., Ruffner, D. E., Kuang, W. J., Dennison, O. E., Hawkins, J. W., Beattie, W. G., & Dugaiczyk, A. (1986). Molecular structure of the human albumin gene is revealed by nucleotide sequence within q11-22 of chromosome 4. *The Journal of Biological Chemistry*, *261*: 6747−6757.

Mulqueen, P. M., & Kronman, M. J. (1982). Binding of naphthalene dyes to the N and A conformers of bovine α-lactalbumin. *Archives of Biochemistry and Biophysics, 215*: 28−39.

Muromoto, R., Sekine, Y., Imoto, S., Ikeda, O., Okayama, T., Sato, N., & Matsuda, T. (2008). BART is essential for nuclear retention of STAT3. *International Immunology*, *20*: 395−403.

Naka, T., Narazaki, M., Hirata, M., Matsumoto, T., Minamoto, S., Aono, A., Nishimoto, N., Kajita, T., Taga, T., Yoshizaki, K., & Akirak, S. (1997). STAT-induced STAT inhibitor. *Nature*, *387*: 924−929.

Olsson, T. S., Williams, M. A., Pitt, W. R., & Ladbury, J. E. (2008). The thermodynamics of protein–ligand interaction and solvation: Insights for ligand design. *Journal of Molecular Biology, 384*: 1002−1017.

Oncley, J. L., Scatchard, G., & Brown, A. (1947). Physical-chemical characteristics of certain of the proteins of normal human plasma. *The Journal of Physical Chemistry*, *51*: 184−198.

Page, B. D. G., Fletcher, S., Yue, P., Li, Z., Zhang, X., Sharmeen, S., Datti, A., Wrana, J. L., Trudel, S., Schimmer, A. D., Turkson, J., & Gunning, P. T. (2011). Identification of a non-phosphorylated, cell permeable, small molecule ligand for the Stat3 SH2 domain. *Bioorganic & Medicinal Chemistry Letters*, *21*: 5605−5609.

Painter, L., Harding, M. M., & Beeby, P. J. (1998). Synthesis and interaction with human serum albumin of the first 3,18-disubstituted derivative of bilirubin. *Journal of the Chemical Society, Perkin Transactions 1, 18*: 3041−3044.

Pajot, P. (1976). Fluorescence of proteins in 6-M guanidine hydrochloride. *European Journal of Biochemistry*, *63*: 263−269.

Pan, Y., Zhou, F., Zhang, R., & Claret, F. X. (2013). Stat3 inhibitor Stattic exhibits potent antitumor activity and induces chemo-and radio-sensitivity in nasopharyngeal carcinoma. *PLoS ONE, 8*: e54565.

Park, I. H., & Li, C. (2011). Characterization of molecular recognition of STAT3 SH2 domain inhibitors through molecular simulation. *Journal of Molecular Recognition*, *24*: 254−265.

Pedranzini, L., Leitch, A., & Bromberg, J. (2004). Stat3 is required for the development of skin cancer. *The Journal of Clinical Investigation*, *114*: 619−622.

Peters Jr., T. (1985). Serum albumin. *Advances in Protein Chemistry*, 37: 161−245.

Peters Jr., T. (1996). *All About Albumin: Biochemistry, Genetics and Medical Applications*. (pp. 432). San Diego: Academic Press.

Petitpas, I., Bhattacharya, A. A., Twine, S., East, M., & Curry, S. (2001). Crystal structure analysis of warfarin binding to human serum albumin anatomy of drug site I. *The Journal of Biological Chemistry, 276*: 22804−22809.

Picó, G. A. (1997). Thermodynamic features of the thermal unfolding of human serum albumin. *International Journal of Biological Macromolecules, 20*: 63−73.

Poli, V., & Alonzi, T. (2003). STAT3 function in vivo. In *Signal Transducers and Activators of Transcription (STATs)* (pp. 493−512). Netherlands: Springer.

Puthier, D., Bataille, R., & Amiot, M. (1999). IL-6 up-regulates Mcl-1 in human myeloma cells through JAK/STAT rather than Ras/MAP kinase pathway. *European Journal of Immunology*, *29*: 3945−3950.

Qin, H. R., Kim, H. J., Kim, J. Y., Hurt, E. M., Klarmann, G. J., Kawasaki, B. T., Serat, M. A. D., & Farrar, W. L. (2008). Activation of signal transducer and activator of transcription 3 through a phosphomimetic serine 727 promotes prostate

tumorigenesis independent of tyrosine 705 phosphorylation. *Cancer Research*, *68*: 7736−7741.

Reed, R. G., Feldhoff, R. C., Clute, O. L., & Peters Jr., T. (1975). Fragments of bovine serum albumin produced by limited proteolysis. Conformation and ligand binding. *Biochemistry, 14*: 4578−4583.

Quinlan, G. J., Martin, G. S., & Evans, T. W. (2005). Albumin: Biochemical properties and therapeutic potential. *Hepatology*, *41*: 1211−1219.

Rinco, O., Brenton, J., Douglas, A., Maxwell, A., Henderson, M., Indrelie, K., Wessels, J., & Widin, J. (2009). The effect of porphyrin structure on binding to human serum albumin by fluorescence spectroscopy. *Journal of Photochemistry and Photobiology A: Chemistry, 208*: 91−96.

Ross, P. D., & Subramanian, S. (1981). Thermodynamics of protein association reactions: Forces contributing to stability. *Biochemistry, 20*: 3096−3102.

Samari, F., Hemmateenejad, B., Shamsipur, M., Rashidi, M., & Samouei, H. (2012). Affinity of two novel five-coordinated anticancer Pt (II) complexes to human and bovine serum albumins: A spectroscopic approach. *Inorganic Chemistry*, *51*: 3454−3464.

Sanner, M. F. (1999). Python: A programming language for software integration and development. *Journal of Molecular Graphics and Modelling, 17*: 57−61.

Scheider, W., Dintzis, H. M., & Oncley, J. L. (1976). Changes in the electric dipole vector of human serum albumin due to complexing with fatty acids. *Biophysical Journal*, *16*: 417−431.

Schust, J., Sperl, B., Hollis, A., Mayer, T. U., & Berg, T. (2006). Stattic: A small-molecule inhibitor of STAT3 activation and dimerization. *Chemistry and Biology,13*: 1235−1242.

Shah, A., & Bano, B. (2011). Spectroscopic studies on the interaction of bilirubin with liver cystatin. *European Biophysics Journal*, *40*: 175−180.

Shahabadi, N., Falsafi, M., & Hadidi, S. (2015). Molecular modeling and multispectroscopic studies of the interaction of hepatitis B drug, adefovir dipivoxil with human serum albumin. *Journal of Luminescence, 167*: 339−346.

Shahlaei, M., Rahimi, B., Nowroozi, A., Ashrafi-Kooshk, M. R., Sadrjavadi, K., & Khodarahmi, R. (2015). Exploring binding properties of sertraline with human serum albumin: Combination of spectroscopic and molecular modeling studies. *Chemico-Biological Interactions*, *242*: 235−246.

Sheng, L., Ding, H., Wang, Z., & Song, G. (2010). Binding of amphiphilic p(DMAEMA$_{79}$-b-AZOM$_5$) diblock copolymer with bovine serum albumin–A spectroscopic investigation with warfarin and ibuprofen as site markers. *Journal of Molecular Structure*, *979*: 152−159.

Shuai, K. (2000). Modulation of STAT signaling by STAT-interacting proteins. *Oncogene*, *19*: 2638−2644.

Siddiquee, K., Zhang, S., Guida, W. C., Blaskovich, M. A., Greedy, B., Lawrence, H. R., Yip, M. L. R., Jove, R., McLaughlin, M. M., Lawrence, N. J., Sebti, S. M., & Turkson, J. (2007). Selective chemical probe inhibitor of Stat3, identified through structure-based virtual screening, induces antitumor activity. *Proceedings of the National Academy of Sciences of the United States of America*, *104*: 7391−7396.

Simon, G. A., & Maibach, H. I. (2000). The pig as an experimental animal model of percutaneous permeation in man: Qualitative and quantitative observations–An overview. *Skin Pharmacology and Physiology*, *13*: 229−234.

Sjöholm, & Ljungstedt, I. (1973). Studies on the tryptophan and drug-binding properties of human serum albumin fragments by affinity chromatography and circular dichroism measurements. *The Journal of Biological Chemistry, 248*: 8434−8441.

Skeel, R. T., & Khleif, S. N. (2011). *Handbook of Cancer Chemotherapy* (8th ed.). (pp. 45−62). Lippincott Williams & Wilkins, Philadelphia.

Song, H., Wang, R., Wang, S., & Lin, J. (2005). A low-molecular-weight compound discovered through virtual database screening inhibits Stat3 function in breast cancer cells. *Proceedings of the National Academy of Sciences of the United State of America, 102*: 4700−4705.

Stamler, J. S., Jaraki, O., Osborne, J., Simon, D. I., Keaney, J., Vita, J., Singel, D., Valeri, C. R., & Loscalzo, J.(1992). Nitric oxide circulates in mammalian plasma primarily as an *S*-nitroso adduct of serum albumin. *Proceedings of the National Academy of Sciences of the United States of America*, *89*: 7674−7677.

Sudlow, G. D. J. B., Birkett, D. J., & Wade, D. N. (1976). Further characterization of specific drug binding sites on human serum albumin. *Molecular Pharmacology, 12*: 1052−1061.

Sugio, S., Kashima, A., Mochizuki, S., Noda, M., & Kobayashi, K. (1999). Crystal structure of human serum albumin at 2.5 Å resolution. *Protein Engineering*, *12*: 439−446.

Sułkowska, A., Maciążek-Jurczyk, M., Bojko, B., Rownicka, J., Zubik-Skupień, I., Temba, E., Pentak D., & Sułkowski, W. W. (2008). Competitive binding of phenylbutazone and colchicine to serum albumin in multidrug therapy: A spectroscopic study. *Journal of Molecular Structure, 881*: 97−106.

Sułkowska, A., Równicka, J., Bojko, B., & Sułkowski, W. (2003). Interaction of anticancer drugs with human and bovine serum albumin. *Journal of Molecular Structure, 651*: 133−140.

Takeda, K., Noguchi, K., Shi, W., Tanaka, T., Matsumoto, M., Yoshida, N., Kishimoto, T., & Akira, S. (1997). Targeted disruption of the mouse Stat3 gene leads to early embryonic lethality. *Proceedings of the National Academy of Sciences of the United States of America*, *94*: 3801−3804.

Tanford, C. (1950). Preparation and properties of serum and plasma proteins. XXIII. Hydrogen ion equilibria in native and modified human serum albumins. *Journal of the American Chemical Society*, *72*: 441−451.

Trynda-Lemiesz, L., Keppler, B. K., & KozłLowski, H. (1999). Studies on the interactions between human serum albumin and imidazolium [trans-tetrachlorobis (imidazol) ruthenate (III)]. *Journal of Inorganic Biochemistry, 73*: 123−128.

Tunc, S., Duman, O., Soylu, I., & Bozoglan, B. K. (2014). Spectroscopic investigation of the interactions of carbofuran ad amitrol herbicides with human serum albumin. *Journal of Luminescence, 151*: 22−28.

Turkson, J., Kim, J. S., Zhang, S., Yuan, J., Huang, M., Glenn, M., Haura, E., Sebti, S., Hamilton, A. D., & Jove, R. (2004a). Novel peptidomimetic inhibitors of signal transducer and activator of transcription 3 dimerization and biological activity. *Molecular Cancer Therapeutics, 3*: 261−269.

Turkson, J., Zhang, S., Palmer, J., Kay, H., Stanko, J., Mora, L. B., Sebti, S., Yu, H., & Jove, R. (2004b). Inhibition of constitutive signal transducer and activator of

transcription 3 activation by novel platinum complexes with potent antitumor activity. *Molecular Cancer Therapeutics*, *3*: 1533−1542.

Turkson, J., Zhang, S., Mora, L. B., Burns, A., Sebti, S., & Jove, R. (2005). A novel platinum compound inhibits constitutive Stat3 signaling and induces cell cycle arrest and apoptosis of malignant cells. *The Journal of Biological Chemistry*, *280*: 32979−32988.

Twine, S. M., Gore, M. G., Morton, P., Fish, B. C., Lee, A. G., & East, J. M. (2003). Mechanism of binding of warfarin enantiomers to recombinant domains of human albumin. *Archives of Biochemistry and Biophysics, 414*: 83−90.

Urlam, M. K., Pireddu, R., Ge, Y., Zhang, X., Sun, Y., Lawrence, H. R., Guida, W. C., Sebti, S. M., & Lawrence, N. J. (2013). Development of new N-arylbenzamides as STAT3 dimerization inhibitors. *Medicinal Chemistry Communications*, *4*: 932−941.

Uversky, V. N., Narizhneva, N. V., Ivanova, T. V., & Tomashevski, A. Y. (1997). Rigidity of human α-fetoprotein tertiary structure is under ligand control. *Biochemistry, 36*: 13638−13645.

Varlan, A., & Hillebrand, M. (2010). Bovine and human serum albumin interactions with 3-carboxyphenoxathiin studied by fluorescence and circular dichroism spectroscopy. *Molecules, 15*: 3905−3919.

Wallevik, K. (1973). Reversible denaturation of human serum albumin by pH, temperature and guanidine hydrochloride. *The Journal of Biological Chemistry, 245*: 2650−2655.

Wang, H. L., Zou, H. F., & Zhang, Y. K. (1997). Determination of drug-protein interactions by combined microdialysis and high-performance liquid chromatography. *Chromatographia, 44*: 205–208.

Wang, Y. Q., Tang, B. P., Zhang, H. M., Zhou, Q. H., & Zhang, G. C. (2009). Studies on the interaction between imidacloprid and human serum albumin: Spectroscopic approach. *Journal of Photochemistry and Photobiology B: Biology, 94*: 183−190.

Ware, W. R. (1962). Oxygen quenching of fluorescence in solution: An experimental study of the diffusion process. *The Journal of Physical Chemistry, 66*: 455−458.

Weinstock, J., & Baldwin, G. S. (1988). Nucleotide sequence of porcine liver albumin. *Nucleic Acids Research*, *16*: 9045.

Xiong, A., Yang, Z., Shen, Y., Zhou, J., & Shen, Q. (2014). Transcription factor STAT3 as a novel molecular target for cancer prevention. *Cancers*, *6*: 926−957.

Yasmeen, S., Riyazuddeen, & Rabbani, G. (2017). Calorimetric and spectroscopic binding studies of amoxicillin with human serum albumin. *Journal of Thermal Analysis and Calorimetry, 127*: 1445−1455.

Yamasaki, K., Maruyama, T., Kragh-Hansen, U., & Otagiri, M. (1996). Characterization of site I on human serum albumin: Concept about the structure of a drug binding site. *Biochimica et Biophysia Acta - Protein Structure and Molecular Enzymology*, *1295*: 147−157.

Yeggoni, D. P., Gokara, M., Mark Manidhar, D., Rachamallu, A., Nakka, S., Reddy, C. S., & Subramanyam, R. (2014). Binding and molecular dynamics studies of 7-hydroxycoumarin derivatives with human serum albumin and its pharmacological importance. *Molecular Pharmaceutics, 11*: 1117−1131.

Yoshikawa, H., Matsubara, K., Qian, G. S., Jackson, P., Groopman, J. D., Manning, J. E., Harris, C. C., & Herman, J. G. (2001). SOCS-1, a negative regulator of the JAK/STAT pathway, is silenced by methylation in human hepatocellular carcinoma and shows growth-suppression activity. *Nature Genetics*, *28*: 29−35.

Yu, C. L., Meyer, D. J., & Campbell, G. S. (1995). Enhanced DNA-binding activity of a Stat3-related protein in cells transformed by the Src oncoprotein. *Science*, *269*: 81−83.

Yu, H., & Jove, R. (2004). The STATs of cancer—New molecular targets come of age. *Nature Reviews Cancer*, *4*: 97−105.

Yu, H., Kortylewski, M., & Pardoll, D. (2007). Crosstalk between cancer and immune cells: Role of STAT3 in the tumour microenvironment. *Nature Reviews Immunology*, *7*: 41−51.

Yu, H., Pardoll, D., & Jove, R. (2009). STATs in cancer inflammation and immunity: A leading role for STAT3. *Nature Reviews Cancer*, *9*: 798−809.

Yu, X. W., Kennedy, R. H., & Liu, S. J. (2003). JAK2/STAT3, not ERK1/2 pathway mediates interleukin-6-elicited inducible NOS activation and decrease in

contractility in adult ventricular myocytes. *The Journal of Biological Chemistry, 278*: 16304−16309.

Yue, Y., Zhang, Y., Li, Y., Zhu, J., Qin, J., & Chen, X. (2008). Interaction of nobiletin with human serum albumin studied using optical spectroscopy and molecular modeling methods. *Journal of Luminescence, 128*: 513−520.

Zhang, H. M., Chen, T. T., Zhou, Q. H., & Wang, Y. Q. (2009). Binding of caffeine, theophylline, and theobromine with human serum albumin: A spectroscopic study. *Journal of Molecular Structure, 938*: 221−228.

Zhang, X., Sun, Y., Pireddu, R., Yang, H., Urlam, M. K., Lawrence, H. R., Guida, W. C., Lawrence, N. J., & Sebti, S. M. (2013). A novel inhibitor of STAT3 homodimerization selective suppresses STAT3 activity and malignant transformation. *Cancer Research*, *73*: 1922−1933.

Zhang, X., Yue, P., Fletcher, S., Zhao, W., Gunning, P. T., & Turkson, J. (2010). A novel small-molecule disrupts Stat3 SH2 domain–phosphotyrosine interactions and Stat3-dependent tumor processes. *Biochemical Pharmacology*, *79*: 1398−1409.

Zhang, Q., Zhang, C., He, J., Guo, Q., Hu, D., Yang, X., Wang, J., Kang, Y., She, R., Wang, Z., Li, D., Huang G., Ma, Z., Mao, W., Zhou, X., Xiao, C., Sun, X., & Ma, J. (2015). STAT3 inhibitor stattic enhances radiosensitivity in esophageal squamous cell carcinoma. *Tumor Biology*, *36*: 2135−2142.

Zhuang, S. (2013). Regulation of STAT signaling by acetylation. *Cellular Signalling*, *25*: 1924−1931.

LIST OF PUBLICATIONS / PRESENTATION

1. **Ida Syazwani M. Affandi**, Lee Wei Qi, Shevin R. Feroz, Saharuddin B. Mohamad and Saad Tayyab (2016). Interaction of stattic, a STAT3 inhibitor with human serum albumin: Spectroscopic and computational study. *Journal of Biomolecular Structure and Dynamics,* DOI: 10.1080/07391102.2016.1264887.

2. **Ida Syazwani Binti Mohd Affandi**, Saharuddin B. Mohamad and Saad Tayyab (2016). Multispectroscopic and molecular docking approach on the transport of stattic, a STAT3 inhibitor with human serum albumin. *Proceedings of the 41st Annual Conference of the Malaysian Society for Biochemistry and Molecular Biology held at Selangor, Malaysia on August 17-18, 2016*. Abstract No. Poster 41, pp. 93.

Journal of Biomolecular Structure and Dynamics, 2016
http://dx.doi.org/10.1080/07391102.2016.1264887

Taylor & Francis
Taylor & Francis Group

LETTER TO THE EDITOR

Interaction of stattic, a STAT3 inhibitor with human serum albumin: spectroscopic and computational study

Ida Syazwani M. Affandi[a], Wei Qi Lee[a], Shevin R. Feroz[a], Saharuddin B. Mohamad[b,c] and Saad Tayyab[a,c]*

[a]*Faculty of Science, Biomolecular Research Group, Biochemistry Programme, Institute of Biological Sciences, University of Malaya, Kuala Lumpur, Malaysia;* [b]*Faculty of Science, Bioinformatics Programme, Institute of Biological Sciences, University of Malaya, Kuala Lumpur, Malaysia;* [c]*Centre of Research for Computational Sciences and Informatics for Biology, Bioindustry, Environment, Agriculture and Healthcare (CRYSTAL), University of Malaya, Kuala Lumpur, Malaysia*

Communicated by Ramaswamy H. Sarma

(*Received 22 August 2016; accepted 15 November 2016*)

Diagnosis of over 14.1 million new cancer patients and 8.2 million deaths each year has made cancer as one of the most life-threatening diseases (Cancer Research UK, 2014). The most commonly used method in treating cancer is chemotherapy, which employs pharmacological agents to treat cancer cells. Despite of their action in killing cancer cells, many of these agents are also toxic to the normal, healthy cells. Due to this problem, search for effective drugs to fight cancer is still continued. Drugs with efficient anticancer potential but minimal effect on normal cells are being discovered from natural sources as well as through chemical synthesis. These drugs usually act as inhibitors against abnormally expressed proteins in cancer cells. Recent *in vivo* studies have reported STAT3 in being constitutively active in a wide range of malignancies including breast, prostate and head and neck tumors as well as multiple myelomas and hematological cancers (Bromberg et al., 1999; Song, Wang, Wang, & Lin, 2005; Turkson et al., 2004). This has made it as an attractive molecular target for the development of novel cancer therapies.

Stattic (ST), whose structure is illustrated in the inset of Figure 1(a), can directly inhibit STAT3 function (Schust, Sperl, Hollis, Mayer, & Berg, 2006) and has shown potential against STAT3-dependent cancer cells such as nasopharynx, ovarian, and breast cancers (Pan, Zhou, Zhang, & Claret, 2013; Schust et al., 2006). Although several studies on ST have been made to show the mechanism of its anticancer action (Pan et al., 2013; Schust et al., 2006), information about its transport in blood circulation is not known.

Being one of the most abundant proteins and a major transporter in the blood circulation, human serum albumin (HSA) has been commonly used as a reagent in the biological study. Different ligands may bind to either of the two high affinity binding sites available on HSA, viz. Sudlow's site I and site II, located in subdomains IIA and IIIA, respectively (Feroz, Mohamad, Bakri, Malek, & Tayyab, 2013). Presence of a solitary tryptophan residue (Trp-214) located in subdomain IIA is advantageous in using fluorescence spectroscopy to probe the binding of any ligand to the protein. Here, we describe the interaction between ST and HSA using fluorescence and CD spectroscopy along with molecular docking techniques.

Materials and methods

Materials

HSA, essentially fatty acid-free, warfarin (WFN), 1-anilinonaphthalene-8-sulfonate (ANS) and ST were procured from Sigma-Aldrich Inc., USA. Diazepam (DZM) was the product of Lipomed AG, Switzerland. All other chemicals were of analytical standard.

Analytical methods

Sodium phosphate buffer (60 mM, pH 7.4) was used to prepare all working solutions. The concentration of the protein (HSA) solution was determined using a molar absorption coefficient of 36,500 M^{-1} cm^{-1} at 280 nm (Kabir et al., 2016).

DZM, WFN, and ST stock solutions were prepared by dissolving 10 mg of their crystals in 10 mL dimethyl sulfoxide (DMSO) and were diluted with the buffer to obtain the desired concentration for the working solutions. The final concentration of DMSO was less than 1% in all experiments. This concentration of DMSO has been shown to cause no affect on HSA conformation and

*Corresponding author. Email: saadtayyab2004@um.edu.my

Poster 41

MULTISPECTROSCOPIC AND MOLECULAR DOCKING APPROACH ON THE TRANSPORT OF STATTIC, A STAT3 INHIBITOR WITH HUMAN SERUM ALBUMIN

Ida Syazwani Binti Mohd Affandi[1], Saharuddin B. Mohamad[1] & Saad Tayyab[1]

[1]*Institute of Biological Sciences, Faculty of Science, University of Malaya, 50604 Kuala Lumpur*

*Corresponding author: saadtayyab2004@um.edu.my

Interaction of stattic (ST), an inhibitor of signal transducer and activation of transcription 3, STAT3, with human serum albumin (HSA), the major transport protein in human blood circulation, was examined using multitude of spectroscopic techniques and molecular docking method. The binding constant of ST-HSA system, as determined by the fluorescence quenching data analysis was found to be within the range $2.60-1.45 \times 10^4$ M^{-1} at three different temperatures, suggesting a moderate binding affinity. The inverse correlation between the binding constant and the temperature revealed involvement of static quenching mechanism, thus affirming ST-HSA complex formation. The complex was found to be stabilized by hydrophobic interactions and hydrogen bonds, as suggested by the thermodynamic data (ΔH = -14.9 kJ mol^{-1} and ΔS = +32.8 J mol^{-1} K^{-1}). The far-UV and the near-UV circular dichroic spectral results showed alteration in both secondary and tertiary structures of HSA upon ST binding. Change in the microenvironment around aromatic fluorophores of HSA consequent to the complex formation was evident from three-dimensional fluorescence spectra. Binding of ST to HSA led to an increase in its stability against heat, as deduced from thermal stability experiments. Competitive ligand displacement using site specific marker ligands (site I marker: warfarin, site II markers: diazepam and ANS) along with molecular docking results suggested Sudlow's site I of HSA as the preferred ST binding site.

Keywords: Stattic, human serum albumin, ligand-protein interaction, fluorescence spectroscopy, molecular docking

BIOGRAPHY

Ida Syazwani was born in Selangor, Malaysia on June 7, 1992. She received her Pre-university education from Malacca Matriculation College in 2010–2011. She was enrolled as an undergraduate student of Biochemistry at the University of Malaya in 2011 and received her B.Sc. degree in Biochemistry in 2015. Then, she joined the laboratory of Professor Saad Tayyab to work as Research Assistant in the HIR grant (UM.C/625/1/HIR/MOHE/SC/02) during April 20, 2015 – April 19, 2016. On October 30, 2015, she registered herself in the Master programme in Biochemistry of the University of Malaya.